博士論文

論文題目　Studies on the Variation of Salinity Responses and Salt-tolerant Mechanisms of *Miscanthus sinensis* Andersson

（ススキの塩ストレスに対する応答および耐塩性機構に関する研究）

氏　名　孫　茜

Studies on the Variation of Salinity Responses and Salt-tolerant Mechanisms of *Miscanthus sinensis* Andersson

（ススキの塩ストレスに対する応答および耐塩性機構に関する研究）

Graduate School of Agricultural and Life Science, University of Tokyo

Department of Agricultural and Environmental Biology

Qian Sun

Supervisor: Prof. Testuo Takano

Thesis submitted in partial fulfilment of the requirement for the degree of

Doctor of Agriculture Science

April 2014

ABSTRACT

The lignocellulosic crop, *Miscanthus* spp. has been identified as a good candidate for biomass production. To satisfy the need for high yield and to avoid competition with food production by growing the crop in marginal areas, we studied the responses of *M. sinensis* to salinity. Effects of salt concentrations (0─360 mM NaCl) on seed germination, growth, photosynthesis, and shoot ion accumulation were examined. In the germination test of 17 accessions, high salt concentration inhibited seed germination in all accessions, while germination percentage varied significantly among the accessions. Two accessions showing variable salt tolerance, JM0119 (salt-tolerant) and JM0099 (salt-sensitive), were selected for a greenhouse study on plant dry weight, leaf chlorophyll content, total leaf area, tiller number, photosynthetic rate (A), stomatal conductance (g_s), PSII operating efficiency ($\Delta F/F'_m$), and shoot ion concentration during various lengths of time. The experiment was performed twice, but for most parameters, no significant differences between runs were observed. Salinity resulted in a reduction of plant growth. A and g_s were adversely affected by all salt treatment levels, while $\Delta F/F'_m$ was not reduced until salt concentrations reached 120 mM NaCl. In contrast to the increases of shoot Na^+ and Cl^- concentrations，shoot K^+ concentration declined in the presence of salt. Overall, this study revealed a great variability for salt tolerance in *M. sinensis* germplasm. The

relative advantage of JM0119 over JM0099 under saline conditions was primarily associated with larger leaf area, a greater number of tillers, greater photosynthetic capacity, and restricted Na^+ accumulation in shoots.

In order to better understand the physiological and biochemical responses of C_4 photosynthesis to salinity in *M. sinensis*, seedlings of two accessions (salt-tolerant 'JM0119' and salt-sensitive 'JM0099') were subjected to 0 (control) or 250 mM NaCl stress for two weeks. The shoot dry weight, leaf chlorophyll content, gas-exchange, chlorophyll *a* fluorescence, activities of phospho*enol*pyruvate carboxylase (PEPC), pyruvate, orthophosphate dikinase (PPDK), NADP-malic enzyme (NADP-ME), NADP-malate dehydrogenase (NADP-MDH), and ribulose-1,5-bisphosphate carboxylase/oxygenase (RuBisCO), and contents of carbohydrates, protein, and foliar total free-amino acids were investigated on five harvest dates. Salt-induced reduction of the relative growth rate related to the inhibited photosynthetic rate. Higher photosynthetic rate, transpiration rate, chlorophyll content, the PSII operating efficiency, coefficient of photochemical quenching, and contents of soluble sugars, protein, and total free-amino acids under salinity were observed in 'JM0119' relative to those in 'JM0099'. Activities of PEPC and PPDK were gradually increased under salt duration in 'JM0119', while they displayed single peak curves in 'JM0099'. NADP-MDH activity enhanced gradually in both accessions under salt duration, with greater increases observed in 'JM0099'. Salt-enhanced activity of NADP-ME was

only observed in ‘JM0099’. The maximum efficiency of PSII photochemistry, activity of RuBisCO, and starch content were slightly affected by salt stress. Greater photosynthetic capacity under salt stress was mainly associated with non-stomatal factors including less chlorophyll loss, higher PSII operating efficiency, enhanced activities of PEPC and PPDK, and lower activity of NADP-ME. Despite the repressive effect on plant photosynthesis due to the imbalanced source-sink relationship, accumulated soluble sugars provided osmotic adjustment and osmprotection in leaves. More efficient nitrate assimilation was also related to salt-tolerance owing to the greater contents of protein and total leaf free-amino acid.

The adaptation responses of genes involved in C_4 path way (*PEPC*, *PPDK*, *NADP-MDH*, *NADP-ME*, and *RbcS*) and genes encoding Na^+/H^+ antiporters, NHX1 and SOS1, to NaCl stress were also examined in JM0119 and JM0099. Based on the sequencing on approximate 600 bp-long cDNA fragments obtained from degenerated PCR, the cDNA sequences of genes examined were highly conserved among the relatives of *M. sinensis*. These salt-induced variation of gene expression investigated by quantitative real-time PCR provided evidences for insights of the molecular mechanisms of salt tolerance in *M. sinensis*. Up-regulation of *PEPC*, *PPDK*, *NADP-MDH*, and *NADP-ME* were observed in both accessions with different patterns, while *RbcS* expression was suppressed by salt stress. Between the accessions, higher *PEPC*, *PPDK*, and *RbcS* expression were related to greater

photosynthetic capacity under salt regime. Expression of *NADP-MDH* and *NADP-ME* may be closely related to each other and partially responsible for the changes in the activity of NADP-MDH and NADP-ME. The expression of *NHX1* was up-regulated by salt stress in JM0119 shoot and root tissues. However, it was hardly affected in JM0099 shoot tissue except for a significant increase at 100 mM salt treatment, and it was salt-suppressed in JM0099 root tissue. Thus, the remarkably higher expression of *NHX1* and *SOS1* were associated with the resistance of Na^+ toxicity by regulation of Na^+ influx, efflux, and sequestration under different salt conditions.

Results in this thesis are expected to provide useful information in screening for salt-tolerant germplasm in *M. sinensis* and they may shed new light on elucidating the physiological and biochemical mechanisms associated with salt stress in this species.

LIST OF ABBREVIATIONS

ϕ_{CO2}, quantum yield of CO_2 assimilation

ϕ_{PSII}, efficiency of light harvesting of photosystem II

A, photosynthetic rate; CVG, velocity of germination

BSC, bundle sheath cell

F_m, maximal fluorenscence of dark-adapted leaf

F_o, minimal fluorenscence of dark-adapted leaf

F_t, steady-state yield of fluorescence

F_v, variable fluorescence of dark-adapted leaf

F_v/F_m, maximum efficiency of PSII photochemistry

F'_m, maximal fluorenscence of light-adapted leaf

ΔF, difference in fluorescence between F'_m and F_t

$\Delta F/F'_m$, PSII operating efficiency

g_s, stomatal conductance

MC, mesophyll cell

NADP-ME, NADP-malic enzyme

NADP-MDH, NADP-malate dehydrogenase

NHX1, Na^+/H^+ exchanger 1

NPQ, the nonphotochemical quenching

PEPC, phospho*enol*pyruvate carboxylase

PPDK, pyruvate, orthophosphate dikinase

PSDW, plant shoot dry weight

qP, the coefficient of photochemical quenching

RuBisCO, ribulose-1,5-bisphosphate carboxylase/oxygenase

RGR, relative growth rate

RL, root length

SL, shoot length

SOS1, Salt Overly Sensitive 1

SPAD, leaf chlorophyll content

TAA, total free-amino acid

TLA, total leaf area

TN, number of tillers

TSS, total soluble sugars

TABLE OF CONTENTS

CHAPTER 1

General Introduction

1.1. *Miscanthus sinensis*, An Important Species Facilitate Bioenergy Crop Development

Miscanthus Andersson, originating from Southeast Asia, Pacific Islands and tropic Africa, is a C_4 perennial lignocellulosic grass genus which has about 14 species. *Miscanthus* plants have been raw material for making paper, thatching material for roofs of traditional houses and buildings, organic fertilizer, livestock feed, and ornamental plant.

One species in this genus, *Miscanthus ×giganteus* (*M. ×giganteus*), demonstrates high yield, high water and nitrogen use efficiency, the ability to enhance soil carbon sequestration, and low susceptibility to pests and diseases; this species has thus been identified as a good candidate for a bioenergy crop, and particularly for energy production by direct combustion (Dohleman *et al.*, 2010; Dohleman and Long, 2009; Grare, 2010; Sang and Zhu, 2011; Zub *et al.*, 2010). Since plant-based liquid biofuels have played an important role in large-scale substitution for petroleum-based fuels but have historically been produced from crops developed for food production, primarily using maize and sugarcane for bioethanol and soybean and rapeseed for biodiesel, it raises concerns about net energy and greenhouse gas effects and potential competition

between use of land for food and fuel production (Somerville *et al.*, 2010). To meet the challenge of developing second-generation energy crops capable of growing on marginal land, perennial plants with high net energy output and little to no CO_2 emission are needed. *M.* ×*giganteus*, a natural triploid hybrid between *Miscanthus sinensis* Anderss. (*M. sinensis*) (2n = 2× = 38) and *Miscanthus sacchariflorus* (Maxim.) Benth. (*M. sacchariflorus*) (2n = 4× = 76) (Greef & Deuter, 1993; Linde-Laursen, 1993; Hodkinson and Renvoize, 2001), introduced from Japan to Denmark as an ornamental in 1935 (Hodkinson *et al.*, 2002) and then recognized and studied in Europe as a bioenergy crop from the 1980s (Long, 1987). However, industry-scale production of bioethanol from lignocellulosic crops has been restrained due to high cost of ethanol production from cellulose at the step of cellulose digestion (Campbell *et al.*, 2009; Ohlrogge *et al.*, 2009). Alternatively, electricity generated from biomass combustion, especially through cofiring with coal, has been considered to initiate large-scale bioenergy production, as energy conversion efficiency of electricity generation through lignocellulosic crops is higher than that of ethanol production (Berndes *et al.*, 2010).

M. sinesis, one of the parents of *M.* ×*giganteus*, is a tall, tufted grass distributing in Far East, most part of Japan, the Korean peninsula, and eastern, central, and southern China. It grows on mountain slopes, highland, open grassy place, and wasteland at altitudes below 2500 m (Sun *et al.*, 2010), and the tightly arranged tillers even allows it scatter between rocks. In Japan, the widespread distribution allow *M.*

sinesis plants grow in silty clay or light clay soil with 14-25% soil water content, sandy or well-drained loamy soils, and neutral or acid-sulfate soil with pH ranging from 3.5-7.5 (Stewart *et al.*, 2009). The growth and development patterns of *M. sinesis* also exhibit high variation due to its large distribution from the north temperate zone to the tropics, and this variation is considered to be resource facilitating breeding selection (Clifton-Brown *et al.*, 2008). Aboveground yields of *M. sinesis* also vary by location and year similar to the variation of the growth and development patterns. And the shoot density and height of the plant are considered to be indexes of *M. sinesis* biomass accumulation (Yoshida, 1976; Clifton-Brown, *et al.*, 2001). The regeneration of *M. sinesis* community usually depends upon vegetative growth of rhizomes and roots rather than upon seed propagation, as seed set of *M. sinesis* flowers was low due to several possible factors such as self-incompatibility. However, developing *M. sinesis* to be a bioenergy crop needs additional reseeding due to insufficient amount of seed in the soil and the "fairy-ring" phenomenon (Kobayashi and Yokoi, 2003). The widespread distribution of *M. sinesis* shows a source of genetic diversity for development of new hybrid bioenergy crops, and the capability of *M. sinesis* to easily propagate and produce high-yield in various abiotic stress environments implies less management for establishment or production and well-adaptation to marginal lands as a bioenergy crop itself.

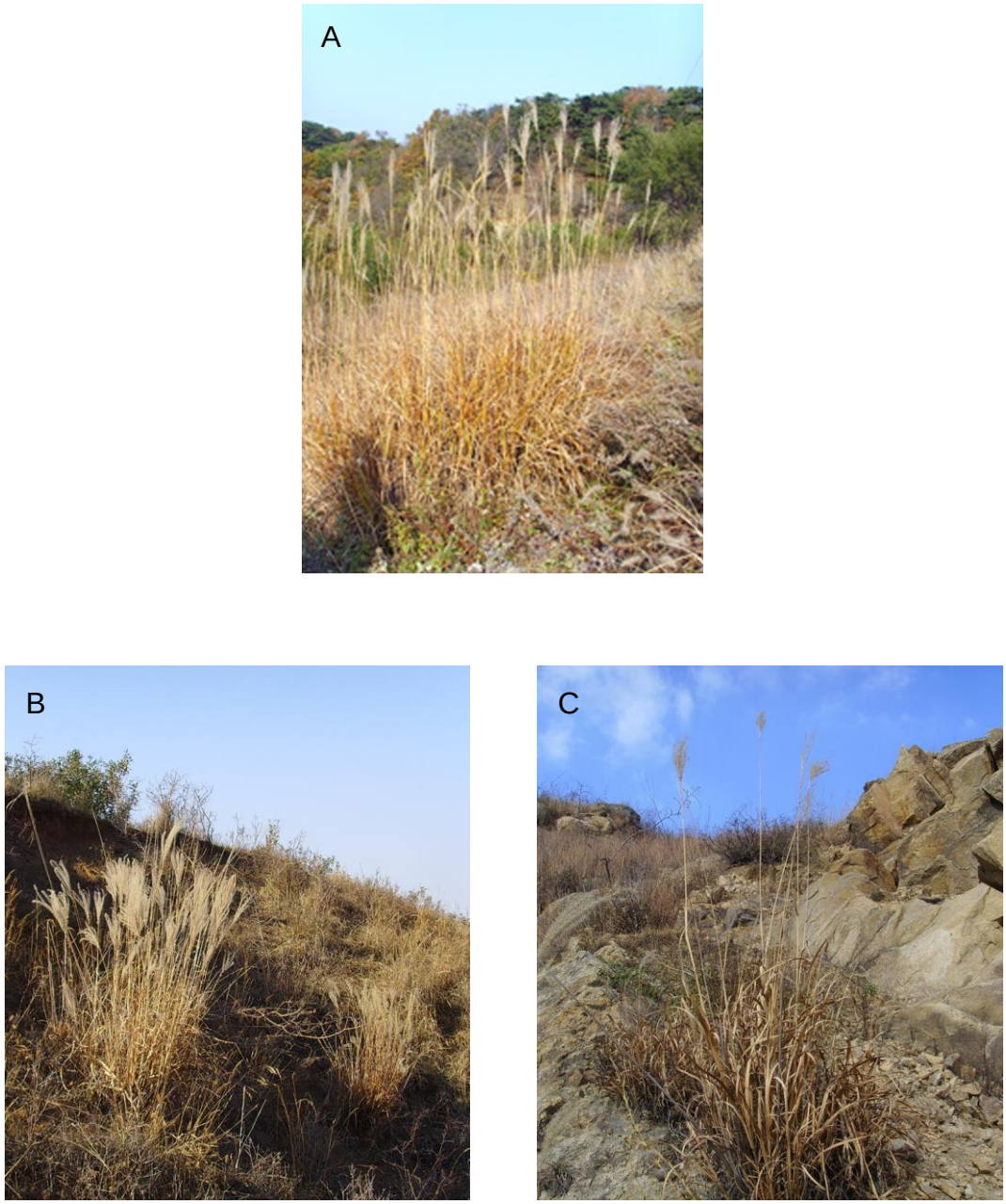

Figure 1-1. *Miscanthus sinensis* plants growing on grassland (a), mountain slope (b), and stony soil (c). This species shows great environmental acclimation.

1.2. Salinity, One of the Most Important Issues in World Agriculture

More than 6% of the world's total land, including 30% of irrigated areas, is salt affected due to natural accumulation of salts from weathering of parental rocks and wind and rain carrying oceanic salts over long periods of time in arid and semiarid regions or due to land clearing and irrigation that lead to rising water tables and concentration of salts in the root zone (Munns and Tester, 2008; Tilbrook and Roy, 2014). Soil salinity which is characterized by a high concentration of soluble salts has become a major limitation to agricultural production. Saline soil defined as ECe $\geq$ 4 dS m^{-1}, which is equivalent to about 40 mM NaCl with an osmotic pressure of nearly 0.2 MPa, would reduce yield of most crops.

Salinity causes both hyperionic and hyperosmotic stresses and finally death of plants (Hasegawa, *et al.*, 2000). Plant responses to salinity occur in two distinct phases, a rapid response to the osmotic stress and a slower response to the ionic stress (Munns and Tester, 2008; Munns, 2010). Cells lose water and shrink when treated with salt stress and the elongation rates in growing tissues are reduced though original turgor and volume of cells can regain over hours, and then leaf and root growth is inhibited resulting in gross changes in vegetative development and reproductive development (Munns, 2010). Salt toxicity affects plants in terms of uptake control of salt by roots, salt transport to leaves, and compartmentalization of the salt within cells. Although plants accumulate salts in the older transpiring leaves, growth of the

younger leaves will be inhibited if toxic concentrations of salts are reached, and leading to death of premature leaves. To cope with effects of salt stress, the mechanisms of salt-tolerance include several categories. Plant response to osmotic stress would result in greater leaf growth and stomatal conductance to overcome reduced cell expansion and stomatal closure (Munns, 2010). Since NaCl is the most widespread soluble salt in the soil to induce salinity, all plants have evolved mechanisms to regulate or exclude NaCl accumulation in favor of nutritional balances. For example, 1) Na^+ exclusion by roots and transport control into leaves ensures less toxic concentrations within leaves; 2) compartmentalization of Na^+ and Cl^- at the cellular and intercellular level avoids toxic concentrations within the cytoplasm of growing tissues; 3) synthesis of compatible osmolytes helps to balance the osmotic pressure of ions in the vacuole (Munns and Tester, 2008; Munns, 2010; Kronzucker and Britto, 2011; Agarwal *et al.*, 2014). Moreover, responses in changes of photosynthetic pathway and membrane structure, induction of antioxidative enzymes, and stimulation of phytohormones were also reported. Based on the physiological studies of plant responses to salinity, new molecular techniques can be utilized to alleviate the impact of salinity stress on plants, and to ameliorate the performance of species to agricultural and environmental sustainability.

1.3. Scope of the Research

To realize the potential of *Miscanthus* to provide a high-yield source of biofuel, and to avoid competition with food production by growing biomass crops in marginal areas, improvement of *M.* ×*giganteus* is needed to overcome its high establishment costs of vegetative propagation from rhizomes or microplants and relatively poor environmental adaptability （Clifton-Brown and Lewandowski, 2000a; Clifton-Brown and Lewandowski, 2000b; Farrell *et al.*, 2006）. As the natural triploid hybrid of *M. sinensis* and *M. sacchariflorus*, *M.* ×*giganteus* is sterile and thus genetic manipulation and improvements of this species are restricted (Zub *et al.*, 2010). Nevertheless, the genetic diversity of other species in this genus (e.g., *M. sinensis*) originating from the sub-tropics to sub-arctic regions in Asia is relatively higher compared with *M.* ×*giganteus*; the self-incompatibility of the fertile, diploid *M. sinensis* can facilitate crossing and genetic studies with the goal of breeding high-yield *Miscanthus* plants. Furthermore, the mineral content (especially Cl, K, N, and S) of *Miscanthus* biomass harvested at the end of the winter could influence the maintenance costs of combustion units, as K and Cl enrichment can cause decreased ash melting point and corrosion issue (Miles *et al.*, 1996; Brosse, *et al.*, 2012). Thus, combustion quality and salt tolerance are linked traits, as ion transporter were essential in both cases.

This study is aim to understand the physiological and biochemical response of *M.*

sinensis to salinity stresses to provide information to the breeders for screening salt-tolerant accessions and developing new energy crops with both high combustion quality and environmental resistance.

CHAPTER 2

Physiological Responses of *Miscanthus sinensis* Accessions to NaCl Stress

2.1. Introduction

Several rapid and effective screening techniques to identify genetic variation in salinity tolerance have been reported (Munns and James, 2003). Seed germination and seedling growth may be considered as possible indicators for determination of tolerance to high salinity (Krishnamurthy, *et al.*, 2007; Zhao *et al.*, 2007; Ezaki *et al.*, 2008). In whole plants, delays in leaf emergence, reduction of leaf expansion and tiller numbers result in decreased shoot growth (Wahid *et al.*, 1997; Netondo *et al.*, 2004a; de Lacerda *et al.*, 2005). Photosynthesis is usually inhibited in plants exposed to salinity (Meinzer *et al.*, 1994; Netondo *et al.*, 2004b; Yan *et al.* 2012). Salt stress decreases photosynthesis through stomatal closure or non-stomatal factors (Heuer, 2005; Chaves *et al.*, 2009). Several factors are related to the non-stomatal events that constrain photosynthesis, including premature loss of chlorophyll (Netondo *et al.*, 2004b; Zhao *et al.*, 2007), damage to the photosynthetic apparatus (Smillie and Nott, 1982; Belkhodja *et al.*, 1994; Netondo *et al.*, 2004b; Jiang *et al.*, 2006; Maricle *et al.*, 2007), and effects on photophosphorylation and CO_2 fixation (Meinzer *et al.*, 1994; Zhu and Meinzer, 1999). Besides osmotic effects, soil salinity can also induce specific

ionic effects on plants that cause toxicity and mineral deficiencies. Because of the complex nature of salinity tolerance and difficulties in maintaining long-term growth experiments, researchers have used K^+/Na^+ discrimination to screen for salt-tolerant germplasm (Yeo and Flowers, 1983; Cramer *et al.*, 1994; Dionisio-Sese and Tobita, 2000; Munns and James, 2003; Netondo *et al.*, 2004a; Zhao *et al.*, 2007; Praxedes *et al.*, 2010).

Grare (2010) discussed the variability of salinity tolerance in two genotypes of *M. sinensis* using whole-plant fresh weight, tiller number, mineral content of shoots, and chlorophyll fluorescence. The genotype MS88-110 had higher fresh weight but showed greater increases in Na^+ and Cl^- concentrations in the shoots, while MS90-2 showed a lower number of photosystem-II (PSII) photosynthetic centers but higher photosynthetic efficiency. Grare (2010) proposed that *in-vitro* propagation and chlorophyll fluorescence can be effectively used to screen for salt tolerance, and that higher anthocyanin content in MS90-2 was a mechanism for protection of the photosynthetic apparatus. To date, aside from the research by Grare (2010), previous stress-tolerance studies about *M. sinensis* mainly focused on chilling, drought, low pH, and heavy metals (Stewart *et al.* 2009; Zub *et al.*, 2010), with few reports related to salinity-response mechanisms. Therefore, it remains unclear which morphological and physiological parameters in *M. sinensis* (e.g., dry mass, relative growth rate [RGR], photosynthesis) will show genotypic variability in response to salinity, and which physiological factors will be responsible for these differences. In this paper,

we examined the effects of salt levels and stress duration on seedling growth, photosynthesis, and ion accumulation using two *M. sinensis* accessions (JM0119 and JM0099) with contrasting tolerance to salt stress. We further discussed some of the physiological mechanisms underlying these accessions' responses to salt stress, to facilitate the selection and breeding of more salt-tolerant *M. sinensis* genotypes.

2.2. Materials and Methods

2.2.1. Germination Experiments

Seventeen accessions of *M. sinensis* collected in Japan and maintained at Hokkaido University (Table 2-1, Fig. 2-1) were subjected to six salt (NaCl) concentrations: 0 (control), 30, 60, 120, 240, and 360 mM, in a completely randomized design with four replications per treatment. All the seeds used for the experiment were obtained from naturally pollinated plants (plants from different accessions were isolated by keeping an appropriate distance). Treatment solutions were prepared with calcium chloride ($CaCl_2$) at 5:1 (NaCl:$CaCl_2$) molar concentration. Seeds (n = 25) of each accession were surface-sterilized with 70% ethanol for 30 s and with 1% (v/v) sodium hypochlorite (NaClO) for 10 min, rinsed three times with distilled water. Seeds were germinated on filter paper in a closed 90-mm Petri dish filled with 25 ml treatment solution in a growth chamber at 28/22 ℃ day/night temperature with 12-h day length, and a light intensity of 300 μmol m^{-2} s^{-1}. Seeds were

considered germinated by emergence of 2 mm-length radicle. The number of germinated seeds was counted daily for 15 days. Shoot and root lengths of each seedling were measured on the 15th day and used to calculate the shoot-to-root ratio. Coefficient of velocity of germination was calculated as $CVG = \left(\sum_{i=1}^{k} f_i \Big/ \sum_{i=1}^{k} f_i x_i \right) \times 100$ (Ranal and Santana, 2006), where f_i is the number of newly germinated seeds on day i, x_i is the number of days from sowing, and k is the last day of germination.

2.2.2. Growth Experiments

Accessions JM0119 and JM0099 were selected based on the results of the germination tests and used in a greenhouse study. Experiments were conducted from February 25th to May 14th, 2012 and repeated from July 23rd to October 5th 2012 in a glasshouse with 25/20 ℃ day/night temperatures, 16 h light, and 70% relative humidity. Five seeds were sown in a 2-l pot filled with mixed peat moss (PRO-MIX PGX; Grower's Nursery Supply, Inc.; Salem, USA) and plants were thinned to three when the seedlings had three fully expanded leaves approximately one month after sowing. Pots were irrigated with tap water until 7 d after the thinning, followed by an additional 7 d irrigation with 0.1% (w/v) salt-free 20:20:20 (N:P:K) commercial fertilizer (Peter's Professional; The Scotts Co.; Marysville, USA). At 14 d after the thinning, 200-ml fertilizer solutions containing 0, 30, 60, 120, 240, and 360 mM

Table 2-1. Origin of 17 accessions of *Miscanthus sinensis*.

No.	Accession	Collecting site	Latitude (ºN)	Longtitude (ºE)
1	JM0015	Fukagawa	43.7	142.1
2	JM0048	Kamui	43.3	140.4
3	JM0050	Iwanai	42.9	140.6
4	JM0051	Niseko	42.8	140.7
5	JM0055	Oshamanbe	42.4	140.3
6	JM0059	Toya	42.6	140.8
7	JM0061	Makkari	42.8	140.8
8	JM0062	Hakodate	41.7	141.0
9	JM0073	Esashi	41.9	140.1
10	JM0075	Onuma	42.0	140.7
11	JM0079	Iozan	43.6	144.4
12	JM0080	Bihoro	43.7	144.2
13	JM0096	Kobuchizawa	35.9	138.4
14	JM0099	Nagasaka	35.6	138.6
15	JM0118	Shiozuka	33.6	133.4
16	JM0119	Kochi	33.6	133.4
17	JM0134	Takachiho	32.4	131.2

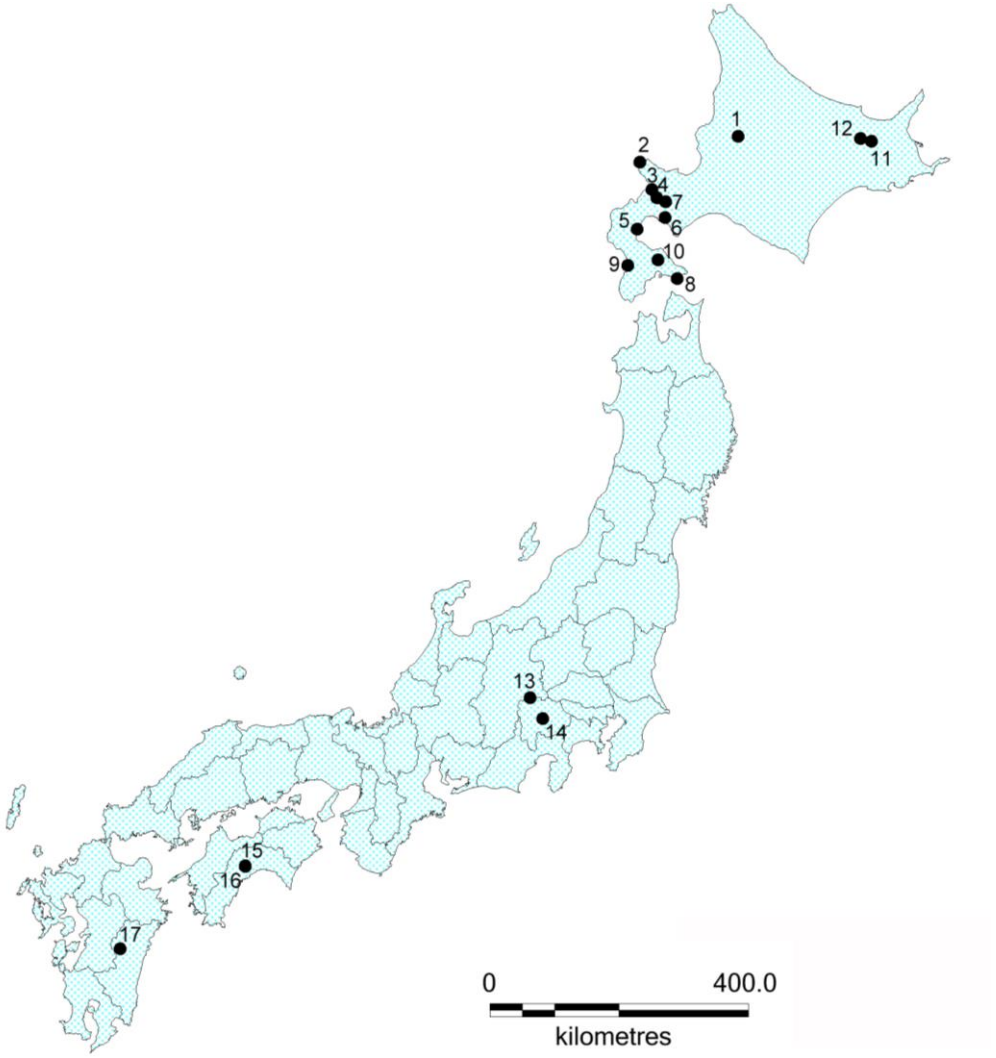

Figure 2-1. Origin locations of 17 accessions of *Miscanthus sinensis* used in the present study. Number one to 17 are JM0015, JM0048, JM0050, JM0051, JM0055, JM0059, JM0061, JM0062, JM0073, JM0075, JM0079, JM0080, JM0096, JM0099, JM0118, JM0119, JM0134.

NaCl (NaCl:$CaCl_2$ = 5:1 molar concentration) were applied daily for each pot. To avoid osmotic shock, salt addition gradually increased at a progressive rate of 60 mM per day until the final treatment levels. Pots were moved randomly to alleviate the effects of variable conditions inside the glasshouse. The experiment ran for 30 days, with the peat moss salinity of 1.0, 3.2, 6.1, 10.5, 23.6, and 27.0 dS m^{-1}, respectively, on day 30 at each treatment. On the day before salt addition (day 0), and on days 6, 14, 22, and 30, plants were harvested and cleaned thoroughly with tap water. The pots were arranged in a completely randomized design with four replications of each treatment for a total of 240 pots (5 harvest dates × 6 salt treatments × 2 accessions × 4 replications).

2.2.2.1. Growth and Leaf Chlorophyll Measurements

On each harvest date, plants were separated into shoots and roots. Dry weights of tissues were determined after tissues were dried at 70 ℃ for 72 h. The relative growth rate (RGR) was calculated according to Kingsbury *et al.* (1984) as $RGR = \frac{(\ln w_2 - \ln w_1)}{(t_2 - t_1)}$, where w_1 and w_2 stand for dry weights (mg) of shoots at times t_1 and t_2 (in days), respectively. On day 30, the number of tillers were recorded, and leaf area was measured with a LI-3000 Leaf Area Meter (LI-COR, Inc.; Lincoln, USA). Leaf chlorophyll was measured using a chlorophyll meter (SPAD-502 Chlorophyll Meter; Konica Minolta, Inc.; Tokyo, Japan) and expressed as the

average of three readings from the base, middle, and tip of the topmost fully expanded leaf blade on days 6, 14, 22, and 30.

2.2.2.2. Gas Exchange and Chlorophyll *a* Fluorescence

Photosynthetic rate (A) and stomatal conductance (g_s) were measured on the topmost fully expanded leaf of each plant in each pot on Day 30, using an infrared, open gas exchange system (LI-6400; LI-COR, Inc.; Lincoln, USA) with a 6400-02B red/blue LED light source at 1000 μmol m^{-2} s^{-1} photosynthetic photon flux density (PPFD) and 400 ppm CO_2 concentration. The area of each leaf in the leaf chamber was determined manually. Chlorophyll *a* fluorescence parameters were also measured on the same leaves before the gas exchange measurement at 6:00 in the early morning in the dark-adapted (30-min) state, followed by a measurement in the 5-min actinic illuminated light-adapted state, using a MINI-PAM (Walz; Effeltrich, Germany) at 650-nm pulse-modulated measuring light (0.15 μmol m^{-2} s^{-1} PAR) for minimal fluorescence (F_o), 800-ms saturating pulse (5000 μmol m^{-2} s^{-1} PAR) for maximal fluorescence of dark-adapted leaves (F_m) and maximal fluorescence of light-adapted leaves (F'_m), and actinic light supplied by light-emitting diodes for steady-state yield of fluorescence (F_t). The maximum efficiency of PSII photochemistry (F_v/F_m) was calculated as (F_m - F_o)/F_m, and the efficiency of energy capture by open reaction centers of PSII for light-adapted leaves ($\Delta F/F'_m$) was

calculated as $(F'_m - F_t)/F'_m$ (Maxwell and Johnson, 2000; Baker, 2008).

2.2.2.3. Tissue Ion Concentration

At the end of the experiment (Day 30), ions were extracted from fine powder of oven-dried plant shoot samples following the procedures described by Munns *et al.* (2010). The Na^+, K^+, and Cl^- concentration were determined by flame atomic absorption spectrometry (Z-6100; Hitachi, Ltd.; Tokyo, Japan), according to the analytical methods of flame atomic absorption spectrometry (Agilent Technologies, Inc.; Santa Clara, USA).

2.2.3. Data Analysis

All data was analyzed by Statistical Product and Service Solutions (SPSS Statistics, Version 20; IBM Corp.; New York, USA). Differences in morphological and physiological traits among accessions and salt treatments were tested by analysis of variance using the general linear model procedures. The least significant difference ($LSD_{0.05}$) test was used to separate treatment means. The significance of the differences between accession means in each treatment group was determined by a t-test. The half maximal effective concentration (EC_{50}) value for germination was calculated using the probit regression. A logistic regression was used to determine the effects of accessions and salt treatments on the germination percentage.

Table 2-2. Effects of salt stress on final germination percentage of *Miscanthus sinensis* accessions.

Accession	NaCl Concentration (mM)						EC_{50}
	0	30	60	120	240	360	(mM)
JM0015	93 bcd	96 a	96 ab	88 cd	74 c	29 a	308.4
JM0048	93 bcd	94 bcd	88 bcd	71 ef	38 e	11 cde	190.3
JM0050	96 abcd	91 bcd	90 abcd	91 bcd	82 abc	16 cd	294.8
JM0051	93 bcd	91 cde	92 abcd	89 cd	73 c	18 bc	288.5
JM0055	97 abc	93 bcd	92 abcd	92 bcd	75 c	10 cde	272.6
JM0059	84 e	71 f	72 e	75 de	33 e	0 f	215.1
JM0061	84 e	78 f	80 de	53 g	39 e	3 ef	187.2
JM0062	100 a	98 ab	95 abc	94 bc	36 e	0 f	205.2
JM0073	93 cde	79 ef	84 de	71 ef	38 e	0 f	234.2
JM0075	94 bcd	94 abcd	93 abcd	83 d	56 d	5 ef	254.9
JM0079	89 de	86 de	86 cde	85 d	78 bc	15 cd	294.6
JM0080	95 bcd	91 cde	92 abcd	86 cd	86 ab	8 def	287.9
JM0096	80 e	83 def	73 e	76 de	57 d	0 f	244.5
JM0099	89 cde	77 f	81 de	58 fg	9 g	0 f	151.6
JM0118	99 ab	99 a	98 a	99 a	89 a	9 ed	284.4
JM0119	94 bcd	95 bcd	95 abc	96 ab	80 bc	26 ab	306.8
JM0134	88 ed	80 ef	83 de	76 de	18 f	0 f	184.9

Means sharing the same letter within a column are not significantly different ($LSD_{0.05}$ test). EC_{50}, half maximal effective concentration of NaCl.

Table 2-3. Deviance table of logistic regression for the germination percentage in relation to accessions and salt treatments and mean squares of two-way analysis of variance on coefficient of velocity of germination (CVG), shoot length (SL), and root length (RL).

Parameters	Germination percentage			CVG (%)	SL (mm)	RL (mm)
	df	Wals	P			
Accession (A)	16	83.84	<0.0001	2.48**	2.31**	5.57**
Salinity (S)	5	110.31	<0.0001	54.38**	48.58**	40.22**
A × S	456.156	80	<0.0001	0.25**	0.34**	0.76**
Error				0.037	0.045	0.038

Level of significance: * P ≤ 0.05; ** P ≤ 0.01; absence of an asterisk denotes a non-significant effect.

2.3. Results

2.3.1. Germination Experiments

High salt concentration inhibited seed germination in all tested accessions, with significantly different responses among accessions (Table 2-2 and 2-3). In the 360 mM salt treatment, germination of JM0059, JM0062, JM0073, JM0096, JM0099, and JM0134 was completely inhibited, while germination of JM0015 and JM0119 were maintained at 31% ±6 and 28% ±12, respectively, of that of the control. The values of EC_{50} indicated the resistant limits of accessions to NaCl stress. Seeds of JM0015 and JM0119 showed much greater salt tolerance than that of JM0099 according to the EC_{50} values. Salinity stress also greatly affected the germination process and seeding growth, with significant differences among accessions (Table 2-3). The velocity of germination was slowed with the increase of NaCl concentration (Fig. 2-2a), suggesting that more days were required to reach a germination peak under salt stress. Decreases of the shoot and root length of seedlings with the increase of NaCl concentration were also observed (Fig. 2-2b and c). Significant effect of salinity ($P < 0.001$) was also observed in the shoot-to-root-length ratio, with each accession showing different patterns in the variation of shoot-to-root-length ratio under salt stress (data not shown).

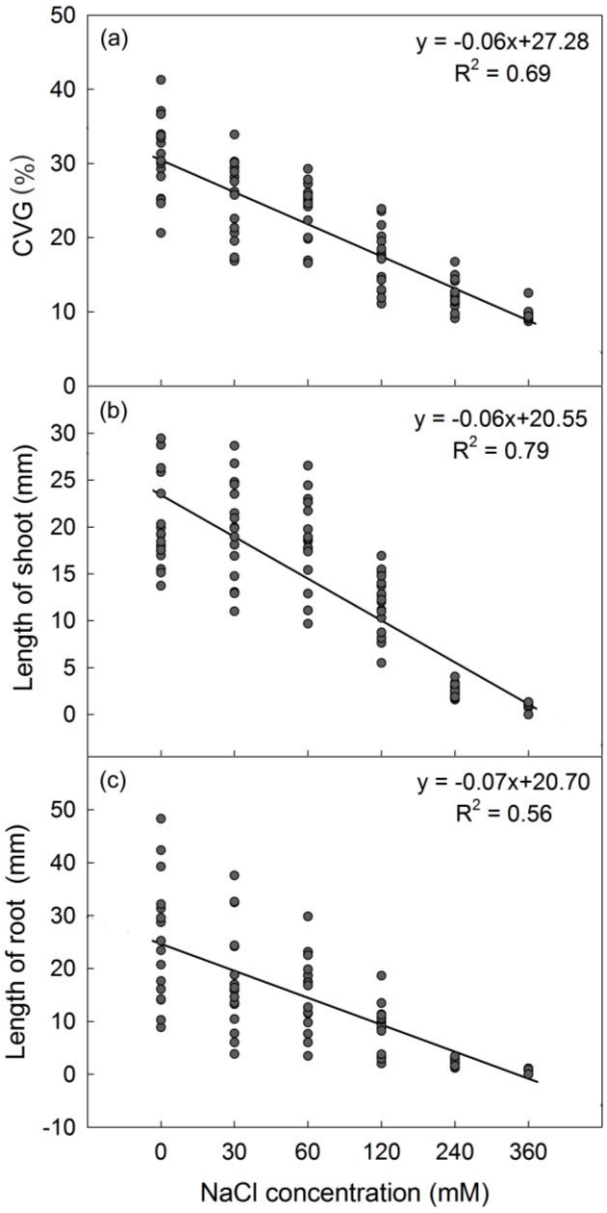

Figure 2-2. Relationship of salt treatment with (a) coefficient of velocity of germination, CVG; (b) shoot length; and (c) root length in 17 *Miscanthus sinensis* accessions.

2.3.2. Growth Experiments

Based on the results of the germination test, accessions JM0119 (salt-tolerant) and JM0099 (salt-sensitive) were selected for the greenhouse study. Effects of accession and salt treatments on most parameters measured in the second run of the experiment followed the same pattern as those in the first run. Therefore, the following discussion is concentrated on the results from the first run of the experiment.

2.3.2.1. Plant Growth

Salt stress led to decreases in RGR. The main effect of salt treatment was significant ($P < 0.01$) from day 6 in the first run, and one week later in the second run (Table 2-4). As indicated by non-significant values for effect of accession, this effect was independent of accession until day 22 in the first run and day 30 in the second run (Table 2-4). The differences in RGR among salt treatments became more significant with prolonged stress (Fig. 2-3). Although the RGR was reduced more under salt stress for JM0099 than for JM0119 from day 14 onward in both runs of the experiment, significant differences ($P < 0.05$) between the two accessions were observed on day 22 in the first run (Fig. 2-3), and on day 30 in the second run.

Significant accession and salt-stress effects ($P < 0.001$) were observed in total leaf area, number of tillers per plant, and shoot dry weight of *M. sinensis*. Accession ×

salinity interactions were only observed in the total leaf area in the second run of the experiment (Table 2-4). Total leaf area was reduced in all salinity treatments and, on day 30, was reduced by 72% ±2.6 and 83% ±2.7, respectively, in JM0119 and JM0099 at 360 mM compared to the control (Fig. 2-4a). Differences in total leaf area between the two accessions increased in treatments with 60 mM or greater NaCl. With 360 mM salt, total leaf area of JM0099 was 42% ±6.1 less than that of JM0119. A large reduction ($P < 0.01$) in number of tillers per plant was not observed until the salinity level reached 120 mM (Fig. 2-4b). At 360 mM salinity, the number of tillers decreased by 56% ±7.7 and 63% ±6.4 relative to the control for JM0119 and JM0099, respectively. The length of tillers was also shortened greatly ($P < 0.01$) by high salt stress, but some tillers were more elongated at low concentrations of NaCl than at control conditions (data not shown). Shoot dry weight was also reduced by all salinity levels. Large decreases ($P < 0.001$) in shoot dry weight were observed under 60 mM and higher salinity on day 30, with a relative decrease of 64% ±5.2 for JM0119, and 78% ±3.1 for JM0099 at 360 mM NaCl compared to the control (Fig. 2-4c). Significant differences ($P < 0.05$) in plant shoot dry weight between the two accessions occurred at salinity levels above 120 mM NaCl concentration. The dry weight of JM0099 shoots was 13% ±9.0, 24% ±7.6, and 36% ±13.4 less than that of JM0119 at 120, 240, and 360 mM salt stress, respectively.

Table 2-4. Analysis of variance (mean square) of the effects of accession and salinity on growth traits, photosynthesis parameters, and ion accumulation for two experimental runs.

Source	First Run				Second Run			
	Accession (A)	Salinity (S)	A × S	Error	Accession (A)	Salinity (S)	A × S	Error
$RGR_{Day\ 6}$	0.49	3.36**	0.09	0.81	0.00	0.86	0.12	1.17
$RGR_{Day\ 14}$	0.01	6.1**	0.63	0.37	1.44	5.31**	0.57	0.45
$RGR_{Day\ 22}$	5.73**	6.96**	0.18	0.15	1.19	6.09**	0.40	0.37
$RGR_{Day\ 30}$	0.67	7.38**	0.15	0.24	6.05**	7.20**	0.19	0.11
$SPAD_{Day\ 6}$	0.99	0.92	0.88	1.03	6.42**	1.36	1.37	0.75
$SPAD_{Day\ 14}$	1.76	6.91**	0.12	0.28	2.40**	6.75**	0.76**	0.20
$SPAD_{Day\ 22}$	0.51	8.96**	0.01	0.05	3.69**	7.83**	0.28*	0.08
$SPAD_{Day\ 30}$	1.29**	8.86**	0.18**	0.01	2.24**	8.56**	0.16**	0.03
TLA	1.68**	8.31**	0.05	0.10	3.26**	7.89**	0.13	0.10
TN	1.52**	8.49**	0.10	0.07	1.26**	8.37**	0.06	0.10
PSDW	1.08**	8.65**	0.08	0.06	3.38**	8.19**	0.02	0.07
A	0.49**	9.15**	0.06**	0.01	0.64**	9.05**	0.08**	0.02
g_s	0.09	8.9**	0.25**	0.03	0.13*	8.75**	0.44**	0.03
$\Delta F/F'_m$	2.2**	8.08**	0.44**	0.06	1.80**	7.20**	0.60*	0.17
Na^+	3.12**	7.9**	0.75**	0.02	1.80**	7.64**	0.79**	0.09
K^+	1.23*	7.0**	0.56*	0.22	1.14**	8.39**	0.25*	0.07
Cl^-	0.18*	9.0**	0.11*	0.04	0.23	8.68**	0.23**	0.06

RGR, relative growth rate; SPAD, leaf chlorophyll content; TLA, total leaf area; TN, number of tillers; PSDW, plant shoot dry weight; *A*, photosynthetic rate; g_s, stomatal conductance; $\Delta F/F'_m$, PSII operating efficiency.

Level of significance: * P ≤ 0.05; ** P ≤ 0.01; absence of an asterisk denotes a non-significant effect.

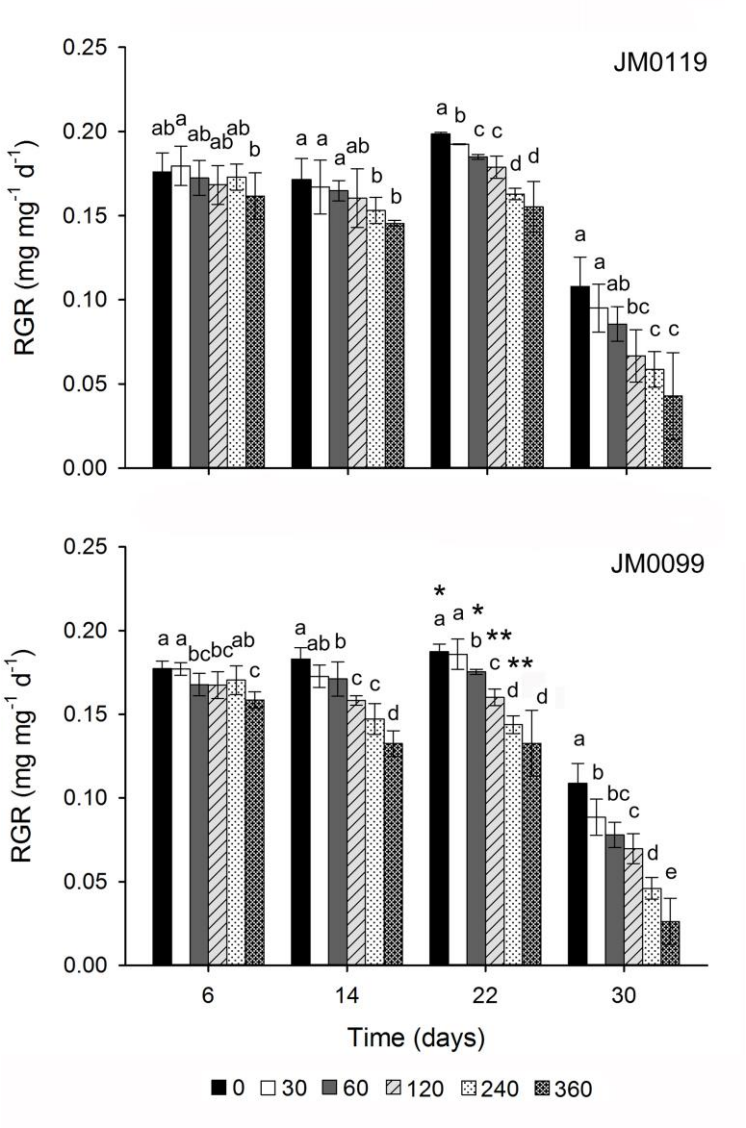

Figure 2-3. Time-course changes in the relative growth rate (RGR) of shoots to increasing NaCl concentration for two *Miscanthus sinensis* accessions. Values are means ± SE of four replicates. Different letters indicate significant differences within each sampling date ($LSD_{0.05}$ test). Asterisks indicate significant differences between accessions for each treatment, * $P \leq 0.05$, ** $P \leq 0.01$, absence of an asterisk denotes a non-significant effect.

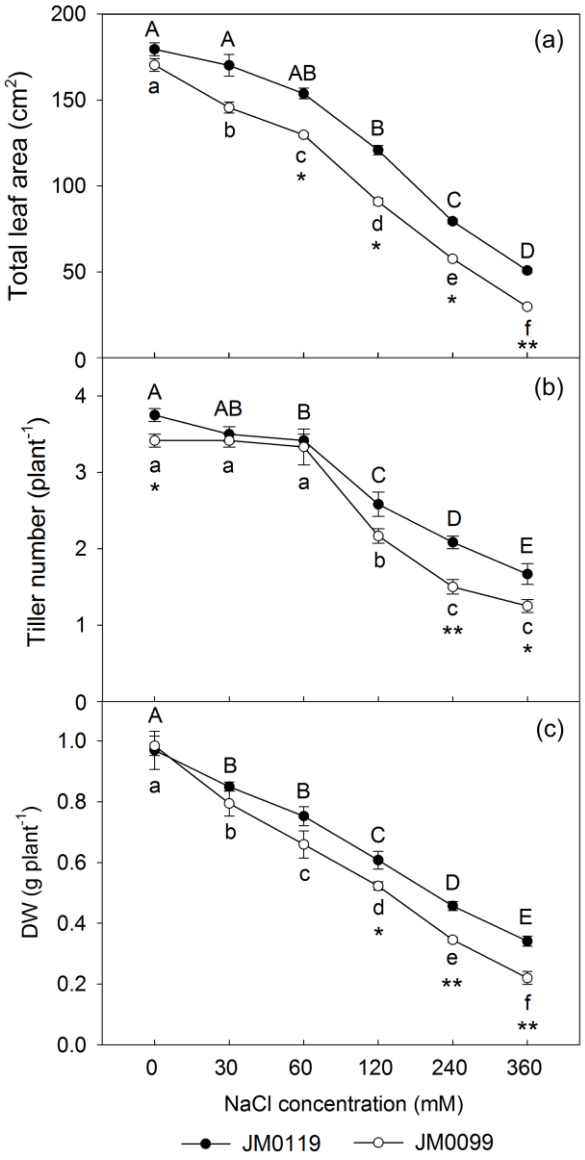

Figure 2-4. Effects of salinity on total leaf area (a), tiller number (b), and plant shoot dry weight (c) of two *Miscanthus sinensis* accessions at day 30 of the experiment. Values are means ± SE of four replicates. Different letters indicate significant differences between salt treatments for each accession ($LSD_{0.05}$ test). Asterisks indicate significant differences between accessions for each treatment, * P ≤ 0.05, ** P ≤ 0.01, absence of an asterisk denotes a non-significant effect.

2.3.2.2. Chlorophyll Content

Leaf chlorophyll content of the two tested accessions was reduced greatly ($P < 0.001$) by high salt levels on all sampling dates after day 14 (Table 2-4, Fig. 2-5). The interaction between accession and salinity also had a significant effect ($P < 0.05$) on leaf chlorophyll content on day 30 in the first run and from day 14 to day 30 in the second run (Table 2-4). Salt-induced marked differences ($P < 0.001$) between the two accessions occurred at the 240 and 360 mM salt levels on day 30 in the first run and at the 120 mM and higher salt levels from day 22 in the second run. Compared with the control, leaf chlorophyll content of the 360 mM NaCl treated seedlings decreased by 39% ±3.2 for JM0119 and by 53% ±1.1 for JM0099 on day 30 (Fig. 2-5).

2.3.2.3. Photosynthetic Responses

Remarkable variation ($P < 0.001$) between accessions and salt treatments was detected, including notable interactions ($P < 0.01$) between these variables in relation to *A* (Table 2-4). Photosynthetic rate declined significantly ($P < 0.01$) relative to the control in all salt treatments (Fig. 2-6a). Significant differences ($P < 0.05$) in *A* were observed between the two accessions at the salinity levels 120, 240, and 360 mM NaCl, with decreases of 35% ±4.5, 61% ±2.7, and 79% ±1.7, respectively, for JM0119 and 47% ±7.4, 72% ±4.4, and 89% ±1.8, respectively, for JM0099, relative to the control, on day 30. Concurrently, salt stress strongly reduced ($P < 0.001$) the g_s of both

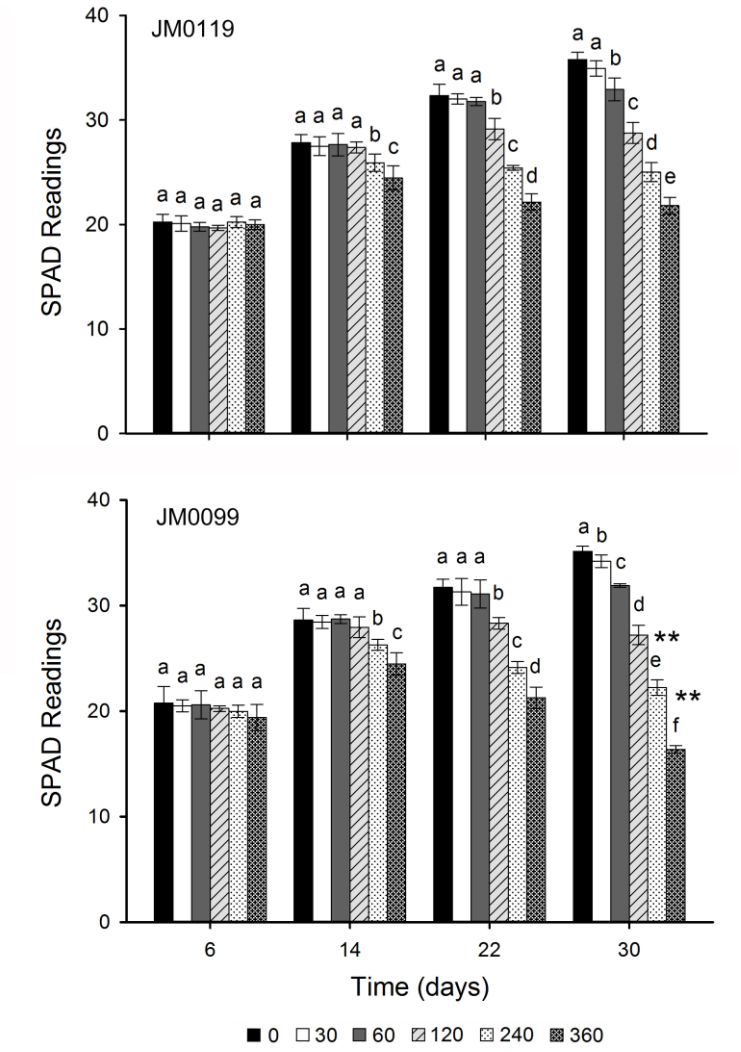

Figure 2-5. Time-course changes in leaf chlorophyll content of two *Miscanthus sinensis* accessions to increasing NaCl concentration. Values are means ± SE of four replicates. Different letters indicate significant differences within each sampling date ($LSD_{0.05}$ test). Asterisks indicate significant differences between accessions for each treatment, * P ≤ 0.05, ** P ≤ 0.01, absence of an asterisk denotes a non-significant effect.

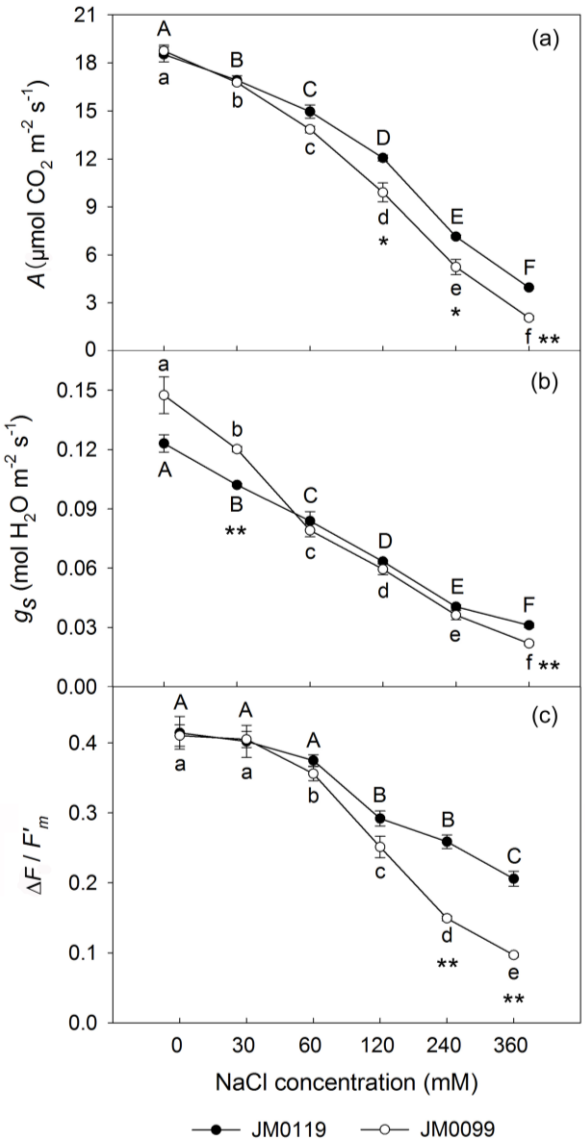

Figure 2-6. Effects of salinity on (a) photosynthetic rate, *A*; (b) stomatal conductance, g_s; and (c) the efficiency of light harvesting of PSII, $\Delta F/F'_m$ of two *Miscanthus sinensis* accessions at day 30 of the experiment. Values are means ± SE of four replicates. Different letters indicate significant differences between salt treatments for each accession ($LSD_{0.05}$ test). Asterisks indicate significant differences between accessions for each treatment, * P ≤ 0.05, ** P ≤ 0.01, absence of an asterisk denotes a non-significant effect.

accessions (Fig. 2-6b). The g_s of JM0099 declined more than that of JM0119, although there was no significant accession effect on g_s in the first run (Table 2-4). At 360 mM salt level on day 30, stomatal conductance decreased by 75% ±0.6 and 85% ±3.3, respectively, in JM0119 and JM0099 relative to the control.

The efficiency of light harvesting of PSII (ϕ_{PSII}), as measured by $\Delta F/F'_m$, was significantly influenced (P <0.001) by accessions and salt levels, and significant interactions (P <0.001) were detected between these two factors (Table 2-4). The notable reduction (P <0.01) in $\Delta F/F'_m$ induced by salt stress was not detected for salt concentrations below 60 mM NaCl for JM0099 and 120 mM NaCl for JM0119 (Fig. 2-6c). Significant differences (P <0.001) between the two accessions were observed at 240 and 360 mM salt concentrations, with 38% ±12.4 and 50% ±2.3 reductions, respectively, in JM0119 and 64% ±3.3 and 76% ±0.8, respectively, in JM0099 relative to the control (Fig. 2-6c).

2.3.2.4. Ion Accumulation

Concentrations of Na^+ and Cl^- in shoot tissue significantly increased (P <0.001) in all salt treatments (Table 2-4, Fig. 2-7a and c), with sharp rises observed in the 240 and 360 mM salinity treatments on day 30. Significant differences (P <0.05) in Na^+ concentration between the two accessions were observed at all salt levels, while Cl^- concentration varied significantly only in the 360 mM salt treatment. Under 360 mM

salt stress, the increase in Na^+ concentration was 94% ±27.4 greater for JM0099 than that for JM0119, and chloride concentration also exhibited an increase of 17% ±14.4 more for JM0099.

Shoot K^+ concentration was also significantly affected by salinity ($P < 0.001$) (Table 2-4), displaying notable decreases at salt concentrations of 120 mM or higher (Fig. 2-7b), while a notable decrease was observed even at 30 mM NaCl in the second run (data not shown). Remarkable differences ($P < 0.05$) between the two accessions were not observed except in the 360 mM salt treatment, with reductions of 34% ±12.8 and 54% ±14.4, respectively, for JM0119 and JM0099 relative to the control. Moreover, the increased Na^+ concentration and decreased K^+ concentration resulted in a severe reduction in the K^+/Na^+ ratio for both accessions.

2.4. Discussion and Conclusion

We screened 17 accessions of *M. sinensis* for salinity tolerance using a seed germination test, and further investigated the responses of two *M. sinensis* accessions, JM0119 and JM0099, to various salt levels over time. JM0119 was more salt tolerant than JM0099 as reflected in a greater germination percentage and greater dry biomass under salt-stress conditions.

Propagation of new *Miscanthus* plants by seed is more cost- and time-effective than by *in vitro* culture or rhizome division. High seed set and germination potential are important to ensure efficient propagation, and these parameters are affected by the

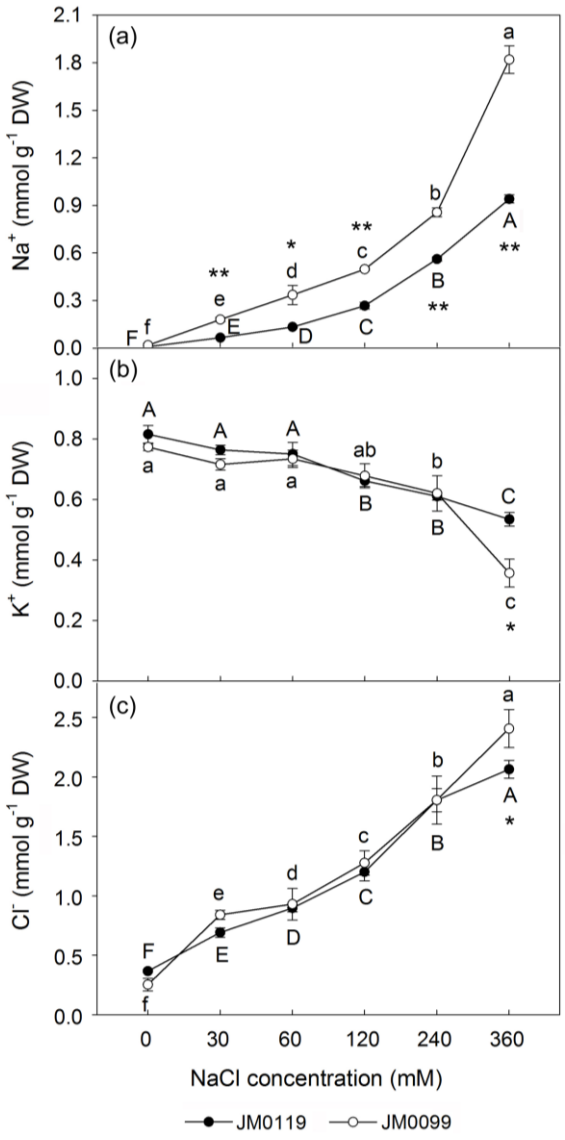

Figure 2-7. Effects of salinity on shoot Na^+ (a), K^+ (b), and Cl^- (c) content of two *Miscanthus sinensis* accessions at day 30 of the experiment. Values are means ± SE of four replicates. Different letters indicate significant differences between salt treatments for each accession ($LSD_{0.05}$ test). Asterisks indicate significant differences between accessions for each treatment, * P ≤ 0.05, ** P ≤ 0.01, absence of an asterisk denotes a non-significant effect.

genotype and the environmental conditions under which plants are grown. We determined that both germination percentage and germination velocity of *M. sinensis* seeds decreased with increasing NaCl concentration, and that germination percentage varied significantly between accessions. These findings are consistent with the results of experiments on germination of some native *Miscanthus* species under salt stress (Hsu, 1990). The salt-resistant limit in germination (germination frequency <50%) was 340 mM NaCl for the seeds of *Miscanthus* spp. (Hsu, 1990; Ezaki *et al.*, 2008), indicating that *Miscanthus* spp. has high salt-tolerance in comparison with other wild species except for halophytes (Ezaki *et al.*, 2008). The accessions tested in the present study showed salt-resistant limits (EC_{50}) from 152 to 309 mM NaCl. This salt-induced variability of seed germination among accessions indicated that seed germination could be considered as a direct salt-tolerance selection criterion for *M. sinensis*. Moreover, Hsu (1990) demonstrated that seeds collected from the littoral displayed higher germination capacity than those from inland sites, and that a higher germination percentage was observed at lower altitudes.

Plant RGR was affected greatly by salt concentration and stress duration, but the reduction in RGR for the salt-tolerant variety (JM0119) was less than that of the salt-intolerant variety (JM0099). The decreased rate of shoot growth could be attributed to a reduction in total leaf area and number of tillers (Table 2-5). It is said that growth rate is specifically related to net assimilation rate and leaf mass fraction (Praxedes *et al.*, 2010). The great reduction in total leaf area may be due to reduced

Table 2-5. Correlation coefficients between the plant shoot dry weight (Day 30) and the growth and photosynthetic parameters and ion contents in salt-treated plants of two accessions.

Traits	Plant shoot dry weight			
	First Run		Second Run	
	JM0119	JM0099	JM0119	JM0099
$SPAD_{Day30}$	0.96**	0.96**	0.94**	0.96**
TLA	0.92**	0.95**	0.90**	0.97**
TN	0.95**	0.88**	0.90**	0.93**
A	0.97**	0.96**	0.94**	0.97**
g_s	0.97**	0.93**	0.93**	0.95**
$\Delta F/F'_m$	0.93**	0.95**	0.82**	0.93**
Na^+	-0.94**	-0.89**	-0.86**	-0.81**
K^+	0.87**	0.73**	0.89**	0.93**
Cl^-	-0.97**	-0.93**	-0.91**	-0.85**

SPAD, leaf chlorophyll content; TLA, total leaf area; TN, number of tillers; *A*, photosynthetic rate; g_s, stomatal conductance; $\Delta F/F'_m$, PSII operating efficiency.

Level of significance: * P ≤ 0.05; ** P ≤ 0.01.

rate of leaf-expansion, delayed or inhibited emergence of leaves and lateral buds, and ion-specific toxicity in older leaves (Munns and Tester, 2008). Leaf rolling occurred in both accessions at the 240 and 360 mM salt levels. This trait could reduce surface area and conserve moisture, and is also related to drought tolerance (Wahid *et al.*, 1997; Clifton-Brown *et al.*, 2002). Over weeks of salinity treatment, salts accumulate in transpiring leaves to excessive levels at which the ability of the cells to compartmentalize salts into the vacuole can be exceeded. Salts then rapidly build up in the cytoplasm and inhibit enzyme activity, and eventually cause marked injury or premature senescence of leaves (Munns, 2010). The effect of salt stress on meristematic tissues results in fewer branches or tillers. Abundant tillers in tolerant genotypes may have a dilution effect by which the salt load is shared with the primary tiller (Wahid *et al.*, 1997). Carbohydrate supply was reported to influence lateral bud development in wheat plants grown in saline soil, as elevated CO_2 increased the number of tillers and reversed the effect of salinity (Nicolas *et al.*, 1993). However, signaling pathways regulate growth rate to maintain a positive carbon balance between source and sink, as the carbohydrate status of growing tissues was not reduced by salinity (Nicolas *et al.*, 1993).

Although Murillo-Amadot *et al.* (2002) found that the chlorophyll content of salt-tolerant cowpea genotypes increased under salt stress, the chlorophyll content of *M. sinensis* decreased with increasing NaCl concentration and stress duration in the present study. This effect may due to inhibition of chlorophyll synthesis or

acceleration of its degradation as a result of salinity (Netondo *et al.*, 2004b; Zhao *et al.*, 2007). We considered the non-destructive measurement of chlorophyll content with the SPAD meter to be an adequate surrogate for measuring extremes in percent dead leaf, as a negative correlation between dead leaf ratio and chlorophyll content was observed in wheat (Munns and James, 2003).

The observed decrease in *A* indicates that photosynthesis in *M. sinensis* was negatively affected by salt stress. The concomitant decrease in g_s in plant leaves implies that the decline in photosynthesis may be attributed primarily to stomatal limitation as observed by Netondo *et al.*, (2004b), Jiang *et al.* (2006), Zhao *et al.* (2007), and Yan *et al.* (2012). The g_s reduction may result from salt-induced perturbation of water status and local synthesis of abscisic acid in stomatal guard cells (Munns and Tester, 2008). However, the salt-induced decline in photosynthesis was reported to be unrelated to stomatal limitations in cowpea leaves (Praxedes *et al.*, 2010). Photosynthetic responses were also related to salt-caused restriction on plant growth (Table 2-5). However, it is difficult to untangle the cause-effect relationships between photosynthesis and growth rate, although a reduced rate of photosynthesis was reported previously to be one of the factors responsible for growth reduction (Heuer, 2005; Zhao *et al.*, 2007). Accumulated unused photosynthate resulting from reduced leaf expansion may induce feedback signals that down-regulate photosynthesis in growing tissues to match the reduced demand arising from growth inhibition (Munns and Tester, 2008). Compared with g_s, the decline in $\Delta F/F'_m$ was

minimal when plants were exposed to low NaCl concentrations. A significant decrease in $\Delta F/F'_m$ occurred at salt concentrations higher than 120 mM, which is consistent with the results reported by Jiang *et al.*, (2006) and Zhao *et al.* (2007). Measurement of $\Delta F/F'_m$ was considered as a rapid method to determine the PSII operating efficiency under different environmental conditions and the value of $\Delta F/F'_m$ was regarded as an indication of overall photosynthesis (Maxwell and Johnson, 2000; Baker, 2008). The consumption rates of NADPH and ATP are considered to be major factors that determine PSII operating efficiency in many situations (Baker, 2008). Salinity-induced stomatal closure could reduce the supply of CO_2 to carboxylation sites and then down-regulate the consumption of NADPH in the Calvin cycle (Trukan and Demiral, 2009), indicating that the reduction of $\Delta F/F'_m$ is related to a decreased quantum yield of CO_2 assimilation (ϕ_{CO2}). Although the maximum quantum efficiency of PSII photochemistry (F_v/F_m) has been thought to provide a simple and rapid way of monitoring stress, stress-induced decreases in efficiency are often complex (Baker, 2008). It was reported that F_v/F_m was not affected by salinity under external NaCl concentrations lower than 200 mM (Netondo *et al.*, 2004b; Praxedes *et al.*, 2010; Yan *et al.*, 2012) and that F_v/F_m declined when salt treatment was increased above this level (Netondo *et al.*, 2004b). Grare (2010), who captured chlorophyll fluorescence images for two *M. sinensis* genotypes, stated that PSII efficiency was greatly influenced by salt concentrations over 100 mM NaCl under both dark and light conditions. However, no significant changes in F_v/F_m were observed in our study

(data not shown), indicating that excess energy was efficiently dispersed without PSII inactivation. Since the *A*, ϕ_{CO2}, and F_v/F_m are factors involved in the determination of photosynthetic efficiency (Jaafar and Ibrahim, 2012), a greater photosynthetic efficiency could be a tolerant response to salt stress.

The exclusion of Na^+ and Cl^- and the maintenance of a high uptake of K^+ are closely related to the salinity tolerance (Munns and James, 2003; Munns *et al.*, 2010; Grare, 2010), while the uptake of other minerals (e.g. N, P, and Ca^{2+}) was hardly affected by salt stress in *M. sinensis* (Grare, 2010). Therefore, measurements of Na^+, K^+, and Cl^- are effective methods for the screen of genetic variation in salinity tolerance of *M. sinensis*. In this study, close relationships between shoot ion concentrations of Na^+, K^+ and Cl^- and shoot dry weight were observed (Table 2-5). Direct ion-specific toxicity is induced by long-term salinity due to the accumulation of high ion concentrations in plant tissue. The main site of Na^+ toxicity for most plants is the leaf blade, so excluding Na^+ from the leaf blades is important, especially for perennial plants in which leaves persist for longer periods of time (Munns and Tester, 2008). Netondo *et al.* (2004a) found that Na^+ concentration saturated in sorghum roots and stems at about 150 mM external salt stress, but Na^+ saturation was not observed in leaves. In our study, Na^+ accumulated significantly in shoots as salinity levels increased, without reaching saturation. This is consistent with reports by Zhao *et al.* (2007) and Grare (2010). Significant differences between accessions observed in our study indicated a negative relationship between Na^+ accumulation and salt tolerance.

Some mechanisms, such as reduced Na^+ delivery to the shoot, tissue- and organ-specific compartmentalization, and recirculation of Na^+ from the photosynthetic organs back to the roots (Shabala and Cuin, 2007; Munns and Tester, 2008) may account for this response. Salinity not only caused high Na^+ accumulation in plants but also decreased uptake of K^+. High shoot Na^+ concentration strongly inhibited K^+ accumulation. A significant decrease in K^+ concentration was observed even at the lowest salinity concentration in the second run of the present experiment. This was in contrast with results reported by Grare (2010) who found that higher Na^+ accumulation did not negatively affect the uptake of K^+, as the K^+ concentration was stable over the salt treatment. The salinity-induced decrease of K^+ concentration may be attributed to several factors, including reduced activity of K^+ resulting from high Na^+ concentration in the soil, competition from Na^+ at uptake sites at the plasma membrane, membrane depolarization resulting from Na^+ cross, and reduction of the available ATP pool by *de novo* synthesis of compatible solutes used for osmo-protection (Shabala and Cuin, 2007). The K^+/Na^+ ratio has been considered as an indicator of salinity tolerance (Munns and James, 2003; de Lacerda *et al.*, 2005; Krishnamurthy *et al.*, 2007). We also found a higher K^+/Na^+ ratio in JM0119 than in JM0099. However, the K^+/Na^+ ratio is not always related to salinity tolerance (Munns and James, 2003; Zhao *et al.*, 2007). This inconsistency may due to the use of shoot (or leaf) tissue K^+ and Na^+ content as a proxy for cytosolic K^+/Na^+ ratio, because the cytosolic K^+/Na^+ ratio determines cell metabolic competence, and ultimately the

ability of a plant to survive in saline environments (Mäser *et al.*, 2002; Shabala and Cuin, 2007). Salt tolerance is reported to be related to the ability of an individual genotype to regulate both Na^+ and Cl^- transport to avoid ionic toxicity. We observed increased Cl^- conctent in shoots with increasing salt levels, in agreement with results reported by Grare (2010). However, a significant difference between accessions was not observed until the salt concentration reached 360 mM NaCl. Several mechanisms related to Cl^- regulation that contribute to salt tolerance have been reported, including Cl^- exclusion from shoots, intercellular compartmentalization, and phloem recirculation and translocation within the plant (Teakle and Tyerman, 2010). In the present study, high concentration of Na^+ and Cl^- found in shoots indicated an intracellular compartmentalization of Na^+ and Cl^- into the vacuoles to avoid toxic concentrations within the cytoplasm. The sharp increase of shoot Na^+ and Cl^- concentration at 240 and 360 mM salt treatments may contribute to accelerated leaf senescence.

In summary, we conclude that salinity stress significantly inhibited morphological (total leaf area and number of tillers) and physiological (chlorophyll content, A, g_s, and $\Delta F/F'_m$) traits of *M. sinensis*. The differences in salt tolerance between accessions were almost unrelated to the changes in RGR, but were associated with maintenance of larger total leaf area, a greater number of tillers, and higher photosynthetic rate. This may be related to relatively lower shoot Na^+ accumulation under salinity, as observed for JM0119. Although our data will be useful in screening

for salt-tolerant germplasm and in elucidating physiological mechanisms associated with salt stress, field research and further study on photosynthesis and ion transport in *M. sinensis* under representative saline environments are necessary to validate our findings.

CHAPTER 3

Salt-tolerant Mechanisms of C_4 Photosynthesis in *Miscanthus sinensis*

3.1. Introduction

The decrease in growth observed in plants subjected to salinity is often accompanied by a decrease in photosynthesis. *M. sinensis* uses the NADP-malic enzyme pathway of C_4 photosynthesis as that in sugarcane, sorghum, and maize. In C_4 plants, photosynthetic reactions is spatial separated between mesophyll cell (MC) and bundle sheath cell (BSC) that are arranged in concentric circles around veins, generating so-called Kranz anatomy, and this separation is achieved by restricting the accumulation of proteins to either BS or M cells (Hibberd and Covshoff, 2010; Langdale, 2011). For NADP-malic enzyme (NADP-ME) pathway, CO_2 enters the M cell cytoplasm and is firstly converted to bicarbonate ions (HCO_3^-) by carbonic anhydrase (CA) and is then fixed by phospho*enol*pyruvate carboxylase (PEPC) to form oxaloacetate (OAA). OAA is subsequently transported from the mesophyll cytoplasm to the mesophyll chloroplast and is converted to malate by NADP-malate dehydrogenase (NADP-MDH). Malate is then transported out of the mesophyll chloroplast into the BS chloroplast via transports across the chloroplast and plasma membranes of both cell types, and decarboxylated by NADP-ME, releasing CO_2 for

ribulose-1,5-bisphosphate carboxylase/oxygenase (RuBisCO) in the Calvin-Benson cycle (C_3 cycle). The pyruvate generated by the decarboxylation reaction is transported back from the BS chloroplast to the M chloroplast where it acts as a substrate for pyruvate, orthophosphate dikinase (PPDK) to regenerate phospho*enol*pyruvate (PEP). The cycle is restarted when PEP is transported from the M chloroplast to the M cell cytoplasm to combine once again with CO_2. The concentration of CO_2 to RuBisCO in C_4 pathway reduces the oxygenation reaction, and in turn limits the wasteful reactions of photorespiration (Hatch, 1987), induce higher yield in C_4 crops than that in C_3 crops.

Salt-induced reduction of photosynthesis may be associated with several factors (Heuer, 2005; Chaves *et al.*, 2009), such as (1) decreased CO_2 supply due to hydroactive closure of the stomata, (2) premature loss of chlorophyll and damage to the photosynthetic apparatus, (3) changes in enzyme activities and gene expression, and (4) negative feedback signals generated by reduced sink activity. Stomatal aperture reflected by the stomatal conductance was reported to be greatly decreased by salinity in lemon [*Citrus limon* (L.) Burm.f.], cucumber (*Cucumis sativus* L.), sugarcane (*Saccharum* spp. hybrid), celery (*Apium graveolens* L.), guava (*Psidium guajava* L.), wheat (*Triticum durum* Desf. and *T. aestivum* L.), rice (*Oryza sativa* L.), lucerne (*Medicago sativa* L.), sorghum [*Sorghum bicolor* (L.) Moench], naked oat (*Avena nuda* L.), and maize (*Zea mays* L.) (Garcialegaz *et al.*, 1993; Chartzoulakis, 1994; Meinzer *et al.*, 1994; Pardossi *et al.*, 1998; Ali-Dinar *et al.*, 1999; Ouerghi *et al.*,

2000; Dionisio-Sese and Tobita, 2000; Anand *et al.*, 2001; Netondo *et al.*, 2004b; Zhao *et al.*, 2007; Omoto *et al.*, 2012). Reduction of chlorophyll content and changes in photosynthetic apparatus were also described in several studies (Smillie and Nott, 1982; Belkhodja *et al.*, 1994; Netondo *et al.*, 2004b; Jiang *et al.*, 2006; Maricle *et al.*, 2007). Chloroplasts aggregate under salinity and ultrastructural changes of the assimilating organs occur in salt-treated plants, including swollen thylakoid membranes, disorganized chloroplast envelope, increased plastoglobuli, and enlarged mesophyll cells (Heuer, 2005; Shu, *et al.*, 2012). However, Omoto *et al.* (2009) indicated that no structural damage was observed in the bundle sheath cell chloroplasts of NADP-ME type C_4 species and that granal stacking developed under salinity condition. Moreover, chlorophyll *a* fluorescence parameters are used to estimate the photosynthetic performance *in vivo* and the limitation extent of the performance by photochemical and nonphotochemical processes (Baker, 2008).

Several molecular mechanisms focusing on enzyme activities may be involved in the maintenance of a relative higher photosynthetic rate in C_4 plants under salinity. As the CO_2-fixing enzyme in C_4 and Crassulacean acid metabolism (CAM) leaves, the activity and content of PEPC and its expression are affected by salt stress. The activity of PEPC and its expression was salt-induced in the facultative CAM plant *Mesembryanthemum crystallinum* L. and it is involved in the switch from C_3 to CAM photosynthesis (Cushman and Bohnert, 1997). PEPC was significantly up-regulated in salt-treated shoots of *Aeluropus lagopoides* (L.) Trin. ex Thw. which is a NAD-ME

subtype C_4 grass (Sobhanian *et al.*, 2010); The enhancement of PEPC was also found in maize (Alla and Hassan, 2012; Omoto *et al.*, 2012) and *Atriplex lentiformis* (Zhu and Meinzer, 1999), though the decrease of PEPC amount and activity was observed in salt-sensitive plants (Bouraima *et al.*, 1987; Alla and Hassan, 2012). PPDK and RuBisCO act as the two rate-limiting enzymes of the C_4 pathway (Sugiyama, 1973; Edwards *et al.*, 1985; Spreitzer and Salvucci, 2002). Increased PPDK activity under salt stress was reported in several studies (Alla and Hassan, 2012; Omoto *et al.*, 2012; Wang *et al.*, 2013), while salt-induced responses of RuBisCO were in dispute. Content and activity of RuBisCO were found to be decreased under salt stress in some studies (Wang *et al.*, 1999; Zhu and Meinzer, 1999; Sobhanian *et al.*, 2010; Omoto *et al.*, 2012; Galmés *et al.*, 2013), though significant effect of salinity on RuBisCO was not found in both tolerant and sensitive genotypes of maize (Alla and Hassan, 2012). And a time-course of salinity effect on RuBisCO *in vitro* activity and content was reported with no decrease until leaves were exposed to salt stress for longer than 20 days (Delfine *et al.*, 1998). NADP-ME is the most studied C_4 decarboxylase. The activity of NADP-ME declined in maize leaves under 3% NaCl stress (Omoto *et al.*, 2012), while induced by salt and salt-alkaline stress (Sun *et al.*, 2003; Wang *et al.*, 2013) with a time-dependent enhancement of expression (Sun *et al.*, 2003). Activity of NADP-MDH was reported to be salt-induced in maize leaves (Eprintsev and Fedorina, 2007; Alla and Hassan, 2012; Omoto *et al.*, 2012) and poplars (Wang *et al.*, 2013).

Amino acids and sugars (e.g. fructose and sucrose) play essential roles in tolerance to salt stress in higher plant as compatible solutes greatly accumulated in the cytosol to balance the osmotic pressure from ions (e.g. Na^+ and Cl^-) sequestered in the vacuole or in the intercellular apoplastic space (Hasegawa, *et al.*, 2000; Heuer, 2005; Munns and Tester, 2008; Sanchez *et al.*, 2008; Krasensky and Jonak, 2012; Tilbrook and Roy, 2014). Changes of these compatible solutes caused by salt stress have been reported in previous studies (Kerepesi and Galiba, 2000; de Lacerda *et al.*, 2005; Chen *et al.*, 2006; Hajlaoui *et al.*, 2010; Boriboonkaset *et al.*, 2013; Hu *et al.*, 2013). Moreover, salt-induced variation in carbohydrates synthesis and export by the source leaves could be a consequence of the altered sink-source relationship, thus the reduced photosynthetic capacity by salinity may also result from the inhibition of certain carbon metabolism processes by feedback signals from the sink tissues (Roitsch, 1999; Heuer, 2005; Parvaiz and Satyawati, 2008).

Although adaptable mechanisms of C_4 photosynthesis to cold and drought have been studied in *Miscanthus*, little is known about the physiological and biochemical responses of its photosynthesis to salinity. To better understand the effects of salinity on C_4 photosynthesis of *M. sinensis*, the gas-exchange, chlorophyll *a* fluorescence, enzyme activities of PEPC, PPDK, NADP-ME, NADP-MDH, and RuBisCO, and contents of carbohydrates, protein, and total free-amino acids were investigated in the leaves of two *M. sinensis* accessions with distinct salt-tolerance, JM0119 (salt-tolerant) and JM0099 (salt-sensitive), under salinity condition.

3.2. Materials and Methods

3.2.1. Plant Materials and Growth Conditions

Seeds of two *Miscanthus* accessions with distinct salt-tolerance, JM0119 (salt-tolerant) and JM0099 (salt-sensitive) were surface-sterilized with 70% ethanol for 30 s and with 1% (v/v) sodium hypochlorite (NaClO) for 10 min, and rinsed three times with distilled water. Twenty-five seeds of each accession were sown in a 2-l pot filled with mixed peat moss (PRO-MIX PGX; Grower's Nursery Supply, Inc.; NE) in growth chamber at 12 h photoperiod with 500 μmol $m^{-2}s^{-1}$ PPF, 70% humidity, and 28/22 ℃ day/night regime and watered with distilled water daily. Seedlings were thinned to ten per pot on 5-leaf stage and then irrigated with salt-free 1/2 Hoagland solution until the seedlings had eight fully expanded leaves. Each pot was treated with 200 ml 1/2 Hoagland solution containing 0 (control) or 250 mM NaCl (split into 3 days at a progressive rate of 83 mM per day to avoid osmotic shock) daily. Samples were harvested just before the treatment (Day 0) and 1 (Day 3), 3 (Day 6), 7 (Day 10), and 14 (Day 17) days after salt application. Leaf samples were immediately immersed in liquid nitrogen and stored at -80 ℃.

3.2.2. Growth and Leaf Chlorophyll Measurements

Shoot dry weight and chlorophyll content of five seedlings were measured as the growth responses to NaCl stress. Shoot dry weight was measured with samples dried

at 70 ℃ for 72 h. The relative growth rate (RGR) was calculated according to Kingsbury *et al.* (1984) as $RGR = \frac{(\ln w_2 - \ln w_1)}{(t_2 - t_1)}$, where w_1 and w_2 stand for dry weights (g) of shoots at times t_1 and t_2 (in days), respectively. Chlorophyll content was assayed using the ethanol-soaking method (Knudson *et al.*, 1977). Centrifuge tubes (15 ml) with the ethanol-soaking samples were covered with aluminum foil and shaken for about 3 d until leaf colors completely disappeared.

3.2.3. Gas Exchange and Chlorophyll *a* Fluorescence

Photosynthetic rate (A), stomatal conductance (g_s), intercellular CO_2 concentration (C_i), intercellular-to-ambient CO_2 concentration ratio (C_i/C_a), and transpiration rate (T_r) were measured on the topmost fully expanded leaf blade of each plant on each harvest date, using an infrared, open gas exchange system (LI-6400; LI-COR, Inc.; Lincoln, USA) at 1000 μmol m^{-2} s^{-1} photosynthetic photon flux density (PPFD) and 400 ppm CO_2 concentration. The area of each leaf in the leaf chamber was determined manually. Chlorophyll *a* fluorescence parameters were also measured on the same leaves on which gas-exchange was measured after 30-min dark adaptation, using a MINI-PAM (Walz; Effeltrich, Germany) at 650-nm pulse-modulated measuring light (0.15 μmol m^{-2} s^{-1} PAR) for minimal fluorenscence (F_o), 800-ms saturating pulse (5000 μmol m^{-2} s^{-1} PAR) for maximal fluorenscence of dark-adapted leaf (F_m) and maximal fluorenscence of light-adapted leaf (F'_m), and

actinic light supplied by light-emitting diodes for steady-state yield of fluorescence (F_t). The maximum efficiency of PSII photochemistry (F_v/F_m) was calculated as (F_m - F_o)/F_m, the efficiency of energy capture by open reaction centers of PSII for light-adapted leaves ($\Delta F/F'_m$) was calculated as (F'_m - F_t)/F'_m, the coefficient of photochemical quenching (*qP*) was calculated from (F'_m - F_t)/ (F'_m - F_o), and the nonphotochemical quenching (*NPQ*) was calculated from (F_m - F'_m)/F'_m as described by the operation handbook of MINI-PAM and Baker (2008).

3.2.4. Enzyme Extraction

Leaves of five seedlings of both control and treated plants were used for enzyme assay. Homogenise about 30 mg of liquid-nitrogen-frozen leaves with 300 μl ice-cold extraction buffer. PEPC (EC 4.1.1.31) was extracted using the methods of Crafts-Brandner and Salvucci (2002) with the following modifications. 50 mM HEPES-NaOH (pH 7.5), 10 mM $MgCl_2$, 0.05 mM EDTA, 1%(w/v) casein, 1% (w/v) polyvinylpyrrolidone, 0.05% (v/v) Triton X-100, and 5 mM dithiothreitol (DTT). The extraction buffer for PPDK (EC 2.7.9.1) was the same as for PEPC kept at room temperature with a modification of 50 mM HEPES-NaOH (pH 8). The extraction of RuBisCO (EC 4.1.1.39) followed the proceducre described by Sharkey *et al.* (1991) with the modified ice-cold extraction buffer as 100 mM HEPES-NaOH pH 7.8, 5 mM $MgCl_2$, 1 mM EDTA, 5 mM DTT, 0.02% (w/v) BSA, 1% (w/v) polyvinyl

polypyrrolidone, and one protease inhibitor cocktail tablet (Roche Applied Science, Indianapolis, USA) per 10 ml of extraction buffer was added to inhibit enzyme degradation. The supernatant of centrifuged extraction (15 s at 15,000 × g) was added with 20 mM $MgCl_2$ and 10 mM $NaHCO_3$ and incubated at room temperature for 10 min to fully activate RuBisCO (Sharkey *et al.*, 1991). NADP-ME (EC 1.1.1.40) extraction buffer was a modification form Iglesias and Andreo (1989), containing 100 mM Tris-HCl, pH 7.3, 10 mM $MgCl_2$, 5 mM DTT, 1 mM EDTA, 10% (w/v) glycerol, and 5% (w/v) polyvinylpyrrolidone. NADP-MDH (EC 1.1.1.82) extraction buffer was according to Ashton *et al.* (1990), containing 100 mM Tris-HCl, pH 8, 10 mM $MgCl_2$, 5 mM DTT, 1 mM EDTA, and 0.05% (v/v) Triton X-100. A 100-µl aliquot of homogenate was added to 5-ml 96% ethanol for total chlorophyll determination. The remainder was centrifuged at 20,000 × g at 4 ℃ for 10 min.

3.2.5. Activities of Key Enzymes in C_4 Photosynthesis

A 50-µl aliquot of crude extract supernatant was immediately added to a cuvette containing 1 ml of the assay buffer for enzyme activities analysis. The activity of PEPC was assayed spectrophotometrically (ultraviolet/visible spectrophotometer UVmini-1240; Shimadzu Corp., Kyoto, Japan) at 340 nm by following the OAA reduction by nicotinamide adenine dinucleotide (NADH) via MDH (Giglioli-Guivarc'h *et al.*, 1996; Ashton *et al.*, 1990). The 1 ml assay buffer contained

100 mM HEPES-NaOH, pH 8.0, 5 mM $MgCl_2$, 5 mM $NaHCO_3$, 0.2 mM NADH, 6.5 Unit NAD-MDH, 5 mM Glc-6-P, and 2 mM DTT. The reaction was initiated by the addition of PEP to 5 mM final concentration and incubated at 30℃. The activity of PPDK was assayed by coupling the production of PEP to NADH via PEPC and MDH with modifications from Ashton *et al.* (1990). The 1 ml assay buffer contained 100 mM HEPES-NaOH, pH 8.0, 15 mM $MgCl_2$, 0.15 mM EDTA, 5 mM $NaHCO_3$, 0.3 mM NADH, 5 mM NH_4Cl, 2.5 mM K_2HPO_4, 1 mM Glc-6-P, 2 Unit MDH, 5 mM DTT, and 1.5 mM ATP. Crude extract was incubated in the assay buffer for 5 min at 25℃ as proposed by Leakey *et al.* (2006). The reaction was initiated by the addition of sodium pyruvate to 2 mM final concentration and 3-Unit PEPC (1U ml^{-1} in 20% glycerol) and incubated at 30℃. The activity of RuBisCO was assayed by coupling the RbBisCO activity to NADH oxidation via 3-phosphoglycerate kinase and glyceraldehyde 3-phosphate dehydrogenase with adaption from Leakey *et al.* (2006). The 1 ml assay buffer contained 100 mM HEPES-NaOH pH 8.0, 10 mM MgCl2, 1 mM EDTA, 20 mM NaCl, 2 mM DTT, 10 mM $NaHCO_3$, 0.3 mM NADH, 2 mM ATP, 5 mM creatine phosphate, 3 Unit creatine phosphokinase, 3-Unit phosphoglycerate kinase, and 10-Unit glyceraldehyde 3-phosphate dehydrogenase. The reaction was initiated by the addition of ribulose-1,5-bisphosphate (RuBP) to 0.66 mM final concentration and incubated at 30℃. Enzyme activity of NADP-ME was determined by monitoring NADPH production at 340 nm with assay buffer minor modified from Iglesias and Andreo (1989). The 1 ml assay buffer contained

100 mM Tris-HCl, pH 8, 20 mM $MgCl_2$, and 0.4 mM $NADP^+$. The recation was initiated by the addition of L-malate to 5 mM final concentration and incubate at 30℃. The activity of NADP-MDH was measured by following the oxidation of NADPH at 340 nm in 1 ml assay buffer modified from Ashton *et al.* (1990) as following, 50 mM Tris-HCl, pH 8.3, 70 mM KCl, 1 mM EDTA, 1 mM DTT, and 0.2 mM NADPH. The reaction was initiated by the addition of OAA^+ to 1 mM final concentration and incubated at 30℃.

3.2.6. Content of Protein, Carbohydrates, and Total Free-amino Acids

Liquid-nitrogen-frozen leaf samples (ca. 30 mg) taken at the indicated dates from leaves of four seedlings were extracted with 300 µl 80% ethanol (v/v) (10 mM Hepes-KOH pH 7.4) at 80℃ for 15 min and centrifuged for 2 min at room temperature (Leakey *et al.,* 2006). A 50-µl aliquot of supernatant was used for each determination of glucose, fructose and sucrose using a continuous enzymatic substrate assay (Maness, 2010). A 16-µl aliquot of the ethanol-extracted supernatant was used for the determination of total free-amino acid contents using a fluorescamine assay (Bantan-Polak *et al.,* 2001) with a fluorescence spectrophotometer (F-2500, Hitachi, Ltd.; Tokyo, Japan). Histidine was used as a standard. Pellets of the ethanol extraction were suspended in l ml 0.1 M NaOH by heating to 95℃ for 30 min. Protein content was assayed with a commercial kit

(Pierce™ BCA Protein Assay Kit, Thermo Fisher Scientific Inc., Rockford, USA) with bovine serum albumin as a standard. The reminder of NaOH solution was then acidified to pH 4.9 with an HCl/sodium-acetate and mixed well. A 50-µl aliquot of the suspension was incubated with 10 µl α-amylase after diluting with 250 µl distilled water at 95°C for 5 minutes and digested with 10 µl 300 U ml^{-1} amyloglucosidase for 15 min at 60 ℃. The starch content was determined by measuring the glucose content.

3.2.7. Data Analysis

All data was analyzed by Statistical Product and Service Solutions (SPSS Statistics, Version 20; IBM Corp.; New York, USA). Differences in morphological and physiological traits among accessions and salt treatments were tested by analysis of variance. The least significant difference ($LSD_{0.05}$) test was used to separate treatment means.

3.3. Results

3.3.1. Growth and Chlorophyll Content

Plant growth was significantly ($P < 0.05$) inhibited after one-week salt treatment in both accessions (Fig. 3-1A). Compared with the control on day 10 and 17, the relative growth rate (RGR) declined by 28% and 44% for JM0119, and 30% and 69% for JM0099, respectively. Remarkable differences were not observed in RGR

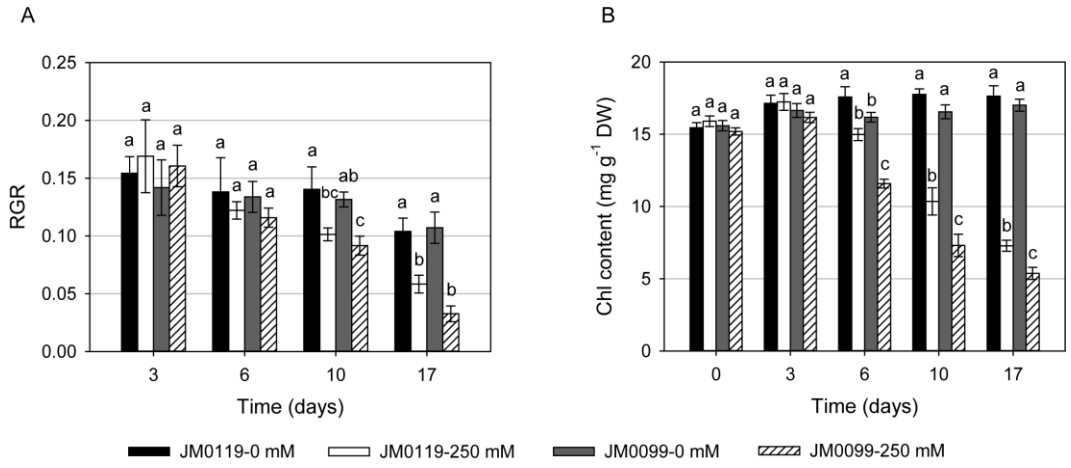

Figure 3-1. Time-course changes in the relative growth rate (RGR) of shoots (A) and leaf chlorophyll content (B) in the absence or presence (250 mM) of NaCl for two *Miscanthus sinensis* accessions. Values are means ± SE of five replicates. Different letters indicate significant differences within each sampling date ($LSD_{0.05}$ test).

between the accessions, though shoot dry weight for JM0099 was significantly (P = 0.018) lower than that for JM0119 on day 17 (data not shown). Chlorophyll content was decreased by salinity even earlier than RGR did (Fig. 3-1B). Marked (P <0.01) decreases were observed from day 6 relative to the control in both accessions, with reduction of 15%, 42%, and 59% for JM0119, and 28%, 56%, and 68% for JM0099, respectively. Notable (P <0.05) differences in chlorophyll content between the accessions also occurred from day 6, which was 26% lower for JM0099 compared with that for JM0119.

3.3.2. Leaf Gas Exchange

Significant (P <0.05) effects of salinity on the photosynthetic rate (A), the stomatal conductance (g_s), and the transpiration rate (T_r) were observed from day 3or later (Fig. 3-2A, B, and D). Compared with the control on day 17, A decreased by 65% for JM0119 and 76% for JM0099, and g_s declined 63% for JM0119 and 71% for JM0099, paralleling with a decrease of 55% in T_r for JM0119 and 66% for JM0099. There was no marked variation in the intercellular CO_2 concentration (C_i) for both accession during salt treatment until day 17 (Fig. 3-2C). A slight increase of C_i was found in salt-treated plants of JM0119 on day 17, while a notable (P = 0.014) increase of C_i was observed in JM0099. Significant (P <0.05) differences between the accessions were only observed in A and T_r from day 10 or later. On day 17, A

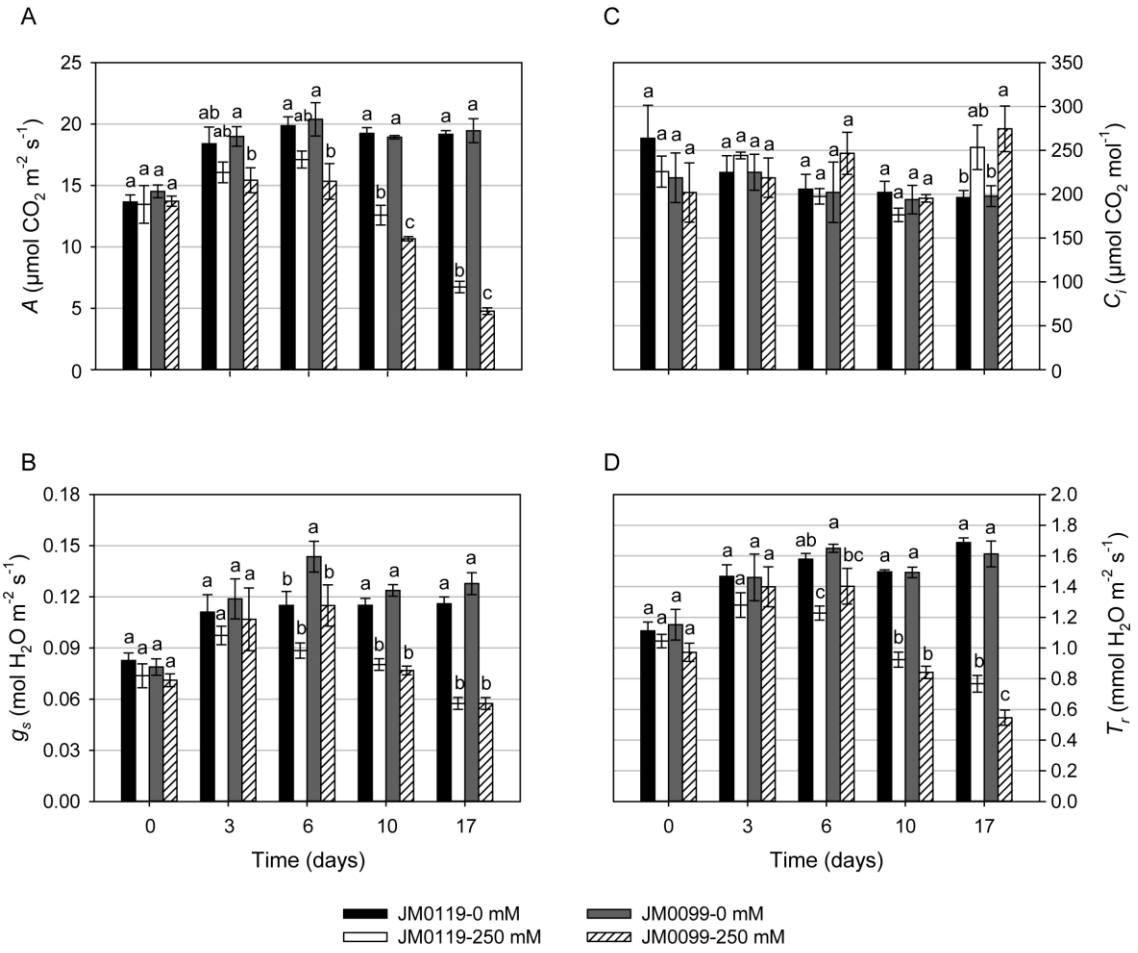

Figure 3-2. Time-course changes in (A) Photosynthetic rate, *A*; (B) stomatal conductance, g_s; (C) intercellular CO_2 concentration, C_i; and (D) transpiration rate, T_r in the absence or presence (250 mM) of NaCl for two *Miscanthus sinensis* accessions. Values are means ± SE of five replicates. Different letters indicate significant differences within each sampling date ($LSD_{0.05}$ test).

and T_r were both 29% lower for JM0099 than those for JM0119. The intercellular-to-ambient CO_2 concentration ratio (C_i/C_a) varied slightly during the salt treatment except for a great (P = 0.003) increase in salt-treated plants of JM0099 on day 17.

3.3.3. Chlorophyll *a* Fluorescence

Salinity did not affect the maximum efficiency of PSII photochemistry (F_v/F_m) significantly in both accessions (Fig. 3-3A), apart from a notable (P = 0.017) decrease in the salt-treated plants of JM0099 on day 10. However, the PSII operating efficiency ($\Delta F/F'_m$) and the coefficient of photochemical quenching (*qP*) were decreased under salt stress (Fig. 3-3B and C). Salt-induced remarkable (P <0.05) reduction occurred on day 6, 10, and 17 in $\Delta F/F'_m$ relative to the control, which were 10%, 15%, and 29%, respectively, for JM0119 and 14%, 26%, and 49%, respectively, for JM0099. In *qP*, the significant (P <0.05) decreases were observed on day 10 and 17 compared with the control, which were 8% and 12%, respectively, for JM0119 and 12% and 27%, respectively, for JM0099. Significant differences between the accessions were observed on day 10 (P = 0.037) and 17 (P <0.001) in $\Delta F/F'_m$ and on day 17 (P = 0.002) in *qP*. On day 17, relative lower $\Delta F/F'_m$ (27%) and *qP* (16%) were found in JM0099 than that in JM0119. In contrast with $\Delta F/F'_m$ and *qP*, the nonphotochemical quenching (*NPQ*) was increased during the salt

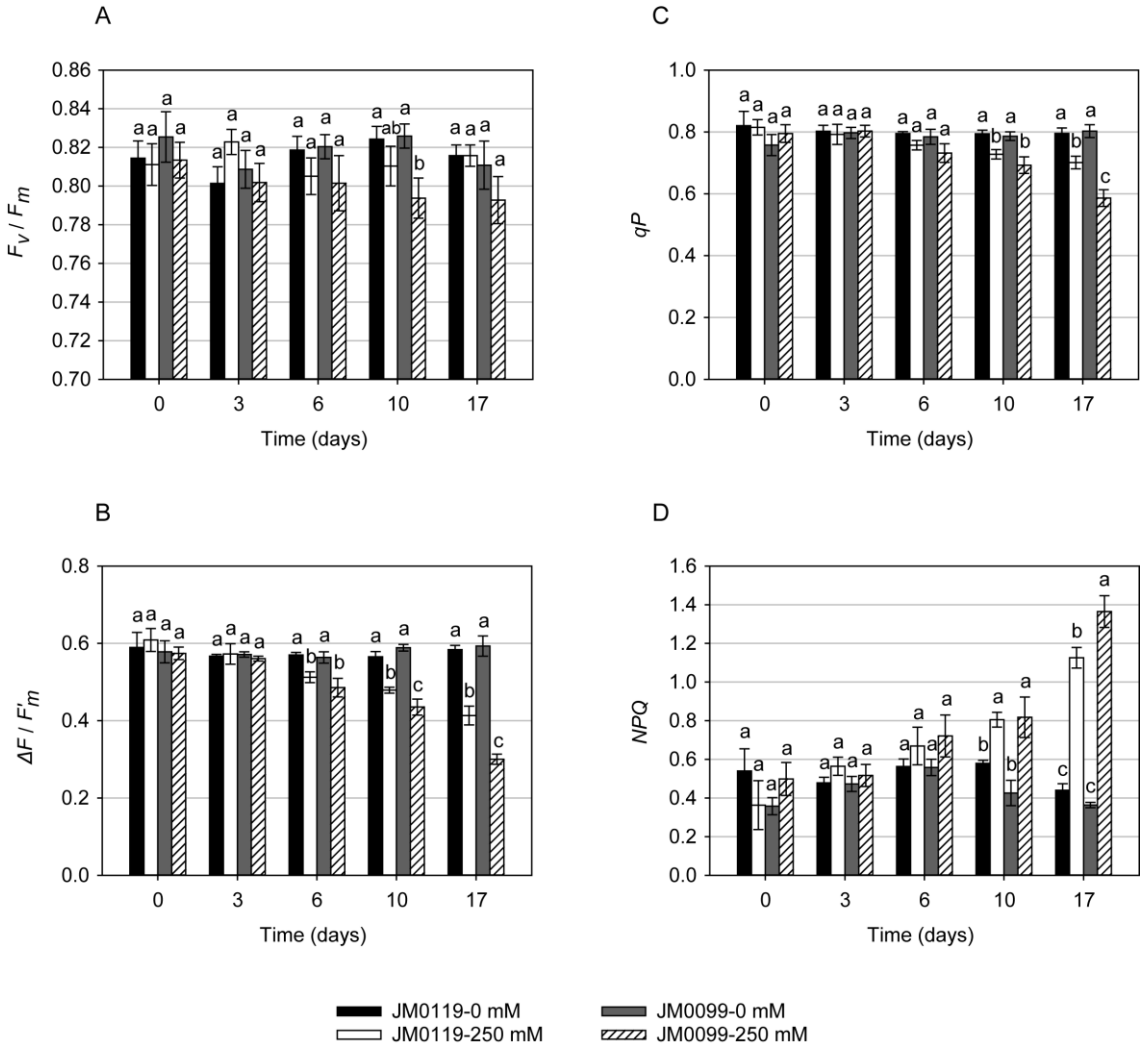

Figure 3-3. Time-course changes in (A) the maximum efficiency of PSII photochemistry, F_v/F_m; (B) the PSII operating efficiency, $\Delta F/F'_m$; (C) the coefficient of photochemical quenching, *qP*; and (D) the nonphotochemical quenching, *NPQ* in the absence or presence (250 mM) of NaCl for two *Miscanthus sinensis* accessions. Values are means ± SE of five replicates. Different letters indicate significant differences within each sampling date ($LSD_{0.05}$ test).

treatment (Fig. 3-3D). Remarkable ($P < 0.05$) increases in salt-treated plants were observed on day 10 and 17, 39% and 156%, respectively, for JM0119 and 92% and 275%, respectively, for JM0099. There was no significant differences between the accessions until day 17 ($P = 0.005$), with the *NPQ* value of 21% greater for JM0099 than that for JM0119.

3.3.4. Activities of Key Enzymes in C_4 photosynthesis

Activities of C_4 photosynthetic enzymes were affected by salinity, except for that of RuBisCO (Fig. 3-4). Activities of PEPC, PPDK, and NADP-MDH were stimulated by salinity with different patterns in each accession (Fig. 3-4A-C). Activities of PEPC and PPDK were enhanced gradually during the salt treatment in salt-treated plants of JM0119. However, single peak curves were observed in the salt-caused variation of PEPC and PPDK activities for JM0099, with increases of 62% and 74% relative to the control at the peak on day 6. On day 17, PEPC and PPDK activity was increased by 133% and 90%, respectively, for JM0119 relative to the control, and they were 42% and 30% greater than those for JM0099. Activity of NADP-MDH enhanced gradually in both accessions, with greater ($P < 0.05$) increases observed in JM0099 than those in JM0119 from day 10. On day 17, NADP-MDH activity increased by 188% and 290% relatively for JM0119 and JM0099 relative to the control. The activity of NADP-ME was hardly affected under

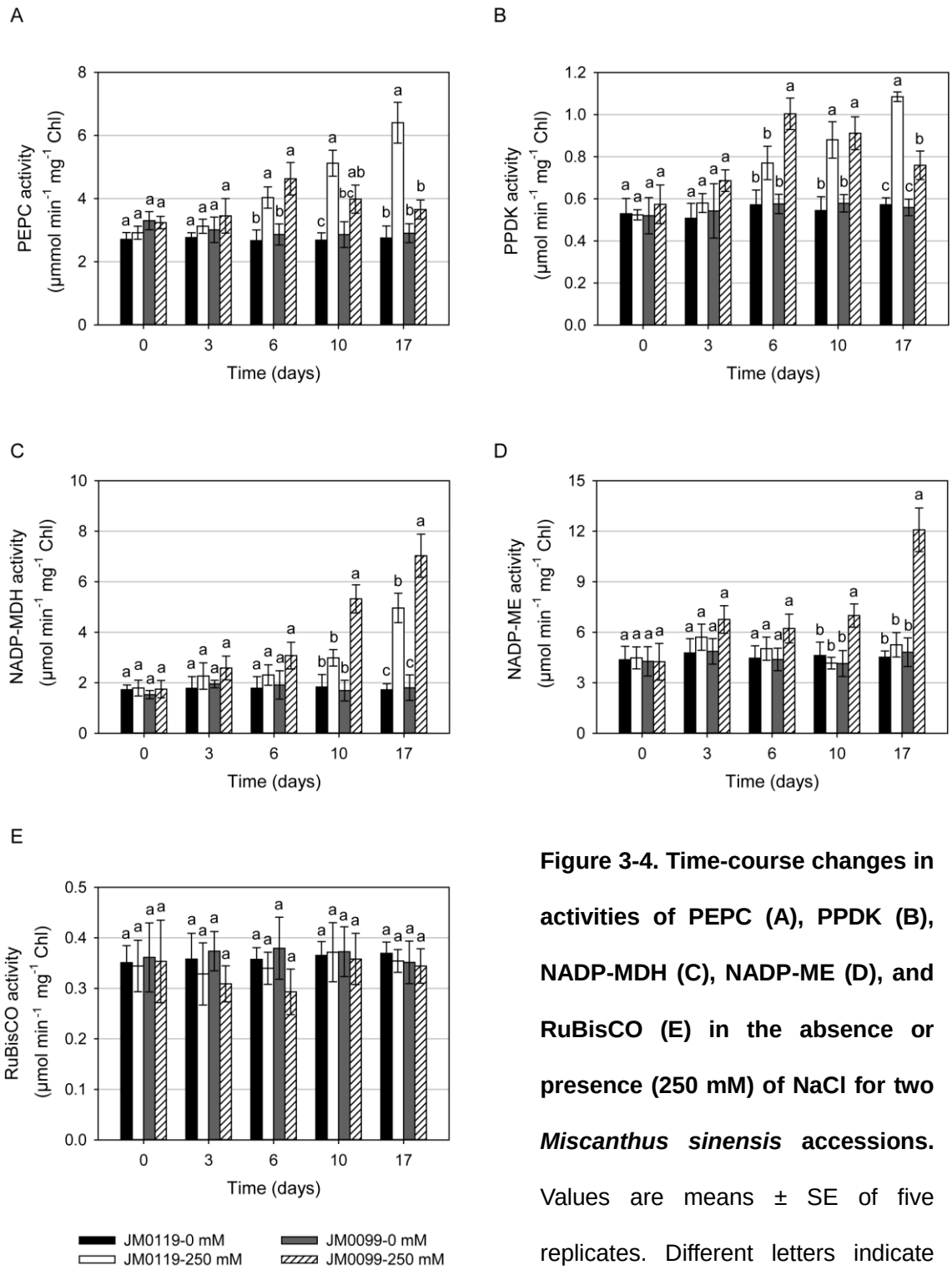

Figure 3-4. Time-course changes in activities of PEPC (A), PPDK (B), NADP-MDH (C), NADP-ME (D), and RuBisCO (E) in the absence or presence (250 mM) of NaCl for two *Miscanthus sinensis* accessions. Values are means ± SE of five replicates. Different letters indicate significant differences within each sampling date ($LSD_{0.05}$ test).

salt stress for JM0119, and was significantly ($P < 0.01$) enhanced from day 10 for JM0099 (Fig. 3-4D). Compared with the control, NADP-ME activity increased by 151% for JM0099 on day 17, and was 130% greater than that for JM0119. When expressed on leaf fresh weight basis instead of chlorophyll basis (data not shown), similar differences between accessions were observed. However, the activities of the enzymes decreased (except for PEPC in JM0119) from day 6 after an increase (except for RuBisCO, activity of which was changeless) on day 3 in both accessions, and activities of PEPC, PPDK, ME, and RuBisCO was even less than that of the control from day 10.

3.3.5. Contents of Carbohydrates, Protein, and Total Free-Amino Acids

Salt-induced strikingly ($P < 0.05$) increase of the contents of soluble sugars including glucose, fructose, and sucrose were observed from day 3 or later in both accessions (Fig. 3-5A-D). Plants of JM0099 possess relative higher level of glucose content under control conditions compared with those of JM0119 do, and varied in a single peak curve, with a peak value 149% greater than the control on day 6, during the time course of salt treatment (Fig. 3-5A). However, content of fructose in the plants of JM0119 was much greater under control relative to JM0099, and increased dramatically on day 3, 123% greater than the control, followed by a valley curve (Fig. 3-5B). Contents of glucose, fructose, and total soluble sugar were significantly

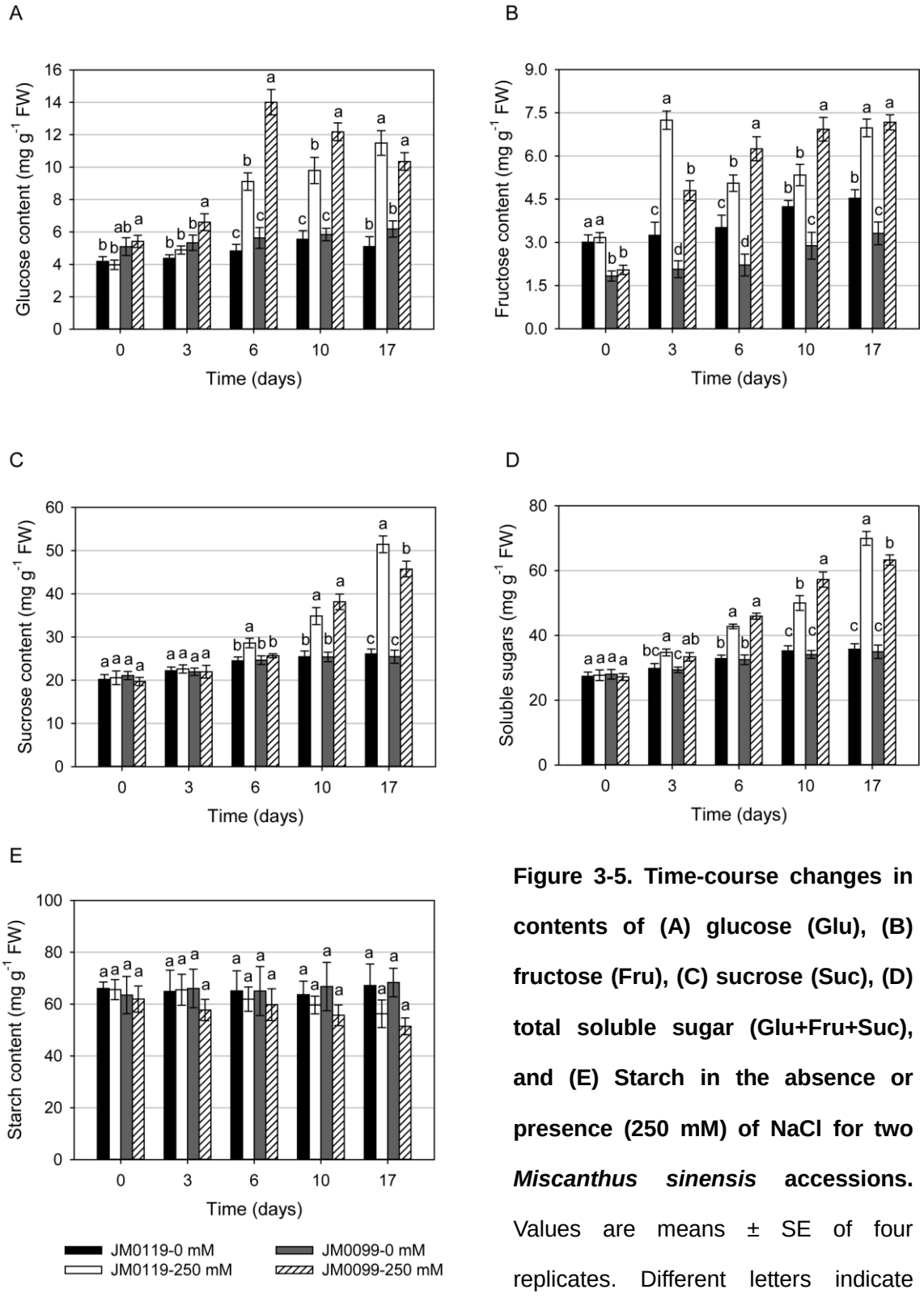

Figure 3-5. Time-course changes in contents of (A) glucose (Glu), (B) fructose (Fru), (C) sucrose (Suc), (D) total soluble sugar (Glu+Fru+Suc), and (E) Starch in the absence or presence (250 mM) of NaCl for two *Miscanthus sinensis* accessions. Values are means ± SE of four replicates. Different letters indicate significant differences within each sampling date ($LSD_{0.05}$ test).

($P < 0.05$) greater in salt-treated plants of JM0099 than those in JM0119 up to day 10, then became lower on day 17. On day 17 relative to the control, contents of glucose, fructose, sucrose, and total soluble sugar increased by 125%, 54%, 97%, and 96%, respectively, for JM0119, and 67%, 116%, 80%, and 81%, respectively, for JM0099. Although the content of starch showed a decline under salt stress from day 10, no significance was observed.

Trifling increases of the protein content in salt-treated plants was found in JM0119 form day 10, paralleling with significant ($P < 0.001$) reduction of that on day 17 in JM0099 (Fig. 3-6A). The content of protein declined 40% relative to the control on day 17 in JM0099. A significant ($P = 0.001$) increase in the content of total free-amino acids relative to the control was observed on day 17 for JM0119, and no remarkable changes were found in that for JM0099 (Fig. 3-6B).

3.4. Discussion and Conclusion

The present study determined that shoot growth of *M. sinensis* was dramatically inhibited by 250 mM NaCl after one week salt application and positively ($P < 0.01$) related to the plant photosynthesis (Table 3-1) in both accessions. There are two major categories associated with photosynthesis reduction: stomatal closure and affected CO_2 fixation. Close correlation ($P < 0.001$) between A and g_s were also observed in the present study. Variation of g_s is the most sensitive and readily

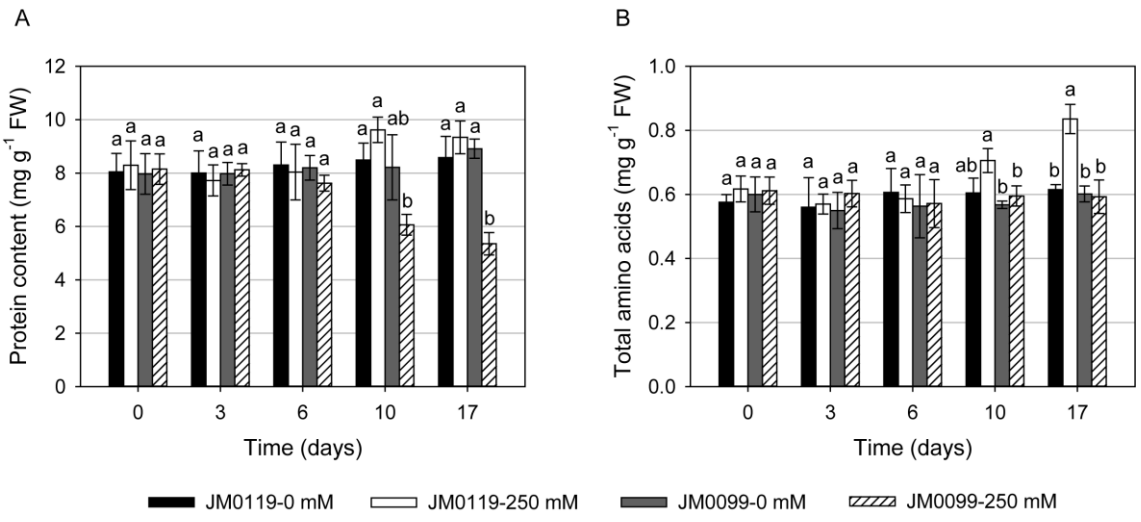

Figure 3-6. Time-course changes in the content of protein (A) and total free-amino acids (B) in the absence or presence (250 mM) of NaCl for two *Miscanthus sinensis* accessions. Values are means ± SE of four replicates. Different letters indicate significant differences within each sampling date ($LSD_{0.05}$ test).

measurable response of the plant to salinity as it is essential in both prevention of desiccation and CO_2 acquisition (Munns and Tester, 2008; Ashraf and Harris, 2013). The reduction of stomatal aperture is usually consequences of decreased leaf turgor, low atmospheric vapour pressure, and chemical signals from the root (Chaves *et al.*, 2009). Furthermore, salt-induced osmotic effect also causes local synthesis of abscisic acid (ABA) in the photosynthetic tissues, especially in the guard cells of stomata, thus leading to a partial stomata closure (Munns and Tester, 2008; Zhao *et al.*, 2009). The C_i was usually declined following the reduction of g_s as a result of stomatal closure and thus decreased the intercellular-to-ambient CO_2 concentration ratio (C_i/C_a) (Zhao *et al.*, 2009; Tavakkoli *et al.*, 2010; Omoto, et al, 2012). However, the absence of significant changes of C_i until day 10 as well as an increase on day 17 in the present study implied that the reduction of CO_2 assimilation after long-term salt duration was not due to the stomatal limitation. Less stomata limitation was found in the photosynthesis in halophytes than that in glycophytes (Heuer, 2005), and the increase of C_i was also found in plant leaves treated with high salt levels (Hu *et al.*, 2013). Stomatal closure also imposes an inhibitory effect on the transpiration of water (Ashraf and Harris, 2013), and this consist with the high correlation coefficients observed between g_s and T_r in Table 3-1. Slight decrease of g_s may save water in plants and improve the plant water-use efficiency (WUE) (Chaves *et al.*, 2009).

Table 3-1. Correlation coefficients between the growth and photosynthetic parameters in salt-treated plants of two accessions.

Trait	Accessio	*A*	RGR	Chl	g_s	C_i	T_r	C_i/C_a	F_v/F_m	$\Delta F/F'_m$	*qP*	*NPQ*
A	JM0119	1.000										
	JM0099	1.000										
RGR	JM0119	**0.441****	1.000									
	JM0099	**0.569****	1.000									
Chl	JM0119	**0.774****	**0.516****	1.000								
	JM0099	**0.834****	**0.617****	1.000								
g_s	JM0119	**0.891****	**0.459****	**0.731****	1.000							
	JM0099	**0.752****	**0.577****	**0.518****	1.000							
C_i	JM0119	-0.304*	-0.016	-0.071	-0.028	1.000						
	JM0099	-0.284*	-0.162	-0.200	0.015	1.000						
T_r	JM0119	**0.887****	**0.434****	**0.754****	**0.901****	-0.072	1.000					
	JM0099	**0.860****	**0.538****	**0.685****	**0.905****	0.016	1.000					
C_i/C_a	JM0119	-0.165	-0.100	-0.287*	0.082	0.309*	-0.034	1.000				
	JM0099	-0.225	-0.112	-0.257	0.151	**0.812****	0.096	1.000				
F_v/F_m	JM0119	0.067	-0.085	0.144	0.054	-0.157	0.012	0.061	1.000			
	JM0099	0.331*	0.249	**0.400****	0.140	-0.139	0.208	-0.141	1.000			
$\Delta F/F'_m$	JM0119	**0.512****	**0.436****	**0.689****	**0.512****	0.079	**0.475****	-0.291*	-0.015	1.000		
	JM0099	**0.711****	**0.690****	**0.808****	**0.567****	-0.297*	**0.648****	**-0.387****	**0.433****	1.000		
qP	JM0119	0.354*	0.395*	**0.473****	**0.404****	0.235	**0.376****	-0.201	-0.286*	**0.889****	1.000	
	JM0099	**0.556****	**0.607****	**0.650****	**0.481****	-0.275	**0.562****	-0.320*	0.145	**0.893****	1.000	
NPQ	JM0119	**-0.576****	**-0.468****	**-0.713****	**-0.531****	0.026	**-0.521****	0.357*	0.246	**-0.896****	**-0.747****	1.000
	JM0099	**-0.698****	**-0.657****	**-0.742****	**-0.597****	0.268	**-0.628****	**0.394****	-0.152	**-0.845****	**-0.654****	1.000

RGR, relative growth rate; *A*, photosynthetic rate; Chl, chlorophyll content; g_s, stomatal conductance; C_i, intercellular CO_2 concentration; T_r, transpiration rate; C_i/C_a, intercellular-to-ambient CO_2 concentration ratio; F_v/F_m, the maximum efficiency of PSII photochemistry; $\Delta F/F'_m$, PSII operating efficiency; *qP*, the coefficient of photochemical quenching; *NPQ*, the nonphotochemical quenching. Level of significance: * P ≤ 0.05; ** P ≤ 0.01; absence of an asterisk denotes a non-significant effect.

CO_2 assimilation showed close ($P < 0.001$) positive correlation with leaf chlorophyll content which is an important component of the non-stomatal limitation factors (Table 3-1), with higher content of leaf chlorophyll observed in the plants of salt-tolerant accession. The salt-induced reduction in the leaf chlorophyll content may be attributed to impaired biosynthesis or accelerated pigment degradation (Matile *et al.*, 1999; Eckardt, 2009; Ashraf and Harris, 2013), and therefore lead to impairment in electron transport to reduce photosynthetic capacity. However, it was argued that chlorophyll breakdown resulted from the increased level of toxic Na^+ was markedly less affected by salt stress than chlorophyll biosynthesis did, because the important precursors of chlorophyll, such as glutamate and 5-aminolaevulinic acid (ALA), decreased in salt-stressed calli and leaves of sunflower (Vieira dos Santos and Caldeira, 1999; Santos, 2004; Akram and Ashraf, 2011).

Chlorophyll *a* fluorescence emission kinetic characteristics have been considered as probes of photosynthesis *in vivo* owing to the insights of the relationships between fluorescence parameters and photosynthetic electron transport in photosystem II (PSII). F_v/F_m is the relative determination of the maximum quantum yield of PSII primary photochemistry used as a sensitive indicator of plant photosynthetic performance under abiotic and biotic stresses (Baker, 2008; Ashraf and Harris, 2013). In the present study, CO_2 assimilation was hardly related to F_v/F_m in the tolerant accession, while a significant ($P < 0.05$) correlation coefficient was found in the sensitive accession (Table 3-1). The decrease of F_v/F_m ratio from day

10 in the plants of sensitive accession indicated the damage or inactivation of a proportion of PSII reaction centers, termed as photoinhibition (Maxwell and Johnson, 2000; Baker and Rosenqvist, 2004). The significant decreases of $\Delta F/F'_m$ and *qP* showed positive correlation with the reduction of *A* and g_s (Table 3-1). $\Delta F/F'_m$ can be used to estimate overall photosynthetic capacity *in vivo*, since it can also be used to estimate the quantum yield of linear electron flux under a given photosynthetically active photon flux density (PPFD) (Maxwell and Johnson, 2000, Baker, 2008). *qP* provides an estimate of the proportion of PSII reaction centers that are open. In the salt-tolerant accession (JM0119), the decreased efficiency of the light absorbed by PSII used for Q_A reduction ($\Delta F/F'_m$) could be mainly attributable to salt-induced closure of PSII reaction centers according to the decline of *qP* values and changeless F_v/F_m ratio. However, slight damage to PSII (indicating by decrease of F_v/F_m) and closure of PSII reaction centers were both responsible for the decline of PSII operating efficiency in JM0099. Since dramatic variation in non-photochemical quenching under dark-adapted leaves (F_v/F_m) was not observed in both accessions, we invested the heat dissipation efficiency induced by light relative to that in the dark (*NPQ*). Significant negative correlation between *NPQ* and *A* (Table 3-1) indicated that the demand for products of electron transport was reduced by CO_2 assimilation decline, and thus thermal dissipation of light energy was increased to avoid oxidative damage (James *et al.*, 2002; Takahashi and Murata, 2008; Stepien and Johnson, 2009).

The activities of photosynthetic enzymes was also reported to influence the CO_2 assimilation. Negative correlations between the activities of PEPC, PPDK, and NADP-MDH and *A* were observed in JM0119, and negative correlations between the activities of PPDK, NADP-ME, and NADP-MDH and *A* were observed in JM0099 (Table 3-2). The salt-enhancement of PEPC activity was reported to support organic acid synthesis owing to maintained malate concentration under salinity (Hatzig, *et al.*, 2010). Another proposal was that the increased activity of PEPC may be a response to scavenge limited substrate to maintain the rate of carboxylation due to decreased CO_2 concentration in mesophyll cells by salt-induced stomatal closure (Carmo-Silva *et al.*, 2008; Omoto, *et al.*, 2012). However, the decreased CO_2 concentration in mesophyll cells may result from a reduced mesophyll conductance rather than stomatal closure due to maintained or even increased C_i in the present study. And this decline of mesophyll conductance may be linked to physical alterations in leaf intercellular structure, biochemistry (bicarbonate to CO_2 conversion), and/or membrane permeability (Chaves *et al.*, 2009). PPDK is consider as one of the rate-limiting enzymes in C_4 photosynthesis. The enhancement of PPDK activity could considered to be contributable to a rapid regeneration of PEP to support accelerated PEPC activity in PEP carboxylation (Aoyagi and Bassham, 1986; Omoto, *et al.*, 2012). This is consistent with the significant correlation found between PEPC and PPDK (Table 3-2), with similar variation pattern between both enzymes displayed in each accession. Nevertheless, the salt-increased PPDK activity

Table 3-2. Correlation coefficients between the photosynthetic rate (*A*) and activities of PEPC, PPDK, NADP-MDH, NADP-ME, and RuBisCO in salt-treated plants of two accessions.

Trait	Accession	*A*	PEPC	PPDK	NAPD-MDH	NADP-ME	RuBisCO
A	JM0119	1.000					
	JM0099	1.000					
PEPC	JM0119	**-0.690****	1.000				
	JM0099	-0.170	1.000				
PPDK	JM0119	**-0.540****	**0.710****	1.000			
	JM0099	**-0.369****	**0.379****	1.000			
NAPD-MDH	JM0119	**-0.541****	**0.609****	**0.634****	1.000		
	JM0099	**-0.680****	0.251	**0.484****	1.000		
NADP-ME	JM0119	-0.073	0.075	0.037	0.285*	1.000	
	JM0099	**-0.603****	0.203	**0.434****	**0.783****	1.000	
RuBisCO	JM0119	0.060	0.009	0.028	0.029	-0.072	1.000
	JM0099	0.101	-0.092	0.129	0.115	0.072	1.000

Level of significance: * P ≤ 0.05; ** P ≤ 0.01; absence of an asterisk denotes a non-significant effect.

was proposed to be examined separately in MC and BMC because PPDK in BSC chloroplast may also function as that in MC chloroplast due to salt-induced damage in MC chloroplast (Omoto, *et al.*, 2012). NADP-MDH is involved in the malate-oxaloacetate shuttle, namely malate valve, facilitating to balance the ATP/NADPH ratio in the chloroplast by the regeneration of the electron acceptor $NADP^+$, particularly when CO_2 assimilation is restricted (Scheibe *et al.*, 2005; Hebbelmann *et al.*, 2012). NADP-MDH catalyzes OAA conversion to malate using excess NADPH. Its activation is inhibited by the product $NADP^+$, thus suppress the export rate of malate (Scheibe *et al.*, 2005). In addition to scavenging substrates, we also agreed with the proposal that the increase in NADP-MDH activity may be a result of the activation of the malate valve by a higher NADPH/$NADP^+$ ratio to alleviate photoinhibition by reactive oxygen species generating from excess reducing equivalents of NADPH (Omoto, *et al.*, 2012). The activity of NADP-ME showed different variation in the accessions, floating around the control level in JM0119 and markedly increased in JM0099. Significant correlation between NADP-MDH and NADP-ME (Table 3-2) was coincident with the fact that NADP-ME is also involved in the regulation of malate which movably storage CO_2 and NADPH in C_4 plants. Although the increased activity of NADP-ME could release more CO_2 for RubisCO, excess NADPH generated simultaneously. Takeuchi *et al.* (2000) indicated that growth inhibition in transgenic rice plants expressing a high level of maize C_4 NADP-ME was attributed to increased photoinhibition

resulted from increased NADPH/$NADP^+$ ratio. Therefore, maintained NADP-ME activity under salt stress is a tolerant behavior to avoid generating more reducing equivalents. The changeless activity of RuBiCO under chlorophyll basis and severe decrease under fresh weight basis indicated a similar decrease in RuBiCO activity as that in chlorophyll content. This reduction may be contributed to the decline of RuBiCO protein content (Omoto, *et al.*, 2012; Galmés *et al.*, 2013).

Compared with the sensitive accession, the salt tolerant accession had pronounced higher fructose content under control condition and showed earlier increase in fructose and sucrose response to salinity, suggesting a constitutive adaptation to osmotic stress. Dramatically raised soluble sugars observed in the leaves of both accessions may result from accumulation effects caused by water loss (Hatzig *et al.*, 2010), thus function as osmolytes in maintenance of cell turgor and protection of membranes and proteins from stress damage. In addition to osmotic adjustment and osmoprotection, an important role in the regulation of photosynthesis under imbalanced source-sink status due to abiotic stress was propounded. In C_4 pathway, photosynthate generated in the Calvin cycle in the BSC chloroplasts is transported to MC chloroplasts and exported to the cytosol to be used for glycolysis or converted to sucrose for local use or export to sink tissues, while starch is a transient storage of excess photosynthate in the chloroplast during the day and breakdown to glucose during the night (Rolland *et al.*, 2006; McCormick *et al.*, 2008). In accordance with the significantly negative relationships between soluble

sugars and CO_2 assimilation in both accessions (Table 3-3), the salt-induced increase of soluble sugars may also be a consequence of reduced sink carbon demand due to the limited growth rate (Roitsch, 1999; McCormick *et al.*, 2008; Hajlaoui *et al.* 2010; Hu *et al.*, 2013). Moreover, the negative correlation between sugar content and chlorophyll content (Table 3-3) may consist with the repressive effect of HXK-dependent sugar signaling on the expression of the gene encoding chlorophyll a/b binding protein (*CAB*) (Criqui *et al.*, 1992; Harter *et al.*, 1993; Krapp *et al.*, 1993). Non-significant changes in starch could be dependent on both triose-phosphate utilization and glucose generation (Paul and Foyer, 2001).

Stable protein content and accumulated total free-amino acids content observed in the tolerant accession indicated better osmotic accommodation to the build-up of ions and resistance to salt-induced protein degradation due to accumulated ionic toxicity (Parvaiz and Satyawati, 2008). The steady-state of total free-amino acids content in the sensitive accession may be due to a balance between the rate at which they were released during protein degradation and the rate at which they were removed by efflux from the leaf (Hajlaoui *et al.* 2010). Since soluble protein and chlorophyll content are markers for leaf N status and total leaf free-amino acid content reflects whole-plant N status (Hirel *et al.*, 2005), the relative higher contents of protein, leaf total free-amino acid, together with less reduced chlorophyll content in the salt-tolerant accession implied that this accession had more efficient nitrate assimilation under low water use induced by salinity.

Table 3-3. Correlation coefficients between the photosynthetic rate (*A*), chlorophyll content, contents of glucose, fructose, sucrose, total soluble sugar (TSS), starch, protein, and total free-amino acids (TAA) in salt-treated plants of two accessions.

Trait	Accession	*A*	Chl	Glucose	Fructose	Sucrose	Sugars	Starch	Protein	TAA
Glucose	JM0119	**-0.538****	**-0.797****	1.000						
	JM0099	**-0.487****	**-0.715****	1.000						
Fructose	JM0119	**-0.408****	**-0.503****	**0.547****	1.000					
	JM0099	**-0.628****	**-0.794****	**0.794****	1.000					
Sucrose	JM0119	**-0.632****	**-0.810****	**0.845****	**0.583****	1.000				
	JM0099	**-0.679****	**-0.826****	**0.586****	**0.742****	1.000				
TSS	JM0119	**-0.629****	**-0.828****	**0.902****	**0.668****	**0.987****	1.000			
	JM0099	**-0.692****	**-0.879****	**0.794****	**0.879****	**0.953****	1.000			
Starch	JM0119	0.063	0.393*	-0.384*	-0.226	-0.280	-0.316*	1.000		
	JM0099	**0.433****	0.341*	-0.271	-0.349*	-0.354*	-0.369*	1.000		
Protein	JM0119	0.184	0.167	-0.220	-0.319*	-0.177	-0.217	0.139	1.000	
	JM0099	**0.628****	**0.681****	**-0.437****	**-0.553****	**-0.646****	**-0.644****	**0.444****	1.000	
TAA	JM0119	**-0.495****	**-0.523****	**0.524****	**0.440****	**0.626****	**0.626****	-0.139	-0.255	1.000
	JM0099	-0.199	0.016	0.080	-0.058	0.033	0.034	-0.120	-0.100	1.000

Level of significance: * P ≤ 0.05; ** P ≤ 0.01; absence of an asterisk denotes a non-significant effect.

In conclusion, the work of this study revealed that greater photosynthetic capacity under salt stress in *M. sinensis* was mainly associated with non-stomatal factors including less chlorophyll loss, higher PSII operating efficiency, enhanced activities of PEPC and PPDK, and lower activity of NADP-ME. Despite the repressive effect on plant photosynthesis due to imbalanced source-sink relationship, accumulated soluble sugars provided osmotic adjustment and osmprotection in leaves. More efficient nitrate assimilation was also related to salt-tolerance owing to greater contents of protein and total leaf free-amino acid.

CHAPTER 4

Adaptation Responses of Genes to NaCl Stress in *Miscanthus sinensis*

4.1. Introduction

Nuclear genes encoding the enzymes in the C_4 pathway have been isolated and identified MC- or BSC-specific expression patterns at the transcript level the same as the observation at the protein level (Sheen, 1999; Hibberd and Covshoff, 2010). It is therefore necessary to address our understanding of C_4 gene expression associated with salt tolerance for the facilitation of insights in transcriptional and posttranscriptional regulations. Expression of *PEPC*, *PPDK*, *NADP-MDH*, and *NADP-ME* were reported to be salt-induced in the common ice plant (*Mesembryanthemum crystallinum* L.) during the switch from C_3 photosynthesis to CAM, while *RbcS* expression was post-transcriptional repressed (DeRocher and Bohnert, 1993; Cushman and Bohnert, 1997).

Salinity affected plants through two stress components: an osmotic stress and an ionic toxicity, especially sodium toxicity as elevated NaCl concentration dominates the saline soil condition. Influx of Na^+ could be achieved through plasma-membrane nonselective cation channels (NSCCs) or anatomical ‘leaks’ in the root endodermis (Davenport and Tester, 2000; Hasegawa *et al.*, 2000; Demidchik and Tester, 2002;

Munns and Tester, 2008), and this striking increase in cytoplasmic Na^+ disrupts enzymatic functions and is toxic to both cells and the whole plants. Therefore, decades of study have been dedicated to the characterization of Na^+ transport and distribution in plants (Hasegawa, *et al.*, 2000; Munns and Tester, 2008; Kronzucker and Britto, 2011; Agarwal *et al.*, 2014). Na^+ transport involves a group of genes that play critical roles in ion homeostasis, and herein the Na^+/H^+ antiporters (SOS1 localized at the plasma membrane and NHX1 located in tonoplasts) facilitate the maintenance of appropriate Na^+ concentration in the cytosol to minimize cytotoxicity. At the cellular level, SOS3, SOS2, and SOS1 are essential components of the *Salt Overly Sensitive* (SOS) signaling pathway that mediate cellular signaling under salt stress (Ji *et al.*, 2013). The primary calcium sensor SOS3 which is a calcineurin-like, myristoylated Ca^{2+}-binding protein perceive the increase in cytosolic Ca^{2+} induced by excess cytosolic Na^+ and activates the serine/threonine protein kinase SOS2 (Liu and Zhu, 1998; Halfter *et al.*, 2000; Liu *et al.*,2000), then in turn activates SOS1 and causes extrusion of excessive Na^+ from the cytosol (Qiu *et al.*, 2002; Quintero *et al.*, 2002; Mart ínez-Atienza *et al.*, 2007; Quintero *et al.*, 2011). At the whole-plant level, SOS1 has been proposed previously to promote Na^+ efflux from roots (Elphick *et al.*, 2001, Ol ás *et al.*, 2009) and facilitate Na^+ retrieval from or delivery to the xylem (Shi *et al.*, 2002; Ol ás *et al.*, 2009; Yadav *et al.*, 2012), maintaining a low-sodium zone at the root (Oh *et al.*, 2009). Compartmentalization of Na^+ into vacuoles is thought to lower toxic Na^+ concentration in the cytoplasm and lower vacuolar osmotic potential

to maintain turgor pressure and cell expansion under salt stress (Munns and Tester, 2008). The sequestration of Na^+ in the central vacuole was proved to be important to salt tolerance by overexpression of NHX in various species, such as tomato (*Solanum lycopersicum* L.), rapeseed (*Brassica napus* L.), rice (*Oryza sativa* L.), maize (*Zea mays* L.), wheat (*Triticum aestivum* L.), cotton (*Gossypium hirsutum* L.), and tobacco (*Nicotiana tabacum* L.) (He *et al.*, 2005; Lu *et al.*, 2005; Ohta *et al.*, 2002; Xue *et al.*, 2004; Yin *et al.*, 2004; Zhang and Blumwald, 2001; Zhang *et al.*, 2001). In addition to the function of vacuolar sequestration of Na^+, NHX1 transporter also plays a role in pH homeostasis (Bassil *et al.*, 2011); in plant development (Hanana *et al.*, 2007; Bassil *et al.*, 2011); in the transport of other monovalent cations include K^+, Li^+, Rb^+, and Cs^+ (Venema *et al.*, 2002; Wu *et al.*, 2005; Leidi *et al.*, 2010); in vesicle trafficking and protein targeting (Sottosanto *et al.*, 2007); and in regulation of stomatal function (Barragán *et al.*, 2012).

In the present study, we reported the adaptation responses of genes involved in C_4 path way (*PEPC*, *PPDK*, *NADP-MDH*, *NADP-ME*, and *RbcS*) and genes encoding Na^+/H^+ antiporters NHX1 and SOS1 to NaCl stress in two *M. sinensis* accessions JM0119 (salt-tolerant) and JM0099 (salt-sensitive). These salt-induced variation of gene expression provided evidences for insights of the molecular mechanisms of salt tolerance in *M. sinensis*.

4.2. Materials and Methods

4.2.1. Plant Materials and Growth Conditions

Seeds of two *M. sinensis* accessions with distinct salt-tolerance, JM0119 (salt-tolerant) and JM0099 (salt-sensitive) were surface-sterilized with 70% ethanol for 30 s and with 1% (v/v) sodium hypochlorite (NaClO) for 10 min, and rinsed three times with distilled water. Seeds of each accession were germinated on filter paper in a closed 90-mm Petri dish filled with 20 ml distilled water in a growth chamber at 12 h photoperiod with 500 μmol $m^{-2}s^{-1}$ PPF, 70% humidity, and 28/22 ℃ day/night regime. Seven-day old uniform seedlings were transplanted into a 500-ml pot and hydroponically acclimated in distilled water for seven days. Seedlings were thinned to ten per pot and grown in salt-free 1/2 Hoagland solution (concentration were gradually increased in five days) for 14 days, following by salt treatments of 1/2 Hoagland solution containing 0 (control), 100, 200, and 300 mM NaCl. Salt addition gradually increased at a progressive rate of 50 mM per day until the final treatment levels to avoid osmotic shock. Leaf and root samples were harvested 24 h after salt application for each treatment and three days after salt application for 300 mM NaCl treatment. Samples were immediately immersed in liquid nitrogen and stored at -80 ℃. Leaf samples for analysis of C_4 genes were obtained as described in 3.2.1.

4.2.2. RNA Extraction, Degenerated PCR, Cloning and Sequencing

Frozen samples from leaf and root tissues of *M. sinensis* harvested on different date were ground in liquid nitrogen and total RNA from each sample was extracted using a TRIzol reagent according to the protocol (Life technologies Corp.; Carlsbad, USA). The first-strand cDNA was synthesized with 2 μg of total RNA with a high capacity RNA-to-cDNA kit (Applied Biosystems, Inc.; Foster, USA) and used as a template for a 50-μl PCR (PrimeSTAR HS DNA Polymerase; TaKaRa Bio Inc.; Otsu, Shiga, Japan) primed with gene-specific degenerated primers (Table 4-1). Primers of DP 1 and DP 2 targeting C_4 *PEPC* were designed based on an alignment of the C_4 PEPC peptide sequences of *Panicum laetum* (GenBank accession number FN999993), *Saccharum officinarum* (AJ293346), *Sorghum verticilliflorum* (AJ293347), and *Z. mays* (NM_001111948). Primers of DP 3 and DP 4 targeting C_4 *PPDK* were designed based on an alignment of the C_4 PPDK peptide sequences of *M. ×giganteus* (AY262272), *Sa. officinarum* (DQ631674), *So. bicolor* (AY268138), and *Z. mays* (HQ697603). Primers of DP 5 and DP 6 targeting *NADP-MDH* were designed based on an alignment of the NADP-MDH peptide sequences of *Saccharum* hybrid (AJ565857), *So. bicolor* (X53453), and *Z. mays* (JF810422). Primers of DP 7 and DP 8 targeting *NADP-ME* were designed based on an alignment of the NADP-ME peptide sequences of *O. sativa* (D16499), *So. bicolor* (AY274836), and *Z. mays* (NM_001111843). Primers of DP 9 and DP 10 targeting

Table 4-1. Sequences of primer pairs used for degenerated PCR in *Miscanthus sinensis*.

Gene		Primers Sequences (5'-3')	T_m(°C)	Degeneracy
PEPC	DP 1	GCCCCTGATCAAGTTCTGCTCntggatgggng	63.5	16
	DP 2	TGGGTGGTGATGGCGtcdatnacrtc	62.7	24
PPDK	DP 3	GAAGGAGCTGGTGGGGcartayaarga	64.8	8
	DP 4	TCCTTGTAGGCGGATGGGttytcraaytg	63.9	8
NADP-MDH	DP 5	CCATACGAGGTGTTCGAGGAygtngaytggg	61.6	16
	DP 6	CATGGCATGGAGAACACGatrtcytcngc	61.9	16
NADP-ME	DP 7	AGTTCGAGGACTTCGCCaaycayaaygc	60.9	8
	DP 8	GGTGGGAAGATGGAGCCCktnwcraartt	62.8	64
RbcS	DP 9	GGCCAGTCTACGGCAACAAGaarttygarac	65.7	8
	DP 10	CACTGGGTCTGCCGGATGttrtcraancc	65.7	16
NHX1	DP 11	CGGCTTCCAGGTGAAGAAGaarcarttytt	63.9	8
	DP 12	CCGGGAGGACTCGGTCacrttrtgcca	64.1	4
SOS1	DP 13	CGAGTCCTCCTTCTCCatggarrtnca	63.9	16
	DP 14	GATGTAGGCGACCATCtcccaraartg	64.5	4

RbcS were designed based on an alignment of the RuBisCO small subunit peptide sequences of *M. ×giganteus* (EU219924), *Saccharum* hybrid (JN591757), *So. bicolor* (AB564718), and *Z. mays* (X06535). Primers of DP 11 and DP 12 targeting *NHX1* were designed based on an alignment of the NHX1 peptide sequences of *Aeluropus lagopoides* (GU199336), *Arabidopsis thaliana* (NM_122597), *Diplachne fusca* (JF933902), *Eutrema halophilum* (DQ995339), *O. sativa* (AB021878), *Phragmites australis* (AB211145), *Puccinellia tenuiflora* (AB628206), and *Z. mays* (NM_001111751). Primers of DP 13 and DP 14 targeting *SOS1* were designed based on an alignment of the SOS1 peptide sequences of *Aegilops speltoides* (FN356230), *Aeluropus littoralis* (JN936862), *Arabidopsis thaliana* (AF256224), *Brachypodium sylvaticum* (FJ234838), *O. sativa* (AY785147), *Ph. australis* (AB244217), *Pu. tenuiflora* (AB628205), and *Triticum aestivum* (AY326952). The PCR was conducted under a regime of 94°C for 4 min, followed by 35 cycles of 98°C for 10 s, 54°C for 15 s (5 s for *SOS1* primers), and 72°C for 60 s. Purified amplicon (Agarose Gel DNA Extraction Kit; TaKaRa Bio Inc.; Otsu, Japan) was ligated into pBluescript II SK (-) vector (Agilent Technologies, Inc.; Santa Clara, USA), and transformed into competent DH5α *Escherichia coli* cells (Life technologies Corp.; Carlsbad, USA). Plasmid DNA was isolated from *E. coli* culture using a GenElute plasmid miniprep kit (Sigma-Aldrich; St. Louis, USA).

Table 4-2. Sequences of gene specific primer pairs used for real-time PCR in *Miscanthus sinensis*.

Gene		Primers Sequences (5'-3')
PEPC	RT 1	TTCCTTCAAACGAGCCCT
	RT 2	GGTAAACACCGAGTCCTCA
PPDK	RT 3	GTGCCGTAAAGATTGCTGTG
	RT 4	GCGGATGGGTTTTCAAACTG
NADP-MDH	RT 5	ATGACAGTTCAAAAGCGTGG
	RT 6	CTTCTGGGGTAGGAGTCACAA
NADP-ME	RT 7	CCACAATGCCTTTGATTTGC
	RT 8	ACCAACCATCTTGAGTGCTG
RbcS	RT 9	TCGAGTTCAGCAAGGAAGGC
	RT 10	TTGGCAGCTTCCACATGGTC
NHX1	RT 11	CGTCTGTTGTGCTCTTCAAT
	RT 12	GAGCAATCCAGTAAACACTCC
SOS1	RT 13	CTTGGAAGAACCTTTGATGC
	RT 14	CCCAGCCACAGTATTGACA
Actin	RT 15	GAAACCTTTGAATGCCCAG
	RT 16	GGAGTCCATCACAATACCAGT

4.2.3. Quantitative Real-time PCR Analysis

Extracted total RNA was purified and treated with RNase-free DNase (Recombinant DNase I; TaKaRa Bio Inc.; Otsu, Shiga, Japan). Quantitative real-time PCR (qRT-PCR) assay was performed on an Applied Biosystems 7500 real-time PCR system (Applied Biosystems, Inc.; Foster, USA), with SYBR *Premix Ex Taq* II (TaKaRa Bio Inc.; Otsu, Japan) according to the manufacturer's instructions. Gene-specific primers for real-time PCR analysis were designed on the basis of the obtained approximately 600 bp-long sequence of each gene (Table 4-2). *Actin* gene of *M. sinensis* (JN983213) was used as the reference gene. The PCR program comprised a denaturation of 95°C for 30 s and 45 cycles of 95°C for 5 s and a combined annealing/extension phase of 60°C for 30 s, followed by a melt curve analysis. C_t (cycle threshold) values were determined in auto C_t mode using Applied Biosystems, 7500 real time PCR system software and used to calculate gene expression relative to an internal control gene.

4.2.4. Data Analysis

All data was analyzed by Statistical Product and Service Solutions (SPSS Statistics, Version 20; IBM Corp.; New York, USA). The significance of the differences between salt treatments means was determined by a Student's t-test ($\alpha < 0.05$).

```
                10         20         30         40         50         60         70
           ....|....|....|....|....|....|....|....|....|....|....|....|....|....|
MISI   1   RDGNPRVTPEVTRDVCLLSRMMAANLYIDQVEDLMFELSMWRCNDELRARAEELQSAPASKKVTKYYIEF
SAOF   1   RDGNPRVTPEVTRDVCLLSRMMAANLYIDQVEDLMFELSMWRCNDELRARAEEVQSTPASKKVTKYYIEF
SOBI   1   RDGNPRVTPEVTRDVCLLSRMMAANLYINQVEDLMFELSMWRCNDELRARAEEVQSTPASKKVTKYYIEF
ZEMA   1   RDGNPRVTPEVTRDVCLLARMMAANLYIDQIEELMFELSMWRCNDELRVRAEELHSSSGSK-VTKYYIEF
FLTR   1   RDGNPRVTPEVTRDVCLLARMMTSNMYFSQIEDLMIEMSMWRCNSELRVRAEELYRT--ARKDVKHYIEF
           ******************:***::*:*:.*:*:**:*:******.***.****:  :  ::  .*:****

                80         90         100        110        120        130        140
           ....|....|....|....|....|....|....|....|....|....|....|....|....|....|
MISI   71  WKQIPSNEPYRVILGAVRDKLYNTRERARHLLATGFSEISEDSVFTKIEEFLEPLELCYKSLCDCGDKAI
SAOF   71  WKQIPPNEPYRVILGAVRDKLYNTRERARHLLATGFSEISVDSVFTNIEEFLEPLELCYKSLCDCGDKAI
SOBI   71  WKQIPPNEPYRVILGAVRDKLYNTRERARHLLATGFSEISEDAVFTKIEEFLEPLELCYKSLCECGDKAI
ZEMA   70  WKQIPPNEPYRVILGHVRDKLYNTRERARHLLASGVSEISAESSFTSIEEFLEPLELCYKSLCDCGDKAI
FLTR   69  WKRIPPNQPYRVILGDVRDKLYNTRERSRHLLVDGKSDIPDEAVYTNVEQLLEPLELCYRSLCDCGDHVI
           **:**.*:******* **********:****. * *:*. :: :*.:*::*********:***:***:.*

                150        160        170
           ....|....|....|....|....|....|...
MISI   141 ADGSLLDLLRQVFXFGLSLVKLDIRQESERHTDVXDAI
SAOF   141 ADGSLLDLLRQVFTFGLSLVKLDIRQESERHTDVIDAI
SOBI   141 ADGSLLDLLRQVFTFGLSLVKLDIRQESERQTDVIDAI
ZEMA   140 ADGSLLDLLRQVFTFGLSLVKLDIRQESERHTDVIDAI
FLTR   139 ADGSLLDFLRQVSTFGLSLVKLDIRQESDRHTEVLDAI
           *******:****  **************:*:*:* ***
```

Figure 4-1. Alignment of partial putative translated polypeptide of C_4-PEPC from *M. sinensis* (MISI), sugarcane (SAOF), sorghum (SOBI), maize (ZEMA), and *F. trinervia* (FLTR). Amino acid sequences were deduced by translation of cDNA from the partial sequence of *C_4-MsPEPC* and from GenBank accession numbers AJ293346 (SAOF), X17379 (SOBI), AJ536629 (ZEMA), and X64143 (FLTR).

4.3. Results

4.3.1. Sequences of C_4 Genes

Based on the degenerated PCR, approximate 600 bp-long cDNA fragments were obtained and sequenced. The cDNA sequences of genes involved in the C_4 pathway were highly conserved. Compared with the other typical C_4 species, the translated putative protein sequence of *C_4-MsPEPC* showed 96%, 95%, 89%, and 73% identity to that of sugarcane, sorghum, maize, and *Flaveria trinervia* (Spreng.) C. Mohr (Fig. 4-1). The translated putative protein sequence of *C_4-MsPPDK* showed 93%, 92%, 92%, 88%, and 77% identity to that of *M. ×giganteus*, sugarcane, sorghum, maize, and *F. trinervia* (Fig. 4-2). The translated putative protein sequence of *C_4-MsNADP-MDH* showed 95%, 95%, 94%, and 89% homologous to that of sugarcane, maize, sorghum, and *F. trinervia* (Fig. 4-3). The translated putative protein sequence of *C_4-MsNADP-ME* showed 97%, 94%, and 76% homologous to that of sorghum, maize, and *F. trinervia* (Fig. 4-4). Moreover, the translated putative protein sequence of *MsRbcS* showed 98%, 98%, 95%, 88%, and 80% identity to that of *M. ×giganteus*, sorghum, sugarcane, maize, and *F. trinervia* (Fig. 4-5).

4.3.2. Real-time PCR Analysis for C_4 genes

The expression of genes involved in the C_4 pathway were strongly affected by salt stress and stress duration (Fig. 4-6). Up-regulation of *PEPC*, *PPDK*, *NADP-MDH*,

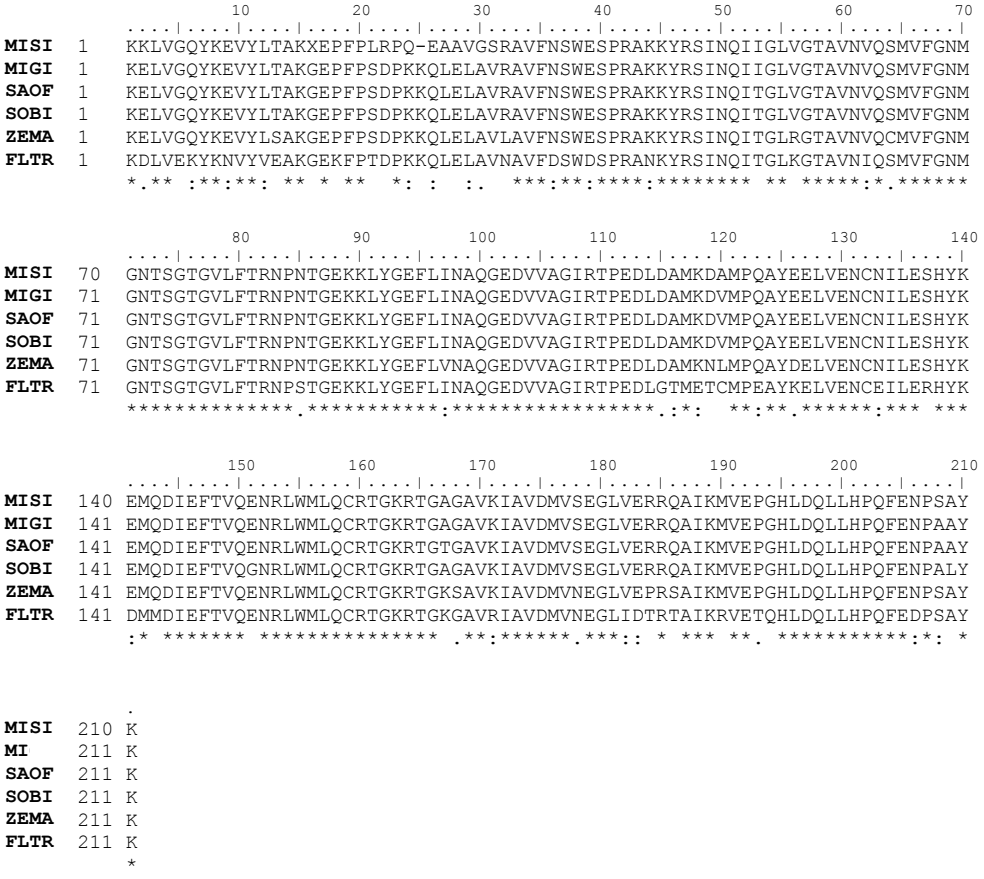

Figure 4-2. Alignment of partial putative translated polypeptide of C_4-PPDK from *M. sinensis* (MISI), *M. ×giganteus* (MIGI), sugarcane (SAOF), sorghum (SOBI), maize (ZEMA), and *F. trinervia* (FLTR). Amino acid sequences were deduced by translation of cDNA from the partial sequence of *C_4-MsPPDK* and from GenBank accession numbers AY262273 (MIGI), DQ631674 (SAOF), AY268138 (SOBI), HQ697603 (ZEMA), and X79095 (FLTR).

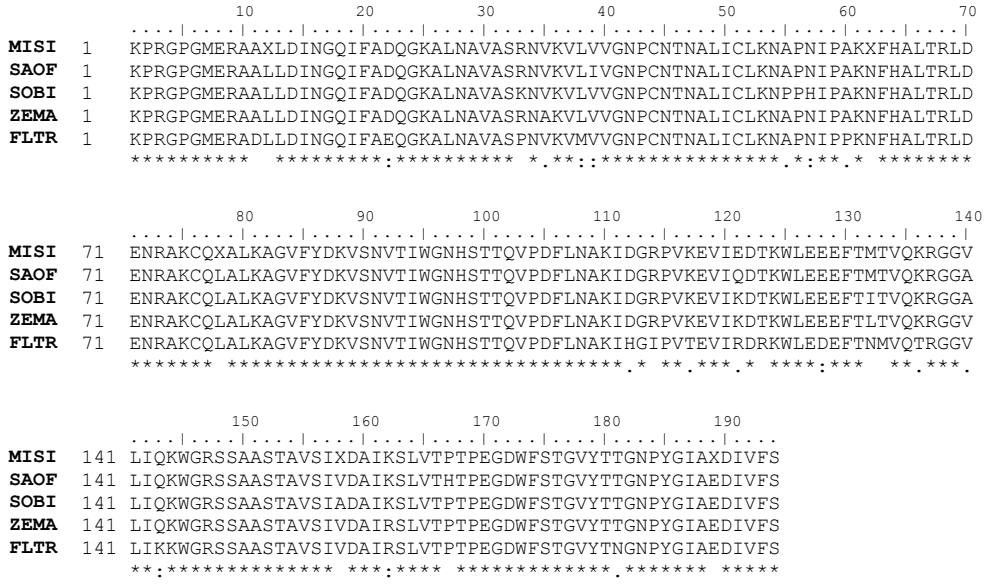

Figure 4-3. Alignment of partial putative translated polypeptide of C_4 NADP-MDH from *M. sinensis* (MISI), sugarcane (SAOF), sorghum (SOBI), maize (ZEMA), and *F. trinervia* (FLTR). Amino acid sequences were deduced by translation of cDNA from the partial sequence of *C_4-MsNADP-MDH* and from GenBank accession numbers AJ344432 (SAOF), X53453 (SOBI), JF810422 (ZEMA), and U22533 (FLTR).

```
                10         20         30         40         50         60         70
           ....|....|....|....|....|....|....|....|....|....|....|....|....|....|
MISI   1   FEDFANHNAFDLLEKYSKSHLVFNDDIQGTASVVLAGLLAALKMVGGTLAEQTYLFLGAGEAGTGIAELI
SOBI   1   FEDFANHNAFDLLEKYSKTHLVFNDDIQGTASVVLAGLLAALKMVGGTLAEQTYLFLGAGEAGTGIAELI
ZEMA   1   FEDFANHNAFDLLEKYSKSHLVFNDDIQGTASVVLAGLLAALKMVGGTLAEQTYLFLGAGEAGTGIAELI
FLTR   1   FEDFANHNAFDLLEKYRTTHLVFNDDIQGTASVVLGGLISALKLVGGSLADQKFLFLGAGEAGTGIAELI
           ***************** .:****************.**::***:***:**:*.:****************

                80         90         100        110        120        130        140
           ....|....|....|....|....|....|....|....|....|....|....|....|....|....|
MISI   71  ALEISKQTKAPIEECRKKVWLVDSKGLIVDSRKNSLAPFKKPWAHEHEPLTTLYDAVQSIKPTVLIGTSG
SOBI   71  ALEMSKQTKAPIEECRKKVWLVDSKGLIVDSRKSSLAPFKKPWAHEHEPLTTLYDAVQSIKPTVLIGTSG
ZEMA   71  ALEISKQTNAPIEECRKKVWLVDSKGLIVDSRKGSLQPFKKPWAHEHEPLKTLYDAVQSIKPTVLIGTSG
FLTR   71  ALEISKQTNIPLEESRKKVWLVDSKGLIVRSRLDSLQHFKKPWAHDHEPVNEFLDAIKTIRPTVLIGSSG
           ***:****: *:**.************** ** .**  *******:***:. : **:::*:******:**

                150        160        170        180        190        200        210
           ....|....|....|....|....|....|....|....|....|....|....|....|....|....|
MISI   141 VGRTFTKEIVEAMASINERPIIFSLSNPTSHSECTAEQAYTWTQGRAVFASGSPFASVEYDGKTFVPGQS
SOBI   141 VGRTFTKEIVEAMASINERPIIFSLSNPTSHSECTAEQAYTWTQGRAVFASGSPFAPVEYDGKTFVPGQS
ZEMA   141 VGRTFTKEIIEAMSSFNERPIIFSLSNPTSHSECTAEQAYTWSQGRSIFASGSPFAPVEYEGKTFVPGQS
FLTR   141 TGQTFTKEVVETMSSLNEKPIILALSNPTSQSECTAEQAYTWSEGRAIFASGSPFKPVEYNGKLYVSGQA
           .*:*****::*:*:*:**:***::******:***********::**::******* .***:** :*.**:

                220        230
           ....|....|....|....|....
MISI   211 NNADIFPGLGLGLVMSGAVRVHEDMLLAA
SOBI   211 NNAYIFPGLGLGLVISGAVRVHEDMLLAA
ZEMA   211 NNAYIFPGLGLGLVISGAVRVHEDMLLAA
FLTR   211 NNAYIFPGFGLGLIISGAIRVHDDMLLAA
           *** ****:****::***:***:******
```

Figure 4-4. Alignment of partial putative translated polypeptide of C_4 NADP-ME from *M. sinensis* (MISI), sorghum (SOBI), maize (ZEMA), and *F. trinervia* (FLTR). Amino acid sequences were deduced by translation of cDNA from the partial sequence of *C_4-MsNADP-ME* and from GenBank accession numbers AY274836 (SOBI), NM_001111843 (ZEMA), and X57142 (FLTR).

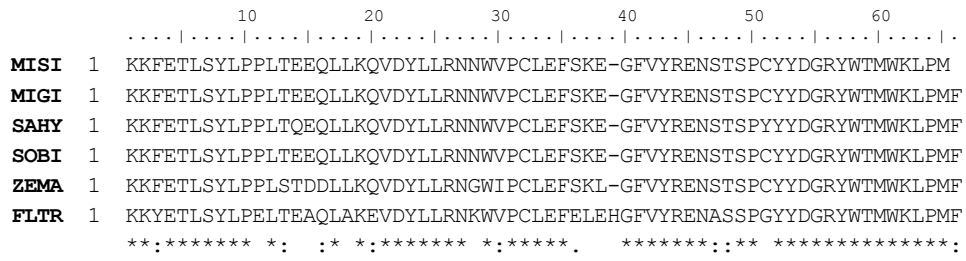

Figure 4-5. Alignment of partial putative translated polypeptide of RuBisCO small subunit from *M. sinensis* (MISI), *M. ×giganteus* (MIGI), sugarcane (SAHY), sorghum (SOBI), maize (ZEMA), and *F. trinervia* (FLTR). Amino acid sequences were deduced by translation of cDNA from the partial sequence of *MsRbcS* and from GenBank accession numbers EU219922 (MIGI), JN591757 (SAHY), AB564718 (SOBI), Y09214 (ZEMA), and X05037 (FLTR).

and *NADP-ME* were observed in both accessions with different patterns, while *RbcS* expression was suppressed by salt stress. Expression of *PEPC* and *PPDK* in JM0119 were progressively raised when the salt treatment lasted, and the expression of both genes showed a single peak curve with the peak value on day 6 in JM0099 (Fig. 4-6A and B). On day 17 relative to the control, the expression of *PEPC* and *PPDK* were increased by about 11-fold and 3-fold, respectively, in JM0119, while regressed to the same level of the control in JM0099. Similar single peak curves were also observed in the expression of *NADP-MDH* and *NADP-ME* in both accessions except for that of *NADP-MDH* in JM0119 (Fig. 4-6C and D). The significant ($P < 0.05$) increase in the expression of *NADP-MDH* in JM0119 was not observed until day 10, and the peak expression of *NADP-ME* in JM0119 was found on day 10 which was later than that in JM0099. Salt-induced expression of both genes were much greater in JM0099 from day 3 than those in JM0119. The peak values of the salt-induced expression of *NADP-MDH* and *NADP-ME* in JM0099 which were observed on day 6 were about 7-fold and 20-fold greater than those of the control, respectively. The decrease in the expression of *RbcS* in both accessions was observed from day 3 (Fig. 4-6E). Although recoveries were observed on day 6 and 10 in JM0099 and JM0119, respectively, the significant ($P < 0.01$) repression in the expression of *RbcS* by salt stress were found on day 17 in both accessions, with 54% and 30% decrease relative to the control in JM0099 and JM0119, respectively.

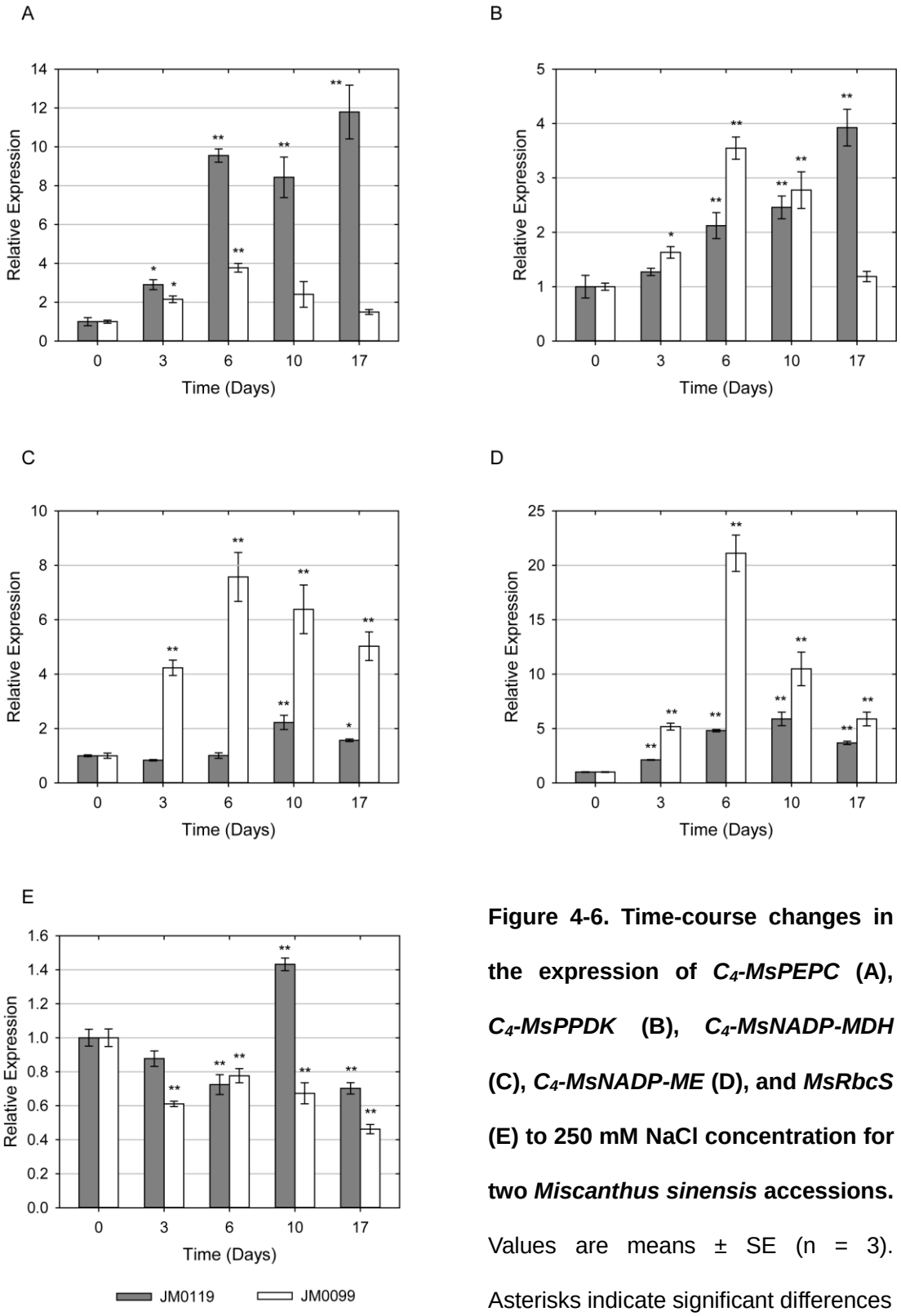

Figure 4-6. Time-course changes in the expression of *C₄-MsPEPC* (A), *C₄-MsPPDK* (B), *C₄-MsNADP-MDH* (C), *C₄-MsNADP-ME* (D), and *MsRbcS* (E) to 250 mM NaCl concentration for two *Miscanthus sinensis* accessions. Values are means ± SE (n = 3). Asterisks indicate significant differences relative to the control (day 0) in each accession, * P ≤ 0.05; ** P ≤ 0.01, absence of an asterisk denotes a non-significant effect (Student's t-test$_{0.05}$).

4.3.3. Sequences of *NHX1* and *SOS1*

The cDNA sequences of genes *NHX1* and *SOS1* were highly conserved. Compared with the other monocotyledon species, the translated putative protein sequence of *NHX1* showed 96%, 94%, 92%, 92%, and 79% identity to that of *Cenchrus americanus* (L.) Morrone, *Diplachne fusca* (L.) Beauv., common reed (*Phragmites australis* (Cav.) Trin. ex Steud.), rice, and maize (Fig. 4-7). The translated putative protein sequence of *MsSOS1* showed 80%, 82%, 82%, 82%, and 79% identity to that of *Distichlis spicata* (L.) Greene, rice, common reed, *Brachypodium sylvaticum* (Huds.) Beauv., and common wheat (*Triticum aestivum* L.) (Fig. 4-8).

4.3.4. Real-time PCR Analysis for *NHX1* and *SOS1*

The expression of the genes encoding the Na^+/H^+ antiporters NHX1 and SOS1 varied under salt stress and treatment duration and showed remarkable differences significantly between accessions (Fig. 4-9). In plant shoots, the expression of *NHX1* was dramatically up-regulated by salt stress in JM0119, while this increase was reduced after 3-days duration under 300 mM NaCl concentration (Fig. 4-9A). Relative to the control, the expression of *NHX1* was 13-fold higher after 24 h treated with 300 mM NaCl and fell to about 4-fold higher after 3-day salt-duration. Significant increase in the expression of *NHX1* was also observed in root tissue of

Figure 4-7. Alignment of partial putative translated polypeptide of NHX1 from *M. sinensis* (MISI), *Dip. fusca* (DIFU), *C. americanus* (CEAM), reed (PHAU), rice (ORSA), and maize (ZEMA). Amino acid sequences were deduced by translation of cDNA from the partial sequence of *MsNHX1* and from GenBank accession numbers JF933902 (DIFU), DQ071264 (CEAM), AB211145 (PHAU), AB021878 (ORSA), and NM_001111751 (ZEMA).

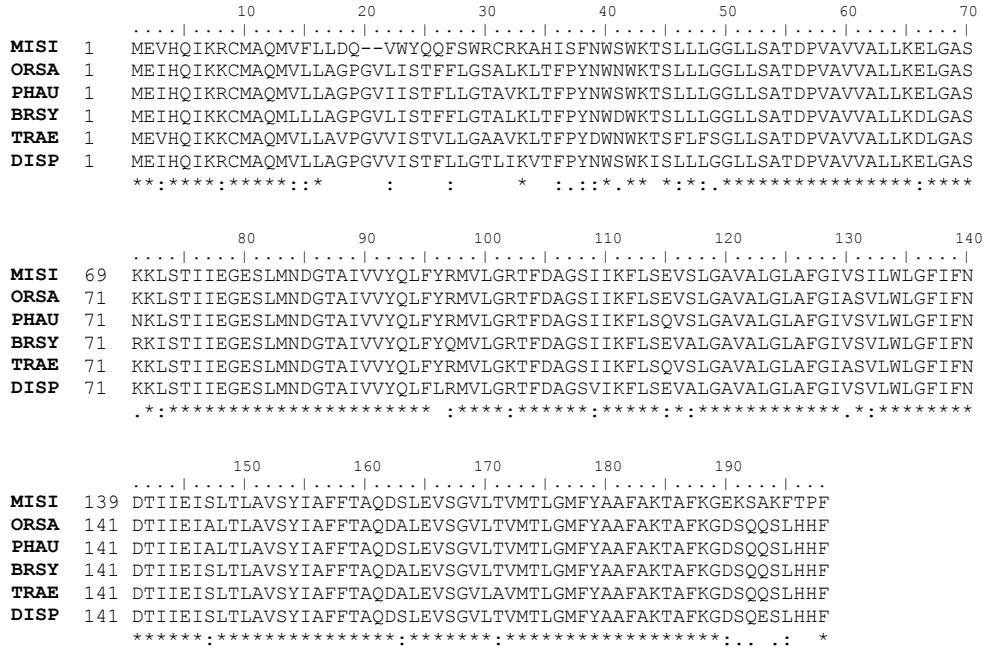

Figure 4-8. Alignment of partial putative translated polypeptide of SOS1 from *M. sinensis* (MISI), rice (ORSA), reed (PHAU), *B. sylvaticum* (BRSY), wheat (TRAE), and *Dis. spicata* (DISP). Amino acid sequences were deduced by translation of cDNA from the partial sequence of *MsSOS1* and from GenBank accession numbers AY785147 (ORSA), AB244217 (PHAU), FJ234838 (BRSY), AY326952 (TRAE), and GU480079 (DISP).

JM0119 under 300 mM salt treatment after the repression at low and moderate salt levels (Fig. 4-9C). However, *NHX1* expression hardly change in shoot tissue of JM0099 except for a significant increase at 100 mM salt treatment, and it was suppressed by salt stress in root tissue of JM0099 (Fig. 4-9A and C). The expression of *SOS1* floated around the control level in the shoot tissues of both accession, while in the root tissue, it was markedly induced by high salt treatment in JM0119 and repressed by all salt treatments in JM0099 (Fig. 4-9B and D).

4.4. Discussion and Conclusion

The genes involved in the C_4 pathway and the genes encoding Na^+/H^+ antiporters showed distinct variation in the accessions under salt regime. Signifcantly higher *PEPC*, *PPDK*, and *RbcS* expression, together with remarkably higher expression of *NHX1* and *SOS1* were associated with salt-tolerance in JM0119.

Variation of C_4 photosynthetic gene expression under salt stress has not been deeply analysed so far attributed to the complex regulation occurring at many levels (Heuer, 2005; Langdale, 2011). The notable reduction in the expression of *RbcS* indicated a marked reduction in the amount of RuBisCO protein. This is consist with the results described in the ice plant and *Aeluropus lagopoides* (DeRocher and Bohnert, 1993; Cushman and Bohnert, 1997; Sobhanian *et al.*, 2010). This salt-

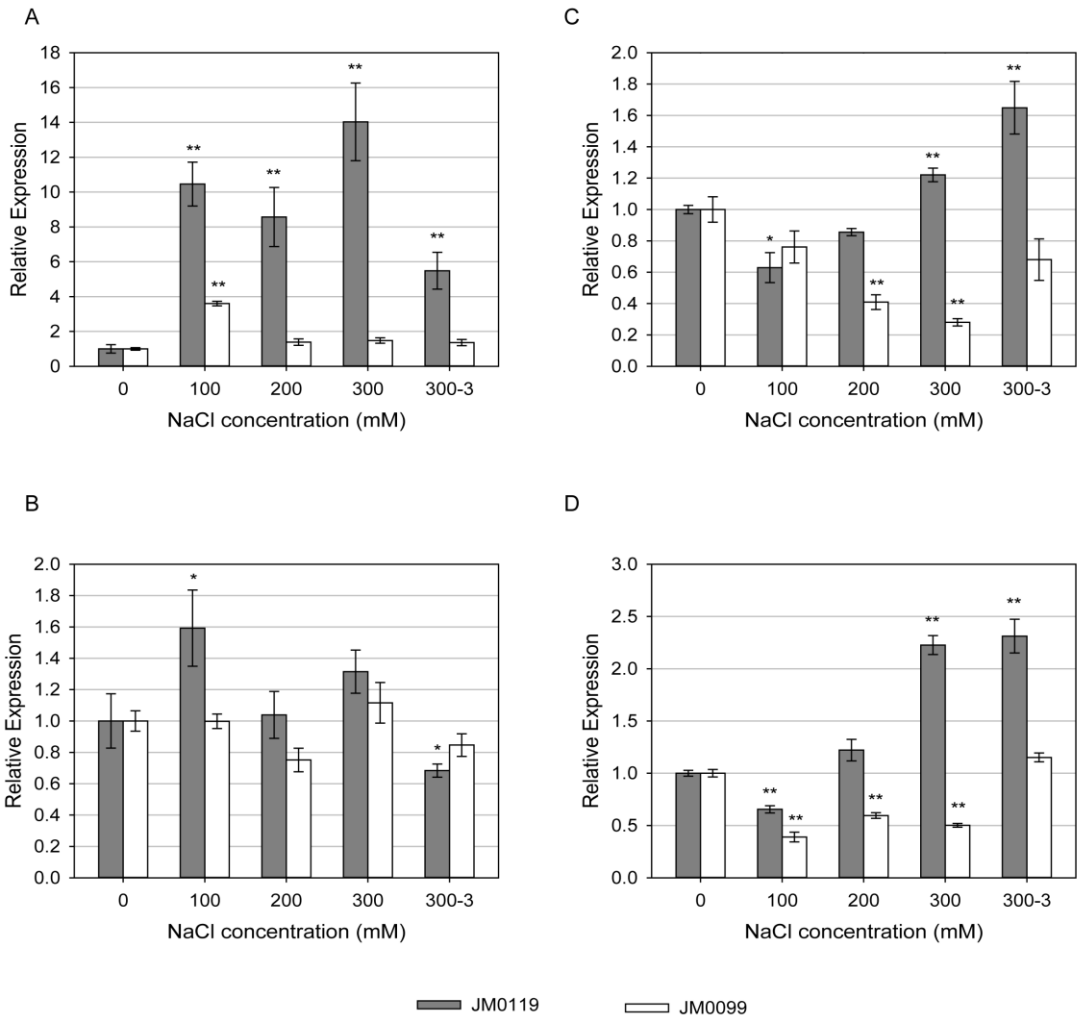

Figure 4-9. Effects of salinity on the expression of *MsNHX1* (A and C) and *MsSOS1* (B and D) in plant shoot（A and B) and root (C and D) tissues to increasing NaCl concentration for two *Miscanthus sinensis* accessions. Values are means ± SE (n = 3). Asterisks indicate significant differences relative to the control (day 0) in each accession, * P ≤ 0.05; ** P ≤ 0.01, absence of an asterisk denotes a non-significant effect (Student's t-test$_{0.05}$).

induced repression of *RbcS* expression was proved to be posttranscriptional regulation to decrease *RbcS* mRNA levels in the ice plant (DeRocher and Bohnert, 1993). Since RuBisCO is considered as one of the rate-limiting proteins in the C_4 pathway, the down-regulation of the *RbcS* expression and subsequently suppressed RuBisCO activity (FW basis) was partially responsible for the decreased photosynthesis by salt stress. The expression of C_4-specific gene may be primarily regulated at the transcriptional level (Cushman and Bohnert, 1997). In the present study, the up-regulation of the expression in *PEPC* and *PPDK* in the present study was in agreement with the proposal that the increased amount of C_4-PEPC and other proteins related to C_4 pathway was a compensation for the suppressed Calvin cycle under salt stress (Sobhanian *et al.*, 2010). The increased NADP-MDH and NADP-ME activities shown in 3.3.4 may be partially influenced by the up-regulated expression of *NADP-MDH* and *NADP-ME* genes, while a posttranscriptional regulation should be responsible for the activity of NADP-ME.

The important mechanism coping with high salinity in plants is the regulation of Na^+ influx, efflux and vacuolar compartmentation (Munns and Tester, 2008). The distinct expression patterns of *SOS1* and *NHX1* during the increase of salt concentration in the salt-tolerant accession (JM0119) indicating different salt-resistant mechanisms. Under 100 mM NaCl stress, *SOS1* and *NHX1* expression were repressed in the salt-treated root tissue of JM0119 and remarkably promoted in the shoot tissue. These phenomena may be the avoidance of the increase in osmotic

stress by sodium extrusion, retainment of Na^+ in stems (Olías *et al.*, 2009), and storage the access Na^+ into cell vacuole of the shoot. When salt stress became more severe (200 mM NaCl), the *SOS1* and *NHX1* expression recovered in the root and less increased in the shoot as the consequences of controlled delivery of Na^+ from the root to the shoot. In roots of JM0119 under high salt stress (300 mM NaCl), both *SOS1* and *NHX1* expression were up-regulated, indicating greatly activated Na^+ extrusion out of the root cells and Na^+ sequestration into the root cell vacuole. In shoots of JM0119, dramatic increase in the expression of *NHX1* suggested that there was strong compartmentation of Na^+ into cell vacuoles. After 3-d under high salinity, shoot *NHX1* and *SOS1* expression were both lower than those measured 24 h after treated with 300 mM NaCl, this may be due to the severe damage to the shoot by Na^+ accumulation. Compared with JM0119, the salt-sensitive accession, JM0099, showed suppressed expression of both genes in the root and changeless expression in the shoot (apart from a significant promotion at 100 mM salt concentration). This was a coincidence of the dramatic increase in Na^+ content in JM0099 shoots described in 2.3.2.4, indicating the lack of the functions of Na^+ efflux and compartmentalization resulted from high Na^+ accumulation in salt-sensitive *M. sinensis* even under moderate salt stress.

In conclusion, higher *PEPC*, *PPDK*, and *RbcS* expression observed in JM0119 were related to greater photosynthetic capacity under salt regime. Expression of *NADP-MDH* and *NADP-ME* may be closely related to each other. Remarkably

higher expression of *NHX1* and *SOS1* were associated with the regulation of Na^+ accumulation in *M. sinensis* by mechanisms involved in Na^+ influx, efflux, and sequestration.

CHAPTER 5

General Discussion

5.1. Screening Methods for Salinity Tolerance of *Miscanthus sinensis*

Despite the inconvenience for the seed set of *M. sinensis* due to its self-incompatibility, it is more cost- and time-effective to obtain *M. sinensis* plants by seeds than by *in vitro* culture or rhizome division. Seed germination could be considered as a direct salt-tolerance selection criterion for *M. sinensis* according to the significant variability of seed germination among accessions under salinity regime. However, it is unavailable to associate the salt-tolerance with seed size, color, or shape, as these factors varied in a large range in native populations of *M. sinensis*. Moreover, environment in the place of origin such as soil and altitude should be studied, since they may be important elements resulting in the differences in salt-tolerance of *M. sinensis* accessions.

Morphological (plant dry weight) and physiological [chlorophyll content (SPAD reading), photosynthetic parameters, and shoot ion contents] traits are also effective measurements in salt-tolerance screening of *M. sinensis*. Salt-induced differences of the plant dry weight between the accessions directly reflect the divergence in salt-tolerance. However, longer-term (at least two weeks) experiments are necessary to detect this divergence, since there was little difference in the shoot dry weight

between the accessions in short-term growth experiment. The measurement of chlorophyll content with the SPAD meter is convenient, non-destructive and is an adequate surrogate for measuring extremes in percent dead leaf. Although F_v/F_m measurement which has been considered to provide a simple and rapid way of monitoring stress (Baker, 2008) was hardly or slightly affected by salt stress and showed minor difference between the accessions of *M. sinensis*., g_s and $\Delta F/F'_m$ are effective measurements reflecting the physiological responses to salinity, especially g_s is one of the most salt-susceptible factors. Shoot ion contents, especially Na^+ content, are also direct evidences for the divergence in salt-tolerance. Content of Na^+ is another salt-susceptible factor in the present study, and is negatively related to salt-tolerance.

5.2. Responses and Mechanisms Acclimated to Salinity

The distinct salt-tolerance between JM0119 and JM0099 were associated with the maintenance of larger total leaf area, a greater number of tillers, higher photosynthetic rate and relatively lower shoot Na^+ accumulation under salinity. The greater photosynthetic capacity under salt regime in JM0119 was mainly associated with non-stomatal factors including less chlorophyll loss, higher PSII operating efficiency, greater activities of PEPC and PPDK which was partially owing to higher *PEPC* and *PPDK* expression, and lower activity of NADP-ME which may be

posttranscriptionally regulated. Moreover, remarkably higher expression of *NHX1* and *SOS1* are associated with the regulation mechanisms of Na^+ accumulation in terms of Na^+ influx, efflux, and sequestration to relieve Na^+ toxicity in plants.

When treated with salt stress, a rapid osmotic stress is exposed on plant due to the salt outside the root. Cells lose water and shrink consequently and leaf stomata are closed (Munns and Tester, 2008; Munns, 2010; Tilbrook and Roy, 2014). Though original turgor and volume of cells can regain over hours owing to osmotic adjustment, including accumulation of compatible solutes such as amino acids and soluble sugars in the cytosol, the leaf expansion rate is reduced over days after salt treatment, paralleling with delayed emergence of new leaves and lateral buds (Munns, 2010). Thus leaf area is decreased, and this decreased leaf area as well as stomatal closure could save water use to lessen the depletion of soil water in the long term. At this timescale, photosynthesis of expanded leaves is also reduced due to stomatal closure. After weeks of salt treatment, the number of tillers declined markedly attributed to the salinity effect on meristematic tissues or signaling regulation transmitted from the roots (Munns, 2010), resulting in a significant reduction in the total leaf area. Therefore, the decreased rate of shoot growth in the vegetative development could be attributed to a gross reduction of the total leaf area and the number of tillers.

Ion toxicity effects, especially Na^+ toxicity, also occur after weeks of salt treatment when salts accumulated in cytoplasm reach excessive levels which exceed the ability of the cells to compartmentalize salts into the vacuole, resulting in injury or

premature senescence in old leaves. Photosynthesis of *M. sinensis* at this time is inhibited mainly attributed to non-stomatal factors, including premature loss of chlorophyll and damage to the photosynthetic apparatus, changes in enzyme activities and gene expression, and negative feedback signals generated by reduced sink activity. The salt-induced reduction in the leaf chlorophyll content may be attributed to impaired biosynthesis or accelerated pigment degradation (Matile *et al.*, 1999; Eckardt, 2009; Ashraf and Harris, 2013), and therefore lead to impairment in electron transport to reduce photosynthetic capacity. The decreased overall photosynthetic capacity, indicating by $\Delta F/F'_m$, for JM0119 could be mainly attributable to salt-induced closure of PSII reaction centers, while slight damage to PSII and closure of PSII reaction centers are both responsible for the decline of $\Delta F/F'_m$ for JM0099. Concurrently, the reduced demand for products of electron transport by CO_2 assimilation decline raises the thermal dissipation of light energy to avoid oxidative damage. Expression of *RbcS* is inhibited by salinity, indicating a reduction of the amount of RuBisCO. In order to compensate the suppression of Calvin cycle by the decreased of the *RbcS* expression, expression of C_4 genes are up-regulated to maintain the photosynthetic capacity. The up-regulation of C_4-gene expression thus partially influence the activities of these enzymes. The activities of PEPC, PPDK, and NADP-MDH are negatively correlated with *A* in both accessions and partially transcriptional regulated. PEPC activities is enhanced to support organic acid synthesis (Hatzig, *et al.*, 2010) and scavenge limited substrate to

maintain the rate of PEP carboxylation, and consequently this reaction needs enhanced PPDK and NADP-MDH activities for the rapid regeneration of PEP and scavenging OAA, respectively. Interestingly, NADP-ME showed different activities between the accessions. Increased activity of NADP-ME could release more CO_2 for RubisCO, while excess NADPH is generated simultaneously. The increase in NADPH/$NADP^+$ ratio would activate the malate valve and promote NADP-MDH activity to alleviate photoinhibition by reactive oxygen species generating from excess reducing equivalents of NADPH. Therefore, NADP-MDH and NADP-ME are both involved in the regulation of malate which movably storage CO_2 and NADPH in C_4 plants. In the whole plant level, the slower growth under salt stress is not considered to be a consequence of limited carbon supply resulted from reduced photosynthesis but is regulated by signaling pathways including a message transmitted from the roots to the shoots (Munns, 2010), since the soluble sugars were remarkably accumulated in shoots as presented in our study. This new relationship between the source and sink tissues would in turn generate feedback signals to fine-tune the rate of photosynthesis to match the reduced sink carbon demand (Roitsch, 1999; McCormick *et al.*, 2008; Hajlaoui *et al.* 2010; Hu *et al.*, 2013). Moreover, the photosynthetic genes expression and photo-assimilate partitioning depend notably on the plant N-status (Scheible, *et al.*, 2004; Rolland *et al.*, 2006) which is reflected by soluble protein, chlorophyll content and total leaf free-amino acid content. Consequently, the photosynthesis is considered to be regulated at the

molecular level by sugar and nitrogen signals through changes in the whole plant C-N balance (Paul and Foyer, 2001; Chikov and Batasheva, 2012).

Striking increase of the cytoplasmic Na^+ disrupts enzymatic functions and is toxic to both cells and the whole plants. Variation in the expression of *NHX1* and *SOS1* indicates different regulation mechanisms of Na^+ influx, efflux and vacuolar compartmentation in JM0119 during the increase of salinity. When treated with low salt treatment, Na^+ is retained in stems and the access Na^+ is stored into leaf cell vacuole to avoid the increase of osmotic stress outside the root by sodium extrusion. Under more severe salt stress, *SOS1* and *NHX1* expression is recovered in the root and less increased in the shoot as the consequences of controlled delivery of Na^+ from the root to the shoot. Under high salt stress, Na^+ is greatly extruded out of the root cells and remainder is compartmentalized into both root and shoot cell vacuoles.

5.3. Future Perspectives

Although our data will be useful in screening for salt-tolerant germplasm and in elucidating physiological and biochemical mechanisms associated with salt stress, further study on photosynthesis and ion transport in *M. sinensis* under representative saline environments are necessary to validate our findings. Studies on PSI and PSII will provide insights to illuminate the factors resulted in the changes in chlorophyll

fluorescence. The activities of C_4 enzymes are under complex regulation at transcriptional, posttranscriptional, translational, and posttranslational levels. For example, it has been known that PEPC is posttranslationally and diurnally regulated by a PEPC kinase (PEPCk), and that PPDK is also reversibly light activated by a small protein kinase. Moreover, there is a contradiction between the proposed repression in photosynthetic genes by sink-source feedback signals (Pego *et al.*, 2000; McCormick, *et al.*, 2008) and the up-regulated expression of C_4 genes. Therefore, further biochemical studies on C_4 enzymes and their regulators will provide insights in the salt-tolerant mechanisms of C_4 photosynthesis. Another driver of the salt-tolerant mechanism research agenda in *M. sinensis* is the need for improved combustion quality. Better regulation of ions and higher mineral translocation capacity (Grare, 2010) in salt-tolerant plants make a possibility of the integration of improved combustion quality and salt tolerance.

ACKNOWLEDGEMENTS

The study described here is conducted with the kind help and support of many people around me in the University of Tokyo. I would like to express my sincere gratitude to all of them.

First and foremost, I would like to express my sincere gratitude to my supervisors Prof. Tetsuo Takano for his guidance and encouragement on my study and life. Meanwhile, I am indebted to Prof. Toshihiko Yamada (Field Science Center for Northern Biosphere, Hokkaido University) for providing experimental materials for this study and for his invaluable suggestions and discussion. I am also grateful to the technical support provided by Prof. Chunlan Lian, Dr. Mariko Norisada, Dr. Dai Kusumoto, and Mr. Kun Zong. My gratitude also goes to Dr. Daisuke Tsugama and Mr. Xuejia Li, both of whom have provided me with valuable experimental skills. Moreover, I would like to extend my gratitude to all members of Takano laboratory. The mutual support, help and friendship in Takano laboratory added great joy to my life during the past three years.

Last, but by no means least, I sincerely thanks my family members, especially my father Yanfei Sun, my mother Xiaoling Zhang, and my husband Yulai Han. Their constant help, encouragement and support have always been motivating my life.

REFERENCES

Agarwal, P.K., N.S. Yadav, and B. Jha. 2014. Role of Na^+/H^+ antiporters in Na^+ homeostasis in halophytic plants. In: N. Tuteja, and S.S. Gill, editors, Climate Change and Plant Abiotic Stress Tolerance. Wiley-VCH Verlag GmbH & Co. KGaA, Weinheim, Germany. p. 685–704.

Akram, M.S. and M. Ashraf. 2011. Exogenous application of potassium dihydrogen phosphate can alleviate the adverse effects of salt stress on sunflower. J. Plant Nutr. 34: 1041–1057.

Ali-Dinar, H.M., G. Ebert, and P. Ludders. 1999. Growth, chlorophyll content, photosynthesis and water relations in guava (*Psidium guajava* L.) under salinity and different nitrogen supply. Gartenbauwissenschaft 64: 54–59.

Alla, M.M.N. and N.M. Hassan. 2012. A possible role for C_4 photosynthetic enzymes in tolerance of *Zea mays* to NaCl. Protoplasma 249: 1109–1117.

Anand, A., M.J. Baig, M. Anuradha, and P.K. Mandal. 2001. Growth and photosynthetic characteristics of lucerne (*Medicago sativa* L.) genotypes as influenced by salinity of irrigation water. Indian Journal of Plant Physio. 6: 158–161.

Aoyagi, K. and J.A. Bassham. 1986. Appearance and accumulation of C_4 carbon pathway enzymes in developing wheat leaves. Plant Physiol. 80: 334–340.

Ashraf, M. and P.J.C. Harris. 2013. Photosynthesis under stressful environments: An

overview. Photosynthetica 51: 163–190.

Ashton, A.R., J.N. Burnell, R.T. Furbank, C.L.D. Jenkins, and M.D. Hatch. 1990. Enzymes of C_4 photosynthesis. In: P.J. Lea, editor, Methods in Plant Biochemistry. Academic Press Limited, London. p. 39–72.

Baker, N.R. 2008. Chlorophyll fluorescence: A probe of photosynthesis in vivo. Annu. Rev. Plant Biol. 59: 89–113.

Baker, N.R. and E. Rosenqvist. 2004. Applications of chlorophyll fluorescence can improve crop production strategies: an examination of future possibilities. J. Exp. Bot. 55: 1607–1621.

Bantan-Polak, T., M. Kassai, and K.B. Grant. 2001. A comparison of fluorescamine and naphthalene-2,3-dicarboxaldehyde fluorogenic reagents for microplate-based detection of amino acids. Anal. Biochem. 297: 128–136.

Barragán, V., E.O. Leidi, Z. Andrés, L. Rubio, A.D. Luca, J.A. Fernández, *et al.* 2012. Ion exchangers NHX1 and NHX2 mediate active potassium uptake into vacuoles to regulate cell turgor and stomatal function in Arabidopsis. Plant Cell 24: 1127–1142.

Bassil, E., H. Tajima, Y.C. Liang, M.A. Ohto, K. Ushijima, R. Nakano, *et al.* 2011. The Arabidopsis Na^+/H^+ antiporters NHX1 and NHX2 control vacuolar pH and K^+ homeostasis to regulate growth, flower development, and reproduction. Plant Cell 23: 3482–3497.

Belkhodja, R., F. Morales, A. Abadia, J. Gomezaparisi, and J. Abadia. 1994.

Chlorophyll fluorescence as a possible tool for salinity tolerance screening in barley (*Hordeum vulgare* L.). Plant Physiol. 104: 667–673.

Berndes, G., J. Hansson, A. Egeskog, and F. Johnsson. 2010. Strategies for 2nd generation biofuels in EU – Co-firing to stimulate feedstock supply development and process integration to improve energy efficiency and economic competitiveness. Biomass Bioenergy 34: 227–236.

Boriboonkaset, T., C. Theerawitaya, N. Yamada, A. Pichakum, K. Supaibulwatana, S. Cha-um, *et al.* 2013. Regulation of some carbohydrate metabolism-related genes, starch and soluble sugar contents, photosynthetic activities and yield attributes of two contrasting rice genotypes subjected to salt stress. Protoplasma 250: 1157–1167.

Bouraima, S., J. Vidal, D. Lavergne, A. Hoarau, and M.L. Champigny. 1987. Effects of sodium chloride stress on phosphoenolpyruvate carboxylase, NADP-malic enzyme and ribulose-1,5-bisphosphate carboxylase in shoots of pearl millet. Phytochemistry 26: 1329–1332.

Brosse, N., A. Dufour, X.Z. Meng, Q.N. Sun, and A. Ragauskas. 2012. *Miscanthus*: a fast-growing crop for biofuels and chemicals production. Biofuels, Bioproducts and Biorefining 6: 580–598.

Campbell, J.E., D.B. Lobell, and C.B. Field. 2009. Greater transportation energy and GHG offsets from bioelectricity than ethanol. Science 324: 1055–1057.

Carmo-Silva, A.E., S.J. Powers, A.J. Keys, M.C. Arrabaca, and M.A.J. Parry. 2008.

Photorespiration in C_4 grasses remains slow under drought conditions. Plant Cell Environ. 31: 925–940.

Chartzoulakis, K.S. 1994. Photosynthesis, water relations and leaf growth of cucumber exposed to salt stress. Sci. Hortic. 59: 27–35.

Chaves, M.M., J. Flexas, and C. Pinheiro. 2009. Photosynthesis under drought and salt stress: regulation mechanisms from whole plant to cell. Ann. Bot. 103: 551–560.

Chen, L.Z., D.H. Li, L.R. Song, C.X. Hu, G.H. Wang, and Y.D. Liu. 2006. Effects of salt stress on carbohydrate metabolism in desert soil alga *Microcoleus vaginatus* Gom.. J Integr. Plant Biol. 48: 914–919.

Chikov, V.I. and S.N. Batasheva. 2012. The role of C to N balance in the regulation of photosynthetic function. In: M. Najafpour, editor, Advances in Photosynthesis - Fundamental Aspects. InTech. p. 273–298.

Clifton-Brown, J.C., Y.C. Chiang, and T.R. Hodkinson. 2008. *Miscanthus*: genetic resources and breeding potential to enhance bioenergy production. In: W. Vermerris, editor, Genetic Improvement of Bioenergy Crops. Springer Science, New York. p. 273–294.

Clifton-Brown, J.C. and I. Lewandowski. 2000a. Overwintering problems of newly established *Miscanthus* plantations can be overcome by identifying genotypes with improved rhizome cold tolerance. New Phytol. 148: 287–294.

Clifton-Brown, J.C. and I. Lewandowski. 2000b. Water use efficiency and biomass partitioning of three different *Miscanthus* genotypes with limited and unlimited

water supply. Ann. Bot. 86: 191–200.

Clifton-Brown, J.C., I. Lewandowski, B. Andersson, G. Basch, D.G. Christian, J.B. Kjeldsen, *et al.* 2001. Performance of 15 *Miscanthus* genotypes at five sites in Europe. Agron. J. 93: 1013–1019.

Clifton-Brown, J.C., I. Lewandowski, F. Bangerth, and M.B. Jones. 2002. Comparative responses to water stress in stay-green, rapid- and slow senescing genotypes of the biomass crop, *Miscanthus*. New Phytol. 154: 335–345.

Crafts-Brandner, S.J. and M.E. Salvucci. 2002. Sensitivity of photosynthesis in a C_4 plant, maize, to heat stress. Plant Physiol. 129: 1773–1780.

Cramer, G.R., G.J. Alberico, and C. Schmidt. 1994. Salt tolerance is not associated with the sodium accumulation of 2 maize hybrids. Aust. J. Plant Physiol. 21: 675–692.

Criqui, M.C., A. Durr, Y. Parmentier, J. Marbach, J. Fleck, and E. Jamet. 1992. How are photosynthetic genes repressed in freshly-isolated mesophyll protoplasts of *Nicotiana sylvestris*? Plant Physiol. Biochem. 30: 597–601.

Cushman, J.C. and H.J. Bohnert. 1997. Molecular genetics of Crassulacean acid metabolism. Plant Physiol. 113: 667–676.

Davenport, R.J. and M. Tester. 2000. A weakly voltage-dependent, nonselective cation channel mediates toxic sodium influx in wheat. Plant Physiol. 122: 823–834.

de Lacerda, C.F., J. Cambraia, M.A. Oliva, and H.A. Ruiz. 2005. Changes in growth

and in solute concentrations in sorghum leaves and roots during salt stress recovery. Environ. Exp. Bot. 54: 69–76.

Delfine, S., A. Alvino, M. Zacchini, and F. Loreto. 1998. Consequences of salt stress on conductance to CO_2 diffusion, Rubisco characteristics and anatomy of spinach leaves. Aust. J. Plant Physiol. 25: 395–402.

Demidchik, V. and M. Tester. 2002. Sodium fluxes through nonselective cation channels in the plasma membrane of protoplasts from Arabidopsis roots. Plant Physiol. 128: 379–387.

DeRocher, E.J. and H.J. Bohnert. 1993. Development and environmental stress employ different mechanisms in the expression of a plant gene family. Plant Cell 5: 1611–1625.

Dionisio-Sese, M.L. and S. Tobita. 2000. Effects of salinity on sodium content and photosynthetic responses of rice seedlings differing in salt tolerance. J. Plant Physiol. 157: 54–58.

Dohleman, F.G., E.A. Heaton, and S.P. Long. 2010. Perennial grasses as second-generation sustainable feedstocks without conflict with food production. In: M. Khanna, J. Scheffran, and D. Zilberman, editors, Handbook of Bioenergy Economics and Policy. Springer Science+Business Media, LLC, Philadelphia. p. 27-37.

Dohleman, F.G. and S.P. Long. 2009. More Productive Than Maize in the Midwest: How Does *Miscanthus* Do It? Plant Physiol. 150: 2104-2115.

Eckardt, N.A. 2009. A new chlorophyll degradation pathway. Plant Cell 21: 700.

Edwards, G.E., H. Nakamoto, J.N. Burnell, and M.D. Hatch. 1985. Pyruvate, Pi Dikinase and NADP-malate dehydrogenase in C_4 photosynthesis: properties and mechanism of light/dark regulation. Annu. Rev. Plant Physiol. Plant Mol. Biol. 36: 255-286.

Elphick, C.H., D. Sanders, and F.J.M. Maathuis. 2001. Critical role of divalent cations and Na^+ efflux in *Arabidopsis thaliana* salt tolerance. Plant Cell Environ. 24: 733–740.

Eprintsev, A.T. and O.S. Fedorina. 2007. Functioning of malate dehydrogenase system in mesophyll and bundle sheath cells of maize leaves under salt stress conditions. Russ. J. Plant Physio. 54: 728–735.

Ezaki, B., E. Nagao, Y. Yamamoto, S. Nakashima, and T. Enomoto. 2008. Wild plants, *Andropogon virginicus* L. and *Miscanthus sinensis* Anders., are tolerant to multiple stresses including aluminum, heavy metals and oxidative stresses. Plant Cell Rep. 27: 951–961.

Farrell, A., J. Clifton-Brown, I. Lewandowski, and M. Jones. 2006. Genotypic variation in cold tolerance influences the yield of *Miscanthus* Ann. Appl. Biol. 149: 337–345.

Galmés, J., I. Aranjuelo, H. Medrano, and J. Flexas. 2013. Variation in Rubisco content and activity under variable climatic factors. Photosynthesis Res. 117: 73–90.

Garcialegaz, M.F., J.M. Ortiz, A. Garcialidon, and A. Cerda. 1993. Effect of salinity on growth, ion content and CO_2 assimilation rate in lemon varieties on different rootstocks. Physiol. Plant. 89: 427–432.

Giglioli-Guivarc'h, N., J.N. Pierre, S. Brown, R. Chollet, J. Vidal, and P. Gadal. 1996. The light-dependent transduction pathway controlling the regulatory phosphorylation of C_4 phospho*enol*pyruvate carboxylase in protoplasts from *Digitaria sanguinalis*. Plant Cell 8: 573–586.

Grare, M.A.R. 2010. Variability of salinity response in *Miscanthus sinensis* - phenotyping and gene expression study. Master's Thesis, Wageningen University, Wageningen UR, Wageningen.

Greef , J.M. and M. Deuter. 1993. Syntaxonomy of *Miscanthus* × *giganteus* Greef et. Deu. . Angew. Bot. 67: 87–90.

Hajlaoui, H., N.E. Ayeb, J.P. Garrec, and M. Denden. 2010. Differential effects of salt stress on osmotic adjustment and solutes allocation on the basis of root and leaf tissue senescence of two silage maize (*Zea mays* L.) varieties. Ind. Crop Prod. 31: 122–130.

Halfter, U., M. Ishitani, and J.K. Zhu. 2000. The Arabidopsis SOS2 protein kinase physically interacts with and is activated by the calcium-binding protein SOS3. Proc. Natl. Acad. Sci. USA 97: 3735–3740.

Hanana, M., O. Cagnac, T. Yamaguchi, S. Hamdi, A. Ghorbel, and E. Blumwald. 2007. A grape berry (*Vitis vinifera* L.) cation/proton antiporter is associated with berry

ripening. Plant Cell Physiol. 48: 804–811.

Harter, K., C. Talkemesserer, W. Barz, and E. Schafer. 1993. Light- and sucrose-dependent gene expression in photomixotrophic cell suspension cultures and protoplasts of rape (*Brassica napus* L.). Plant J. 4: 507–516.

Hasegawa, P.M., R.A. Bressan, J.K. Zhu, and H.J. Bohnert. 2000. Plant cellular and molecular responses to high salinity. Annu. Rev. Plant Physiol. Plant Mol. Biol. 51: 463–499.

Hatch, M.D. 1987. C_4 photosynthesis: a unique blend of modified biochemistry, anatomy and ultrastructure. Biochim. Biophys. Acta 895: 81–106.

Hatzig, S., A. Kumar, A. Neubert, and S. Schubert. 2010. PEP-carboxylase activity: A comparison of its role in a C_4 and a C_3 species under salt stress. J Agron. Crop Sci. 196: 185–192.

He, C.X., J.Q. Yan, G.X. Shen, L.H. Fu, A.S. Holaday, D. Auld, *et al.* 2005. Expression of an arabidopsis vacuolar sodium/proton antiporter gene in cotton improves photosynthetic performance under salt conditions and increases fiber yield in the field. Plant Cell Physiol. 46: 1848–1854.

Hebbelmann, I., J. Selinski, C. Wehmeyer, T. Goss, I. Voss, P. Mulo, *et al.* 2012. Multiple strategies to prevent oxidative stress in Arabidopsis plants lacking the malate valve enzyme NADP-malate dehydrogenase. J. Exp. Bot. 63: 1445–1459.

Heuer, B. 2005. Photosynthetic carbon metabolism of crops under salt stress. In: M. Pessarakli, editor, Handbook of Photosynthesis. Taylor & Francis Group, Boca

Raton, Florida. p. 779–792.

Hibberd, J.M. and S. Covshoff. 2010. The regulation of gene expression required for C_4 photosynthesis. Annu. Rev. Plant Biol. 61: 181–207.

Hirel, B., B. Andrieu, M.H. Valadier, S. Renard, I. Quillere, M. Chelle, *et al.* 2005. Physiology of maize II: Identification of physiological markers representative of the nitrogen status of maize (*Zea mays*) leaves during grain filling. Physiol. Plant. 124: 178–188.

Hodkinson, T.R., M.W. Chase, C. Takahashi, I.J. Leitch, M.D. Bennett, and S.A. Renvoize. 2002. The use of DNA sequencing (ITS and trnL-F), AFLP, and fluorescent in situ hybridization to study allopolyploid *Miscanthus* (Poaceae). Am. J. Bot. 89: 279–286.

Hodkinson, T.R. and S.A. Renvoize. 2001. Nomenclature of *Miscanthus* × *giganteus* (Poaceae). Kew Bull. 56: 759–760.

Hsu, F.H. 1990. Effects of salt stress on germination of *Miscanthus* species and the physiological response to salt stress. Journal of Taiwan Livestock Research 23: 113–124.

Hu, T., L. Hu, X. Zhang, P. Zhang, Z. Zhao, and J. Fu. 2013. Differential responses of CO_2 assimilation, carbohydrate allocation and gene expression to NaCl stress in perennial ryegrass with different salt tolerance. Plos One 8(6): e66090.

Iglesias, A.A. and C.S. Andreo. 1989. Purification of NADP-malic enzyme and phospho*enol*pyruvate carboxylase from sugar cane leaves. Plant Cell Physiol. 30:

399–405.

Jaafar, H.Z.E. and M.H. Ibrahim. 2012. Photosynthesis and quantum yield of oil palm seedlings to elevated carbon dioxide. In: M.M. Najafpour, editor, Advances in Photosynthesis - Fundamental Aspects. InTech, Croatia. p. 321–340.

James, R.A., A.R. Rivelli, R. Munns, and S. von Caemmerer. 2002. Factors affecting CO_2 assimilation, leaf injury and growth in salt-stressed durum wheat. Funct. Plant Biol. 29: 1393–1403.

Ji, H., J.M. Pardo, G. Batelli, M.J.V. Oosten, R.A. Bressan, and X. Li. 2013. The salt overly sensitive (SOS) pathway: established and emerging roles. Mol. Plant 6: 275–286.

Jiang, Q.Z., D. Roche, T.A. Monaco, and S. Durham. 2006. Gas exchange, chlorophyll fluorescence parameters and carbon isotope discrimination of 14 barley genetic lines in response to salinity. Field Crops Res. 96: 269–278.

Kerepesi, I. and G. Galiba. 2000. Osmotic and salt stress-induced alteration in soluble carbohydrate content in wheat seedlings. Crop Sci. 40: 482–487.

Kingsbury, R.W., E. Epstein, and R.W. Pearcy. 1984. Physiological responses to salinity in selected lines of wheat. Plant Physiol. 74: 417–423.

Knudson, L.L., T.W. Tibbitts, and G.E. Edwards. 1977. Measurement of ozone injury by determination of leaf chlorophyll concentration. Plant Physiol. 60: 606–608.

Kobayashi, K. and Y. Yokoi. 2003. Spatiotemporal patterns of shoots within an isolated *Miscanthus sinensis* patch in the warm-temperate region of Japan. Ecol.

Res. 18: 41-51.

Krapp, A., B. Hofmann, C. Schafer, and M. Stitt. 1993. Regulation of the expression of *rbcS* and other photosynthetic genes by carbohydrates: a mechanism for the 'sink regulation' of photosynthesis? Plant J. 3: 817–828.

Krasensky, J. and C. Jonak. 2012. Drought, salt, and temperature stress-induced metabolic rearrangements and regulatory networks. J. Exp. Bot. 63: 1593–1608.

Krishnamurthy, L., R. Serraj, C.T. Hash, A.J. Dakheel, and B.V.S. Reddy. 2007. Screening sorghum genotypes for salinity tolerant biomass production. Euphytica 156: 15–24.

Kronzucker, H.J. and D.T. Britto. 2011. Sodium transport in plants: a critical review. New Phytol. 189: 54–81.

Langdale, J.A. 2011. C_4 cycles: past, present, and future research on C_4 photosynthesis. Plant Cell 23: 3879–3892.

Leakey, A.D.B., M. Uribelarrea, E.A. Ainsworth, S.L. Naidu, A. Rogers, D.R. Ort, *et al.* 2006. Photosynthesis, productivity, and yield of maize are not affected by open-air elevation of CO_2 concentration in the absence of drought. Plant Physiol. 140: 779–790.

Leidi, E.O., V. Barragán, L. Rubio, A. El-Hamdaoui, M.T. Ruiz, B. Cubero, *et al.* 2010. The AtNHX1 exchanger mediates potassium compartmentation in vacuoles of transgenic tomato. Plant J. 61: 495–506.

Linde-laursen, I. 1993. Cytogenetic analysis of *Miscanthus* 'Giganteus', an

interspecific hybrid. Hereditas 119: 297–300.

Liu, J.P., M. Ishitani, U. Halfter, C.S. Kim, and J.K. Zhu. 2000. The *Arabidopsis thaliana* SOS2 gene encodes a protein kinase that is required for salt tolerance. Proc. Natl. Acad. Sci. USA 97: 3730–3734.

Liu, J.P. and J.K. Zhu. 1998. A calcium sensor homolog required for plant salt tolerance. Science 280: 1943–1945.

Long, S. 1987. The productivity of C4 cord-grasses and galingale. In: G. Grassi, and H. Zibetta, editors, Energy from Biomass I. Commission of the European Communities/Elsevier Applied Science, London. p. 95–99.

Lu, S.Y., Y.X. Jing, S.H. Shen, H.Y. Zhao, L.Q. Ma, X.J. Zhou, *et al.* 2005. Antiporter gene from *Hordum brevisubulatum* (Trin.) Link and its overexpression in transgenic tobaccos. J Integr. Plant Biol. 47: 343–349.

Maness, N. 2010. Extraction and analysis of soluble carbohydrates. In: R. Sunkar, editor, Plant Stress Tolerance: Methods and Protocols. Humana Press, New York, USA. p. 341–370.

Maricle, B.R., R.W. Lee, C.E. Hellquist, O. Kiirats, and G.E. Edwards. 2007. Effects of salinity on chlorophyll fluorescence and CO_2 fixation in C_4 estuarine grasses. Photosynthetica 45: 433–440.

Mart ńez-Atienza, J., X. Jiang, B. Garciadeblas, I. Mendoza, Jian-Kang Zhu, J.M. Pardo, *et al.* 2007. Conservation of the salt overly sensitive pathway in rice. Plant Physiol. 143: 1001–1012.

Mäser, P., M. Gierth, and J.I. Schroeder. 2002. Molecular mechanisms of potassium and sodium uptake in plants. Plant Soil 247: 43–54.

Matile, P., S. Hortensteiner, and H. Thomas. 1999. Chlorophyll degradation. Annu. Rev. Plant Physiol. Plant Mol. Biol. 50: 67–95.

Maxwell, K. and G.N. Johnson. 2000. Chlorophyll fluorescence - a practical guide. J. Exp. Bot. 51: 659–668.

McCormick, A.J., M.D. Cramer, and D.A. Watt. 2008. Changes in photosynthetic rates and gene expression of leaves during a source-sink perturbation in sugarcane. Ann Bot. 101: 89–102.

Meinzer, F.C., Z. Plaut, and N.Z. Saliendra. 1994. Carbon-isotope discrimination, gas-exchange, and growth of sugarcane cultivars under salinity. Plant Physiol. 104: 521–526.

Miles, T.R., T.R.J. Miles, L.L. Baxter, R.W. Bryers, B.M. Jenkins, and L.L. Oden. 1996. Boiler deposits from riffing biomass fuels. Biomass Bioenergy 10: 125–138.

Munns, R. 2010. Approaches to identifying genes for salinity tolerance and the importance of timescale. In: R. Sunkar, editor, Plant Stress Tolerance: Methods and Protocols. Humana Press, New York. p. 25–38.

Munns, R. and R.A. James. 2003. Screening methods for salinity tolerance: a case study with tetraploid wheat. Plant Soil 253: 201–218.

Munns, R. and M. Tester. 2008. Mechanisms of salinity tolerance. Annu. Rev. Plant

Biol. 59: 651–681.

Munns, R., P.A. Wallace, N.L. Teakle, and T.D. Colmer. 2010. Measuring soluble ion concentrations (Na^+, K^+, Cl^-) in salt-treated plants. In: R. Sunkar, editor, Plant Stress Tolerance: Methods and Protocols. Humana Press, New York. p. 371–382.

Murillo-Amador, B., E. Troyo-Dieguez, R. LopezAguilar, A. Lopez-Cortes, C.L. Tinoco-Ojanguren, H.G. Jones, *et al.* 2002. Matching physiological traits and ion concentrations associated with salt stress in cowpea genotypes. Aust. J. Agric. Res. 53: 1243–1255.

Netondo, G.W., J.C. Onyango, and E. Beck. 2004a. Sorghum and salinity: I. Response of growth, water relations, and ion accumulation to NaCl salinity. Crop Sci. 44: 797–805.

Netondo, G.W., J.C. Onyango, and E. Beck. 2004b. Sorghum and salinity: II. Gas exchange and chlorophyll fluorescence of sorghum under salt stress. Crop Sci. 44: 806–811.

Nicolas, M.E., R. Munns, A.B. Samarakoon, and R.M. Gifford. 1993. Elevated CO_2 improves the growth of wheat under salinity. Aust. J. Plant Physiol. 20: 349–360.

Oh, D.H., E. Leidi, Q. Zhang, S.M. Hwang, Y. Li, F.J. Quintero, *et al.* 2009. Loss of halophytism by interference with SOS1 expression. Plant Physiol. 151: 210–222.

Ohlrogge, J., D. Allen, B. Berguson, D. DellaPenna, Y. Shachar-Hill, and S. Stymne. 2009. Driving on biomass. Science 324: 1019–1020.

Ohta, M., Y. Hayashi, A. Nakashima, A. Hamada, A. Tanaka, T. Nakamura, *et al.*

2002. Introduction of a Na^+/H^+ antiporter gene from *Atriplex gmelini* confers salt tolerance to rice. FEBS Lett. 532: 279–282.

Ol ás, R., Z. Eljakaoui, J. Li, P. Alvarez De Morales, M. Carmen Marin-Manzano, J.M. Pardo, *et al.* 2009. The plasma membrane Na^+/H^+ antiporter SOS1 is essential for salt tolerance in tomato and affects the partitioning of Na^+ between plant organs. Plant Cell Environ. 32: 904–916.

Omoto, E., M. Kawasaki, M. Taniguchi, and H. Miyake. 2009. Salinity induces granal development in bundle sheath chloroplasts of NADP-malic enzyme type C_4 plants. Plant Prod. Sci. 12: 199–207.

Omoto, E., M. Taniguchi, and H. Miyake. 2012. Adaptation responses in C_4 photosynthesis of maize under salinity. J. Plant Physiol. 169: 469–477.

Ouerghi, Z., G. Cornic, M. Roudani, A. Ayadi, and J. Brulfert. 2000. Effect of NaCl on photosynthesis of two wheat species (*Triticum durum* and *T. aestivum*) differing in their sensitivity to salt stress. J. Plant Physiol. 156: 335–340.

Pardossi, A., F. Malorgio, D. Oriolo, R. Gucci, G. Serra, and F. Tognoni. 1998. Water relations and osmotic adjustment in *Apium graveolens* during long-term NaCl stress and subsequent relief. Physiol. Plant. 102: 369–376.

Parvaiz, A. and S. Satyawati. 2008. Salt stress and phyto-biochemical responses of plants – a review. Plant Soil Environ. 54: 89–99.

Paul, M.J. and C.H. Foyer. 2001. Sink regulation of photosynthesis. J. Exp. Bot. 52: 1383–1400.

Pego, J.V., A.J. Kortstee, C. Huijser, and S.C.M. Smeekens. 2000. Photosynthesis, sugars and the regulation of gene expression. J. Exp. Bot. 51: 407–416.

Praxedes, S.C., C.F. de Lacerda, F.M. DaMatta, J.T. Prisco, and E. Gomes-Filho. 2010. Salt tolerance is associated with differences in ion accumulation, biomass allocation and photosynthesis in cowpea cultivars. J Agron. Crop Sci. 196: 193–204.

Qiu, Q.S., Y. Guo, M.A. Dietrich, K.S. Schumaker, and J.K. Zhu. 2002. Regulation of SOS1, a plasma membrane Na^+/H^+ exchanger in *Arabidopsis thaliana*, by SOS2 and SOS3. Proc. Natl. Acad. Sci. USA 99: 8436–8441.

Quintero, F.J., J. Martinez-Atienza, I. Villalta, X. Jiang, W.-Y. Kim, Z. Ali, *et al.* 2011. Activation of the plasma membrane Na/H antiporter Salt-Overly-Sensitive 1 (SOS1) by phosphorylation of an auto-inhibitory C-terminal domain. Proc. Natl. Acad. Sci. USA 108: 2611–2616.

Quintero, F.J., M. Ohta, H.Z. Shi, J.K. Zhu, and J.M. Pardo. 2002. Reconstitution in yeast of the Arabidopsis SOS signaling pathway for Na^+ homeostasis. Proc. Natl. Acad. Sci. USA 99: 9061-9066.

Ranal, M.A. and D.G.D. Santana. 2006. How and why to measure the germination process? Revista Brasil. Bot. 29: 1–11.

Roitsch, T. 1999. Source-sink regulation by sugar and stress. Curr. Opin. Plant Biol. 2: 198–206.

Rolland, F., E. Baena-Gonzalez, and J. Sheen. 2006. Sugar sensing and signaling in

plants: conserved and novel mechanisms. Annu. Rev. Plant Biol. 57: 675–709.

Sanchez, D.H., M.R. Siahpoosh, U. Roessner, M. Udvardi, and J. Kopka. 2008. Plant metabolomics reveals conserved and divergent metabolic responses to salinity. Physiol. Plant. 132: 209–219.

Sang, T. and W.X. Zhu. 2011. China's bioenergy potential. GCB Bioenergy 3: 79–90.

Santos, C.V. 2004. Regulation of chlorophyll biosynthesis and degradation by salt stress in sunflower leaves. Sci. Hortic. 103: 93–99.

Scheibe, R., J.E. Backhausen, V. Emmerlich, and S. Holtgrefe. 2005. Strategies to maintain redox homeostasis during photosynthesis under changing conditions. J. Exp. Bot. 56: 1481–1489.

Scheible, W.R., R. Morcuende, T. Czechowski, C. Fritz, D. Osuna, N. Palacios-Rojas, et al. 2004. Genome-wide reprogramming of primary and secondary metabolism, protein synthesis, cellular growth processes, and the regulatory infrastructure of Arabidopsis in response to nitrogen. Plant Physiol. 136: 2483–2499.

Shabala, S. and T.A. Cuin. 2007. Potassium transport and plant salt tolerance. Physiol. Plant. 133: 651–669.

Sharkey, T.D., L.V. Savitch, and N.D. Butz. 1991. Photometric method for routine determination of k_{cat} and carbamylation of rubisco. Photosynthesis Res. 28: 41–48.

Sheen, J. 1999. C_4 gene expression. Annu. Rev. Plant Physiol. Plant Mol. Biol. 50: 187–217.

Shi, H.Z., F.J. Quintero, J.M. Pardo, and J.K. Zhu. 2002. The putative plasma membrane Na^+/H^+ antiporter SOS1 controls long-distance Na^+ transport in plants. Plant Cell 14: 465–477.

Shu, S., S.R. Guo, J. Sun, and L.Y. Yuan. 2012. Effects of salt stress on the structure and function of the photosynthetic apparatus in *Cucumis sativus* and its protection by exogenous putrescine. Physiol Plant. 146: 285–296.

Smillie, R.M. and R. Nott. 1982. Salt tolerance in crop plants monitored by chlorophyll fluorescence *in vivo*. Plant Physiol. 70: 1049–1054.

Sobhanian, H., N. Motamed, F.R. Jazii, T. Nakamura, and S. Komatsu. 2010. Salt stress induced differential proteome and metabolome response in the shoots of *Aeluropus lagopoides* (Poaceae), a halophyte C_4 plant. J Proteome Res. 9: 2882–2897.

Somerville, C., H. Youngs, C. Taylor, S.C. Davis, and S.P. Long. 2010. Feedstocks for Lignocellulosic Biofuels. Science 329: 790–792.

Sottosanto, J.B., Y. Saranga, and E. Blumwald. 2007. Impact of AtNHX1, a vacuolar Na^+/H^+ antiporter, upon gene expression during short-term and long-term salt stress in *Arabidopsis thaliana*. BMC Plant Biol. 7: 18.

Spreitzer, R.J. and M.E. Salvucci. 2002. Rubisco: Structure, regulatory interactions, and possibilities for a better enzyme. Annu. Rev. Plant Biol. 53: 449–475.

Stepien, P. and G.N. Johnson. 2009. Contrasting responses of photosynthesis to salt stress in the glycophyte Arabidopsis and the halophyte Thellungiella: role of the

plastid terminal oxidase as an alternative electron sink. Plant Physiol. 149: 1154–1165.

Stewart, J.R., Y. Toma, F.G. Fernández, A. Nishiwaki, T. Yamada, and G. Bollero. 2009. The ecology and agronomy of *Miscanthus sinensis*, a species important to bioenergy crop development, in its native range in Japan: a review. GCB Bioenergy 1: 126–153.

Sugiyama, T. 1973. Purification, molecular, and catalytic properties of pyruvate phosphate dikinase from the maize leaf. Biochemistry 12: 2862–2868.

Sun, Q., Q. Lin, Z.L. Yi, Z.R. Yang, and F.S. Zhou. 2010. A taxonomic revision of *Miscanthus* s.l. (Poaceae) from China. Bot. J. Linn. Soc. 164: 178–220.

Sun, S.B., Q.R. Shen, J.M. Wan, and Z.P. Liu. 2003. Induced expression of the gene for NADP-malic enzyme in leaves of *Aloe vera* L. under salt stress. Acta Bioch. Bioph. Sin. 35: 423–429.

Takahashi, S. and N. Murata. 2008. How do environmental stresses accelerate photoinhibition? Trends Plant Sci. 13(4): 178–182.

Takeuchi, Y., H. Akagi, N. Kamasawa, M. Osumi, and H. Honda. 2000. Aberrant chloroplasts in transgenic rice plants expressing a high level of maize NADP-dependent malic enzyme. Planta 211: 265–274.

Tavakkoli, E., P. Rengasamy, and G.K. McDonald. 2010. High concentrations of Na^+ and Cl^- ions in soil solution have simultaneous detrimental effects on growth of faba bean under salinity stress. J. Exp. Bot. 61: 4449–4459.

Teakle, N.L. and S.D. Tyerman. 2010. Mechanisms of Cl^- transport contributing to salt tolerance. Plant Cell Environ. 33: 566–589.

Tilbrook, J. and S. Roy. 2014. Salinity tolerance. In: M.A. Jenks and P.M. Hasegawa, editors, Plant Abiotic Stress. John Wiley & Sons, Inc., Hoboken, USA. p. 133–178.

Turkan, I. and T. Demiral. 2009. Recent developments in understanding salinity tolerance. Environ. Exp. Bot. 67: 2–9.

Venema, K., F.J. Quintero, J.M. Pardo, and J.P. Donaire. 2002. The Arabidopsis Na^+/H^+ exchanger AtNHX1 catalyzes low affinity Na^+ and K^+ transport in reconstituted liposomes. J. Biol. Chem. 277: 2413–2418.

Vieira dos Santos, C.L. and G. Caldeira. 1999. Comparative responses of *Helianthus annuus* plants and calli exposed to NaCl: I. Growth rate and osmotic regulation in intact plants and calli. J. Plant Physiol. 155: 769–777.

Wahid, A., A.U.R. Rao, and E. Rasul. 1997. Identification of salt tolerance traits in sugarcane lines. Field Crops Res. 54: 9–17.

Wang, H.M., W.J. Wang, H.Z. Wang, Y. Wang, H.N. Xu, and Y.G. Zu. 2013. Effect of inland salt-alkaline stress on C_4 enzymes, pigments, antioxidant enzymes, and photosynthesis in leaf, bark, and branch chlorenchyma of poplars. Photosynthetica 51: 115–126.

Wang, Y.M., Y.L. Meng, H. Ishikawa, T. Hibino, Y. Tanaka, N. Nii, *et al.* 1999. Photosynthetic adaptation to salt stress in three-color leaves of a C_4 plant

Amaranthus tricolor. Plant Cell Physiol. 40: 668–674.

Wu, Y.Y., Q.J. Chen, M. Chen, J. Chen, and X.C. Wang. 2005. Salt-tolerant transgenic perennial ryegrass (*Lolium perenne* L.) obtained by *Agrobacterium tumefaciens*-mediated transformation of the vacuolar Na^+/H^+ antiporter gene. Plant Sci. 169: 65–73.

Xue, Z.Y., D.Y. Zhi, G.P. Xue, H. Zhang, Y.X. Zhao, and G.M. Xia. 2004. Enhanced salt tolerance of transgenic wheat (*Tritivum aestivum* L.) expressing a vacuolar Na^+/H^+ antiporter gene with improved grain yields in saline soils in the field and a reduced level of leaf Na^+. Plant Sci. 167: 849–859.

Yadav, N.S., P.S. Shukla, A. Jha, P.K. Agarwal, and B. Jha. 2012. The SbSOS1 gene from the extreme halophyte *Salicornia brachiata* enhances Na^+ loading in xylem and confers salt tolerance in transgenic tobacco. BMC Plant Biol. 12: 188–205.

Yan, K., P. Chen, H. Shao, S. Zhao, L. Zhang, L. Zhang, *et al.* 2012. Responses of photosynthesis and photosystem II to higher temperature and salt stress in sorghum. J Agron. Crop Sci. 198: 218–226.

Yeo, A.R. and T.J. Flowers. 1983. Varietal differences in the toxicity of sodium-ions in rice leaves. Physiol. Plant. 59: 189–195.

Yin, X.Y., A.F. Yang, K.W. Zhang, and J.R. Zhang. 2004. Production and analysis of transgenic maize with improved salt tolerance by the introduction of AtNHX1 gene. Acta Bot. Sin. 46: 854–861.

Yoshida, S. 1976. *Miscanthus sinensis* type grassland from the view point of grassland

science. In: Study of Susuki. Professor Isao Hirayoshi Memorial Volume. Gifu University, Gifu, Japan (in Japanese). p. 45–68.

Zhang, H.X. and E. Blumwald. 2001. Transgenic salt-tolerant tomato plants accumulate salt in foliage but not in fruit. Nat. Biotechnol. 19: 765–768.

Zhang, H.X., J.N. Hodson, J.P. Williams, and E. Blumwald. 2001. Engineering salt-tolerant *Brassica* plants: Characterization of yield and seed oil quality in transgenic plants with increased vacuolar sodium accumulation. Proc. Natl. Acad. Sci. USA 98: 12832–12836.

Zhao, G.Q., B.L. Ma, and C.Z. Ren. 2007. Growth, gas exchange, chlorophyll fluorescence, and ion content of naked oat in response to salinity. Crop Sci. 47: 123–131.

Zhao, X., H.J. Tan, Y.B. Liu, X.R. Li, and G.X. Chen. 2009. Effect of salt stress on growth and osmotic regulation in Thellungiella and Arabidopsis callus. Plant Cell Tiss. Org. Cult. 98: 97–103.

Zhu, J. and F.C. Meinzer. 1999. Efficiency of C_4 photosynthesis in *Atriplex lentiformis* under salinity stress. Aust. J. Plant Physiol. 26: 79–86.

Zub, H.W. and M. Brancourt-Hulmel. 2010. Agronomic and physiological performances of different species of *Miscanthus*, a major energy crop. A review. Agron. Sustain. Dev. 30: 201–214.